AGRICULTURE JOURNAL IJOEAR

VOLUME-12, ISSUE-4, APRIL 2026

NAAS Rating: 4.23

Download Now

+91-7665235235 www.ijoear.com info@ijoear.com

Preface

We would like to present, with great pleasure, the volume-12, Issue-4, April 2026 of a scholarly journal, *International Journal of Environmental & Agriculture Research*. This journal is part of the AD Publications series *in the field of Environmental & Agriculture Research Development*, and is devoted to the gamut of Environmental & Agriculture issues, from theoretical aspects to application-dependent studies and the validation of emerging technologies.

This journal was envisioned and founded to represent the growing needs of Environmental & Agriculture as an emerging and increasingly vital field, now widely recognized as an integral part of scientific and technical investigations. Its mission is to become a voice of the Environmental & Agriculture community, addressing researchers and practitioners in below areas.

Environmental Research:

Environmental science and regulation, Ecotoxicology, Environmental health issues, Atmosphere and climate, Terrestric ecosystems, Aquatic ecosystems, Energy and environment, Marine research, Biodiversity, Pharmaceuticals in the environment, Genetically modified organisms, Biotechnology, Risk assessment, Environment society, Agricultural engineering, Animal science, Agronomy, including plant science, theoretical production ecology, horticulture, plant, breeding, plant fertilization, soil science and all field related to Environmental Research.

Agriculture Research:

Agriculture, Biological engineering, including genetic engineering, microbiology, Environmental impacts of agriculture, forestry, Food science, Husbandry, Irrigation and water management, Land use, Waste management and all fields related to Agriculture.

Each article in this issue provides an example of a concrete industrial application or a case study of the presented methodology to amplify the impact of the contribution. We are very thankful to everybody within that community who supported the idea of creating a new Research with *IJOEAR*. We are certain that this issue will be followed by many others, reporting new developments in the Environment and Agriculture Research Science field. This issue would not have been possible without the great support of the Reviewer, Editorial Board members and also with our Advisory Board Members, and we would like to express our sincere thanks to all of them. We would also like to express our gratitude to the editorial staff of AD Publications, who supported us at every stage of the project. It is our hope that this fine collection of articles will be a valuable resource for *IJOEAR* readers and will stimulate further research into the vibrant area of Environmental & Agriculture Research.

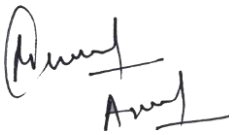

Mukesh Arora

(Managing Editor)

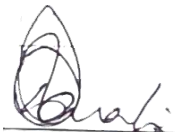

Dr. Bhagawan Bharali

(Chief Editor)

Fields of Interests

Agricultural Sciences	
Soil Science	Plant Science
Animal Science	Agricultural Economics
Agricultural Chemistry	Basic biology concepts
Sustainable Natural Resource Utilisation	Management of the Environment
Agricultural Management Practices	Agricultural Technology
Natural Resources	Basic Horticulture
Food System	Irrigation and water management
Crop Production	
Cereals or Basic Grains: Oats, Wheat, Barley, Rye, Triticale, Corn, Sorghum, Millet, Quinoa and Amaranth	Oilseeds: Canola, Rapeseed, Flax, Sunflowers, Corn and Hempseed
Pulse Crops: Peas (all types), field beans, faba beans, lentils, soybeans, peanuts and chickpeas.	Hay and Silage (Forage crop) Production
Vegetable crops or Olericulture: Crops utilized fresh or whole (wholefood crop, no or limited processing, i.e., fresh cut salad); (Lettuce, Cabbage, Carrots, Potatoes, Tomatoes, Herbs, etc.)	Tree Fruit crops: apples, oranges, stone fruit (i.e., peaches, plums, cherries)
Tree Nut crops: Hazlenuts. walnuts, almonds, cashews, pecans	Berry crops: strawberries, blueberries, raspberries
Sugar crops: sugarcane. sugar beets, sorghum	Potatoes varieties and production.
Livestock Production	
Animal husbandry	Ranch
Camel	Yak
Pigs	Sheep
Goats	Poultry
Bees	Dogs
Exotic species	Chicken Growth
Aquaculture	
Fish farm	Shrimp farm
Freshwater prawn farm	Integrated Multi-Trophic Aquaculture

Milk Production (Dairy)	
Dairy goat	Dairy cow
Dairy Sheep	Water Buffalo
Moose milk	Dairy product
Forest Products and Forest management	
Forestry/Silviculture	Agroforestry
Silvopasture	Christmas tree cultivation
Maple syrup	Forestry Growth
Mechanical	
General Farm Machinery	Tillage equipment
Harvesting equipment	Processing equipment
Hay & Silage/Forage equipment	Milking equipment
Hand tools & activities	Stock handling & control equipment
Agricultural buildings	Storage
Agricultural Input Products	
Crop Protection Chemicals	Feed supplements
Chemical based (inorganic) fertilizers	Organic fertilizers
Environmental Science	
Environmental science and regulation	Ecotoxicology
Environmental health issues	Atmosphere and climate
Terrestric ecosystems	Aquatic ecosystems
Energy and environment	Marine research
Biodiversity	Pharmaceuticals in the environment
Genetically modified organisms	Biotechnology
Risk assessment	Environment society
Theoretical production ecology	horticulture
Breeding	plant fertilization

Board Members

Dr. Bhagawan Bharali (Chief Editor)

Professor & Head, Department of Crop Physiology, Faculty of Agriculture, Assam Agricultural University, Jorhat-785013 (Assam).

Mr. Mukesh Arora (Managing Editor)

M.Tech (Digital Communication), BE (Electronics & Communication), currently serving as Associate Professor in the Department of EE, BIET, Sikar.

Dr. Kusum Gaur (Associate Editor)

Dr. Kusum Gaur working as professor Community Medicine and member of Research Review Board of Sawai Man Singh Medical College, Jaipur (Raj) India.

She has awarded with WHO Fellowship for IEC at Bangkok. She has done management course from NIHFW. She has published and present many research paper in India as well as abroad in the field of community medicine and medical education. She has developed Socio-economic Status Scale (Gaur's SES) and Spiritual Health Assessment Scale (SHAS). She is 1st author of a book entitled " Community Medicine: Practical Guide and Logbook.

Research Area: Community Medicine, Biostatics, Epidemiology, Health and Hospital Management and Spiritual Health

Dr. Darwin H. Pangaribuan

Associate Professor in Department of Agronomy and Horticulture, Faculty of Agriculture, University of Lampung, Indonesia.

Educational background: (Ir.) from Faculty of Agriculture, IPB University, Bogor, Indonesia; (Dipl. Eng) in Land Evaluation from the University of Tweente (UT-ITC), Enschede, The Netherlands; (M.Sc) in Crop Production from Wageningen University (WU), The Netherlands. (Ph.D) in Horticulture from University of Queensland (UQ), Brisbane, Australia.

Research Interest: Vegetable Production & Physiology; Biostimulant & Biofertilizers; Organic Farming, Multiple Cropping, Crop Nutrition, Horticulture.

Dr Peni Kistijani Samsuria Mutalib

Working as Research coordinator and HOD in the department of Medical Physics in University of Indonesia.

Dr. Govindaraj Kamalam Dinesh, PhD

Department of Biochemistry, Physiology, Microbiology and Environmental Science College of Agriculture, Iroisemba

Central Agricultural University, Imphal, Manipur – 795004, India

Specialization: Ecosystem services, Conservation agriculture, Climate change, Agroecology, Greenhouse gas emissions from agriculture, Agricultural ornithology, Carbon sequestration

Academic Qualifications: B.Sc. (Agriculture), Annamalai University, M.Sc. (Environmental Science), Tamil Nadu Agricultural University (TNAU), Ph.D. (Environmental Sciences), ICAR-IARI, New Delhi (UGC-JRF, IARI PhD SRF, All India Rank – 5)

Professor Jacinta A.Opara

Working full-time and full-ranked Professor and Director, Centre for Health and Environmental Studies at one of the top 10 leading public Universities in Nigeria, the University of Maiduguri-Nigeria founded in 1975.

Dr. Samir B. Salman AL-Badri

Samir Albadri currently works at the University of Baghdad / Department of Agricultural Machines and Equipment. After graduation from the Department of Plant, Soils, and Agricultural Systems, Southern Illinois University Carbondale. The project was 'Hybrid cooling to extend the saleable shelf life of some fruits and vegetables. I worked in many other subject such as Evaporative pad cooling.

Orchid ID: https://orcid.org/0000-0001-9784-7424

Publon Profile: https://publons.com/researcher/1857228/samir-b-albadri

Dr. Goswami Tridib Kumar

Presently working as a Professor in IIT Kharagpur from year 2007, He Received PhD degree from IIT Kharagpur in the year of 1987.

Prof. Khalil Cherifi

Professor in Department of Biology at Faculty of Sciences, Agadir, Morocco.

Dr. Josiah Chidiebere Okonkwo

PhD Animal Science/ Biotech (DELSU), PGD Biotechnology (Hebrew University of Jerusalem Senior Lecturer, Department of Animal Science and Technology, Faculty of Agriculture, Nau, AWKA.

Dr. Jadala Shankaraswamy

Specialization: Horticulture, Post-Harvest Technology, Phytochemistry, Nanobiotechnology, 3D Food Printing

Academic Qualifications: B.Sc. (Horticulture), M.Sc. (Post-Harvest Technology of Horticultural Crops), Ph.D. (Horticulture)

Assistant Professor (Senior Scale - IX), College of Horticulture, Mojerla, Sri Konda Laxman Telangana State Horticultural University, Telangana, India

Dr. Jadala Shankaraswamy is an Assistant Professor (Senior Scale – IX) at Sri Konda Laxman Telangana State Horticultural University, Telangana, India. His research focuses on post-harvest technology, phytochemistry, nanobiotechnology, and value addition in horticultural crops. He has contributed to innovative product development, holds patents in horticultural science, and has received several national and international awards for his research excellence.

Dr. Tarun Kumar Maheshwari

Dr. Tarun Kumar Maheshwari, Head of Agricultural Engineering at Dr. BRA College of Agricultural Engineering and Technology, Etawah, specializes in farm machinery and power engineering. He holds a Ph.D. from Sam Higginbottom University and an M.Tech. from IIT Kharagpur.

Prof. Özhan ŞİMŞEK

Agriculture Faculty, Department of Horticulture, Çukurova University, Adana, 01330 Turkey.

Dr. Anka Ozana Čavlović

Working as Professor in the department of Faculty of Forestry, University of Zagreb, Svetošimunska 25, Zagreb.

Dr. Rakesh Singh

Professor in Department of Agricultural Economics, Institute of Agricultural Sciences, Banaras Hindu University, Also Vice President of Indian Society of Agricultural Economics, Mumbai.

Dr. Sunil Wimalawansa

MD, PhD, MBA, DSc, is a former university professor, Professor of Medicine, Chief of Endocrinology, Metabolism & Nutrition, expert in endocrinology; osteoporosis and metabolic bone disease, vitamin D, and nutrition.

Dr. Smruti Sohani

Dr. Smruti Sohani, has Fellowship in Pharmacy & Life Science (FPLS) and Life member of International Journal of Biological science indexed by UGC and e IRC Scientific and Technical Committee. Achieved young women scientist award by MPCOST. Published many Indian & UK patents, copyrights, many research and review papers, books and book chapters. She Invited as plenary talks at conferences and seminars national level, and as a Session chair on many International Conference organize by Kryvyi Rih National University, Ukraine Europe. Designated as state Madhya Pradesh Coordinator in International conference collaborated by RCS. Coordinator of two Professional Student Chapter in collaboration with Agriculture Development society and research Culture Society. her enthusiastic participation in research and academia. She is participating on several advisory panels, scientific societies, and governmental committees. Participant in several worldwide professional research associations; member of esteemed, peer-reviewed publications' editorial boards and review panels. Many Ph.D., PG, and UG students have benefited from her guidance, and these supervisions continue.

Dr. Ajeet singh Nain

Working as Professor in GBPUA&T, Pantnagar-263145, US Nagar, UK, India.

Dr. Salvinder Singh

Presently working as Associate Professor in the Department of Agricultural Biotechnology in Assam Agricultural University, Jorhat, Assam.

Dr. Salvinder received MacKnight Foundation Fellowship for pre-doc training at WSU, USA – January 2000-March 2002 and DBT overseas Associateship for Post-Doc at WSU, USA – April, 2012 to October, 2012.

Dr. V K Joshi

Professor V.K.Joshi is M.Sc., Ph.D. (Microbiology) from Punjab Agricultural University, Ludhiana and Guru Nanak Dev University, Amritsar, respectively with more than 35 years experience in Fruit Fermentation Technology, Indigenous fermented foods, patulin ,biocolour ,Quality Control and Waste Utilization. Presently, heading the dept. of Food Science and Technology in University of Horticulture and Forestry, Nauni-Solan (HP), India.

Dr. Mahendra Singh Pal

Presently working as Professor in the dept. of Agronomy in G. B. Pant University o Agriculture & Technology, Pantnagar-263145 (Uttarakhand).

Dr. Sanjoy Kumar Bordolui

M.Sc. (Ag.), PhD, FSTA, FSIESRP, Assistant Professor, Department of Seed Science and Technology, Bidhan Chandra Krishi Viswavidyalaya, Mohanpur, Nadia. W.B., India. He received CWSS Young Scientist Award-2016, conferred by Crop and Weed Science Society, received Best Young Faculty Award 2019 conferred by Novel Research Academy, received Innovative Research & Dedicated Teaching Professional Award 2020 conferred by Society of Innovative Educationalist & Scientific Research Professional, Chennai.

Dr.Chiti Agarwal

Dr. Chiti Agarwal works as a postdoctoral associate at the University of Maryland in College Park, Maryland, USA. Her research focuses on fungicide resistance to fungal diseases that affect small fruits such as strawberries. She graduated from North Dakota State University in Fargo, North Dakota, with a B.S. in biotechnology and an M.S. in plant sciences. Dr. Agarwal completed her doctorate in Plant Pathology while working as a research and teaching assistant. During her time as a graduate research assistant, she learned about plant breeding, molecular genetics, quantitative trait locus mapping, genome-wide association analysis, and marker-assisted selection. She wants to engage with researchers from many fields and have a beneficial impact on a larger audience.

DR. Owais Yousuf

Presently working as Assistant professor in the Department of Bioengineering, Integral University-Lucknow, Uttar Pradesh, India.

Dr. Vijay A. Patil

Working as Assistant Research Scientist in Main Rice Research Centre, Navsari Agricultural University, Navsari. Gujarat- 396 450 (India).

Dr. Amit Kumar Maurya

Working asJunior Research Assistantin the Department of Plant Pathology at Sam Higginbottom University of Agriculture, Technology and Sciences, Prayagraj, U.P. India.

Prof. Salil Kumar Tewari

Presently working as Professor in College of Agriculture and Joint Director, Agroforestry Research Centre (AFRC) / Program Coordinator in G.B. Pant University of Agric. & Tech., Pantnagar - 263 145, Uttarakhand (INDIA).

Dr. S. K. Jain

Presently working as Officer Incharge of All India Coordinated Sorghum Improvement Project, S. D. Agricultural University, Deesa, Gujarat.

Dr. Deshmukh Amol Jagannath

Presently working as Assistant Professor in Dept. of Plant Pathology, College of Agriculture polytechnic, NAU, Waghai.

Mr. Anil Kumar

Working as Junior Research Officer/Asstt. Prof. in the dept. of Food Science & Technology in Agriculture & Technology, Pantnagar.

Mr. Jiban Shrestha

Scientist (Plant Breeding & Genetics)

Presently working as Scientist (Plant Breeding and Genetics) at National Maize Research Programme (NMRP), Rampur, Chitwan under Nepal Agricultural Research Council (NARC), Singhdarbar Plaza, Kathmandu, Nepal.

Mr. Aklilu Bajigo Madalcho

Working at Jigjiga University, Ethiopia, as lecturer and researcher at the College of Dry land Agriculture, department of Natural Resources Management.

Mr. Isaac Newton ATIVOR

MPhil. in Entomology, from University of Ghana.

He has extensive knowledge in tree fruit orchard pest management to evaluate insecticides and other control strategies such as use of pheromone traps and biological control to manage insect pests of horticultural crops. He has knowledge in agronomy, plant pathology and other areas in Agriculture which I can use to support any research from production to marketing.

Mr. Bimal Bahadur Kunwar

He received his Master Degree in Botany from Central Department of Botany, T.U., Kirtipur, Nepal. Currently working as consultant to prepare CCA-DRR Plan for Hariyo Ban Program/CARE in Nepal/GONESA.

Table of Contents

Volume-12, Issue-4, April 2026

International Journal of Environmental & Agriculture Research (IJOEAR)
ISSN: [2454-1850]
[Vol-12, Issue-4, April- 2026]
Website: www.ijoear.com
Journal DOI: 10.25125/agriculture-journal

Management Strategy against Invasive *Leucoptera malifoliella* (Lepidoptera: Lyonetiidae) on Apple (Malus domestica) in Kashmir Himalayas

Sheikh Khursheed[1*]; Abu Manzar[2]; Baseerat Ul Ann[3]; Shugufta Parveen[4]; Muzafar Mir[5]; Bilal Ahmad Pandit[6]; Hamidullah Itoo[7]

[1,3,4,7]Ambri Apple Research Centre, Shopian, Faculty of Horticulture, Shalimar, Sher-e-Kashmir University of Agricultural Sciences and Technology of Kashmir, Srinagar, 192303, India
[2]Division of Entomology, Faculty of Horticulture, Shalimar, Sher-e-Kashmir University of Agricultural Sciences and Technology of Kashmir, Srinagar, 190025, India
[5]KVK, Poonch, Sher-e-Kashmir University of Agricultural Sciences and Technology of Jammu-185101, India
[6]KVK, Shopian, Sher-e-Kashmir University of Agricultural Sciences and Technology of Kashmir, Srinagar, 192303, India
*Corresponding Author

Received:- 04 March 2026/ Revised:- 28 March 2026/ Accepted:- 05 April 2026/ Published: 30-04-2026

Abstract— *The proliferation of invasive insect pests is often facilitated by favorable environmental conditions, abundant host availability, and the absence of natural enemies. Leucoptera malifoliella (Lepidoptera: Lyonetiidae), commonly known as the apple blotch leaf miner, was first reported in India in 2021, causing significant damage to apple orchards in Kashmir. Given its potential threat to the regional apple industry, a two-year field study (2022–2023) was conducted to assess the efficacy of seven insecticidal treatments. Results demonstrated that Thiamethoxam 12.6% + Lambda-Cyhalothrin 9.5% ZC and Quinalphos 25EC + Thiamethoxam 25WG were highly effective in reducing leaf infestation (1.0–6.0% and 3.0–8.33%) and live larval populations (1.0–2.33 and 1.33–2.67 larvae per 20 infested leaves) compared to untreated controls (up to 92.0% infestation and 21 larvae per 20 infested leaves). Similar trends were observed in 2023. The enhanced efficacy of neonicotinoid-containing combinations is attributed to their systemic/translaminar activity and complementary modes of action. These findings suggest that insecticide combinations, particularly those incorporating neonicotinoids, offer promising options for managing L. malifoliella in apple orchards in Kashmir.*

Keywords— Leucoptera malifoliella; apple; management; insecticides; efficacy.

I. INTRODUCTION

Apple (*Malus domestica* Borkh.) is one of the oldest cultivated fruit crops and remains a cornerstone of temperate fruit production worldwide. Globally, it ranks as the fourth most consumed fruit after oranges, bananas, and grapes (Forsline et al., 2010). Its widespread cultivation in temperate regions is attributed to its economic importance, nutritional value, and diverse cultivars (Musacchi and Serra, 2018). In India, the apple industry plays a pivotal role in the agricultural economy, particularly in the Kashmir Valley, which contributes over 75% of the nation's apple production (Rather and Buhroo, 2015). Apples in Kashmir are renowned for their unique taste, crispness, and quality, making them highly sought after in domestic and international markets. According to the Directorate of Horticulture (2021), apple cultivation spans approximately 160,000 hectares in the Valley, producing nearly 180,000 metric tonnes annually, with a significant portion exported globally. Despite its vast area under cultivation, apple productivity in Kashmir remains below global standards. This gap is largely due to suboptimal orchard management practices, lack of high density planting systems, and the recurring impact of insect pests and diseases. Among the biotic constraints, insect pests have emerged as major limiting factors affecting yield

and fruit quality. While many insect species are associated with apple trees, only a few reach economically damaging levels that warrant urgent and sustained management interventions.

A recent and alarming addition to this pest complex is the apple leaf blotch miner, *Leucoptera malifoliella* (Lepidoptera: Lyonetiidae). This invasive species, previously unreported in India, was first detected in Kashmir in 2021. It is suspected that the pest entered the region through the import of infested apple planting material. Since its introduction, *L. malifoliella* has exhibited rapid population growth across the apple-producing areas of South Kashmir, attaining the status of a major pest by 2023. Growers have reported significant economic losses due to premature defoliation and reduced fruit yield and quality.

L. malifoliella is a typical phytophagous pest that completes up to four overlapping generations per year under the temperate conditions of Kashmir. The larvae mine the upper surface of apple leaves, feeding on mesophyll tissue while leaving the epidermis intact. These solitary miners produce circular blotch mines that evolve from small whitish lesions into larger brown patches with characteristic concentric frass rings. Though fruits are not directly attacked, severe infestations exceeding 40 mines per leaf can cause premature defoliation by August or early September (Baufeld and Freier, 1991). This defoliation compromises the photosynthetic capacity of the tree, weakens bud differentiation, and adversely affects fruit size and quality (Subic, 2015).

Feeding by *L. malifoliella* larvae also induces significant biochemical and physiological stress in host plants. Such stress often manifests as a reduction in chlorophyll content, disruption of photosynthetic pathways, and altered plant defense responses (Gomez et al., 2004; Golawska et al., 2010). Chlorophyll plays a central role in plant-insect interactions, and its decline due to herbivory can severely impair plant growth and productivity (Sammour et al., 2018; Biondi et al., 2018). In addition, the pest pupates on fruit surfaces, and the presence of visible silken cocoons further lowers the commercial value of the produce and creates export-related quarantine challenges. Because of the small size and cryptic behavior of this pest, initial infestations often go unnoticed until significant damage occurs (Rovesti and Deseö, 1991).

The rapid spread and establishment of *L. malifoliella* in Kashmir are attributed in part to the absence of natural enemies. No natural enemies of *L. malifoliella* have been reported in India so far. Invasive insect species frequently experience ecological release in new environments due to the lack of native predators, parasitoids, or pathogens. This facilitates their unchecked proliferation and makes them especially difficult to manage (Kenis et al., 2009). Given the absence of natural enemies, the use of insecticides is currently regarded as the conventional and most practical method for managing leaf miner infestations (Guedes et al., 2016). While chemical control is often criticized for its ecological implications, it remains the primary line of defense in the early stages of invasive pest outbreaks. However, selecting the appropriate insecticides is critical to achieving effective control while minimizing resistance development, environmental contamination, and non-target effects. Hence, identifying efficacious and safe insecticidal options is vital for integration into future Integrated Pest Management (IPM) frameworks.

Given the recency of *L. malifoliella's* introduction in India and the lack of documented control strategies, this study was undertaken to evaluate the field efficacy of seven insecticides, each representing different chemical groups and modes of action, against *L. malifoliella* in Kashmir. Field trials conducted over two consecutive years aimed to determine the most promising options for managing this invasive pest and reducing the economic burden on apple growers. The findings are expected to provide a foundational basis for developing science-based control strategies and contribute to safeguarding apple production in the temperate regions of India.

II. MATERIALS AND METHODS

2.1 Study Site and Orchard Selection

The study was conducted from May 2022 to October 2023 in a commercial apple (*Malus domestica* cv. Red Delicious) orchard located at Bapora, Zainapora village in District Shopian, Jammu and Kashmir, India. The site was selected based on its status as a hotspot for the apple blotch leaf miner, *Leucoptera malifoliella*. The orchard is situated at an elevation of 1,594 meters above mean sea level (33°77′N latitude, 75°01′E longitude). The experimental plot consisted of Red Delicious trees spaced 5.49 meters apart both within and between rows, with an average planting density of 250 trees per hectare.

2.2 Experimental Design and Trial Layout

The experiment was laid out in a Randomized Block Design (RBD) with three replications per treatment. Each replication consisted of a single tree, resulting in a total of 24 trees in the trial. To prevent cross-contamination from spray drift, buffer rows were maintained between treatment blocks. Three trees were designated as untreated controls and received only water

sprays. All trees selected for experimentation were labeled and marked with red paint one week prior to treatment application.

Two foliar spray applications were conducted per season: the first at the third fruit developmental stage and the second at the fourth fruit developmental stage. Sprays were applied using a petrol-operated Honda Power Sprayer equipped with an Aspee HTP pump (30 L capacity) and a hollow-cone nozzle to ensure even coverage, including the undersides of leaves and trunks, as recommended by Khursheed and Raj (2013). Prior to bud break, one application of dormant horticultural mineral oil was applied uniformly across the orchard to control San Jose scale and European red mite. Other cultural practices, including fertilization, pruning, and irrigation, were carried out according to standard guidelines for temperate apple cultivation.

2.3 Insecticidal Treatments and Application

Seven insecticidal treatments were evaluated for their efficacy against *L. malifoliella*. The insecticides tested included:

- Chlorpyrifos 50EC + Cypermethrin 5EC
- Thiamethoxam 12.6% + Lambda-Cyhalothrin 9.5% ZC
- Thiamethoxam 25WG
- Quinalphos 25EC + Thiamethoxam 25WG
- Thiacloprid 21.7 SC
- Quinalphos 25EC + Thiacloprid 21.7 SC
- Quinalphos 25EC

Commercial formulations of each insecticide were prepared using clean running water and applied at field-recommended concentrations as per the label. Applications were conducted in the morning between 15 °C and 25 °C ambient temperature to minimize volatilization and maximize coverage. All treatments were repeated in both 2022 and 2023 seasons.

In addition to chemical control, the following physical and cultural practices were implemented uniformly across the orchard: complete orchard sanitation in November (removal and destruction of fallen leaves, pruned branches, and fruits), mechanical grass cutting with a brush cutter in June and August, and burlapping and brushing to remove pupae from tree trunks.

2.4 Data Collection and Observations

Leaf Infestation: Post-treatment assessment of leaf infestation was carried out at 10, 20, 30, and 40 days after each spray. From each treated tree, 100 leaves were randomly sampled, totaling 300 leaves per treatment. The percentage of infested leaves was calculated using the formula:

Leaf infestation (%) = (Number of leaves infested / Total number of leaves selected) × 100

Larval Population: Live larval counts were also recorded on the same schedule. Ten infested leaves were randomly collected from each treated tree (30 leaves per treatment). The upper epidermis of each mined leaf was carefully dissected using a needle, and larvae were extracted with a fine camel hair brush. Each larva was then gently pressed with the brush; individuals failing to respond were considered dead. Only live larvae were recorded for efficacy evaluation.

2.5 Statistical Analysis

Each treatment was replicated three times, and the entire experiment was conducted over two consecutive years. The data were analyzed separately for 2022 and 2023 using SPSS version 16.0. Percentage values were transformed (using the arcsine square root) before analysis of variance (ANOVA) to normalize the data. Mean comparisons were made using Duncan's Multiple Range Test (DMRT) at a significance level of $P \leq 0.05$. Averages of observations across all intervals were used for statistical analysis, and the results were interpreted accordingly.

III. RESULTS

The results from this two-year field study provide clear evidence of the efficacy of various insecticidal treatments in reducing both leaf infestation and larval populations of *Leucoptera malifoliella* in apple orchards. All insecticidal treatments performed significantly better than the untreated control in minimizing pest incidence.

3.1 Year 2022

Following two foliar spray applications, all tested insecticides led to a significant reduction in leaf infestation at 10, 20, 30, and 40 days after each application when compared to the untreated check. Among the treatments, Thiamethoxam 12.6% + Lambda-cyhalothrin 9.5% ZC and Quinalphos 25EC + Thiamethoxam 25WG were the most effective.

Thiamethoxam + Lambda-cyhalothrin consistently showed the lowest leaf infestation rates, ranging from 1.00% to 6.00%, with the minimum recorded 20 days after the second spray. Quinalphos + Thiamethoxam also performed well, with infestation levels between 3.00% and 6.33%, showing best results at 40 days post-first spray. Quinalphos 25EC + Thiacloprid 21.7 SC showed moderate efficacy, with infestations ranging from 5.00% to 15.67%, particularly effective 10 days after the first spray. In contrast, Quinalphos 25EC applied alone was the least effective, with infestation levels ranging from 14.33% to 71.00%, while the untreated control exhibited infestation levels from 21.33% to 91.00% (Table 1).

TABLE 1

EFFICACY OF DIFFERENT INSECTICIDES AGAINST LEAF MINER ON APPLE AT BAPORA ZAINAPORA DURING 2022

Treatments	Dosage (ml/liter of water)	Percent Leaf infestation*							
		10DA1S	20DA1S	30DA1S	40DA1S	10DA2S	20DA2S	30DA2S	40DA2S
Chlorpyrifos 50EC + Cypermethrin 5EC	1.25	6.00 (14.14)	8.67 (16.99)	15.00 (22.75)	27.67 (31.66)	35.67 (36.63)	34.67 (36.05)	43.00 (40.96)	45.33 (42.29)
Thiamethoxam 12.6% + Lambda-Cyhalothrin 9.5% ZC	0.5	1.00 (4.62)	1.33 (6.53)	2.67 (9.36)	2.00 (6.55)	4.00 (11.47)	3.33 (10.34)	5.00 (12.87)	6.00 (14.14)
Thiamethoxam 25WG	0.5	7.00 (15.31)	6.00 (14.14)	10.67 (19.02)	19.00 (25.81)	30.00 (33.15)	28.33 (32.12)	28.67 (32.35)	33.33 (35.24)
Quinalphos 25EC + Thiamethoxam 25WG	1ml + 0.2g	3.00 (9.88)	2.33 (8.74)	2.00 (7.94)	3.33 (6.73)	7.67 (16.02)	7.00 (15.31)	7.00 (15.23)	8.33 (16.50)
Thiacloprid 21.7 SC	0.6	8.00 (16.40)	8.00 (16.29)	10.67 (19.02)	15.67 (23.22)	25.00 (29.98)	28.67 (32.35)	30.67 (33.59)	38.67 (38.42)
Quinalphos 25EC + Thiacloprid 21.7 SC	1 + 0.4	5.00 (12.87)	6.00 (14.14)	7.00 (15.31)	8.67 (17.11)	11.67 (19.89)	11.00 (19.27)	13.67 (21.63)	15.67 (23.28)
Quinalphos 25EC	1.25	14.33 (22.16)	30.33 (33.39)	37.33 (37.63)	42.67 (40.76)	61.00 (51.37)	64.67 (53.55)	65.00 (53.76)	71.00 (57.44)
Control (water)	—	21.33 (27.45)	36.00 (36.80)	55.00 (47.86)	69.33 (56.55)	82.33 (65.46)	87.67 (69.93)	91.33 (72.97)	92.00 (77.56)
CD (P=0.05)		3.48	4.69	3.79	6.28	7.87	6.92	5.41	9.08

Figures in parentheses are arc sine transformed values

DA1S = days after 1st spray; DA2S = days after 2nd spray

Correspondingly, all treatments significantly reduced larval populations compared to the control. The mean number of live larvae per 20 infested leaves across treatments ranged from 1.00 to 12.33, with the lowest larval counts recorded in plots treated with Thiamethoxam + Lambda-cyhalothrin (1.00–2.33 larvae) and Quinalphos + Thiamethoxam (1.33–2.67 larvae). Moderate control was observed with Quinalphos + Thiacloprid (2.33–4.00 larvae), while the highest larval populations were recorded in trees treated with Quinalphos alone (8.00–12.33 larvae) and the untreated control (11.67–21.00 larvae) (Table 2).

TABLE 2

EFFICACY OF DIFFERENT INSECTICIDES AGAINST LEAF MINER ON APPLE AT BAPORA ZAINAPORA DURING 2022

Treatments	Dosage (ml/liter of water)	Mean number of live larvae/20 infested leaves*							
		10DA1S	20DA1S	30DA1S	40DA1S	10DA2S	20DA2S	30DA2S	40DA2S
Chlorpyrifos 50EC + Cypermethrin 5EC	1.25	4.33 (2.29)	6.33 (2.70)	8.67 (3.10)	10.33 (3.36)	5.33 (2.50)	6.33 (2.70)	10.67 (3.41)	11.33 (3.51)
Thiamethoxam 12.6% + Lambda-Cyhalothrin 9.5% ZC	0.5	1.00 (1.38)	1.33 (1.52)	2.00 (1.71)	3.33 (2.06)	1.00 (1.38)	1.67 (1.63)	3.33 (2.06)	2.33 (1.82)
Thiamethoxam 25WG	0.5	4.67 (2.35)	4.67 (2.36)	7.33 (2.88)	9.00 (3.16)	5.00 (2.44)	4.00 (2.23)	4.33 (2.29)	5.33 (2.50)
Quinalphos 25EC + Thiamethoxam 25WG	1ml + 0.2g	1.33 (1.52)	2.33 (1.82)	3.33 (2.06)	4.33 (2.28)	4.67 (2.36)	2.33 (1.82)	2.67 (1.90)	2.67 (1.91)
Thiacloprid 21.7 SC	0.6	4.00 (2.23)	6.00 (2.64)	9.33 (3.21)	10.33 (3.36)	7.67 (2.94)	7.00 (2.82)	9.33 (3.21)	9.00 (3.16)
Quinalphos 25EC + Thiacloprid 21.7 SC	1 + 0.4	5.67 (2.57)	6.33 (2.69)	6.67 (2.76)	6.67 (2.74)	5.33 (2.50)	4.00 (2.23)	4.67 (2.36)	4.33 (2.31)
Quinalphos 25EC	1.25	8.00 (3.00)	10.00 (3.31)	14.00 (3.87)	15.67 (4.08)	11.33 (3.51)	11.00 (3.46)	11.33 (3.51)	12.33 (3.64)
Control (water)	—	11.67 (3.55)	12.33 (3.65)	19.33 (4.51)	21.00 (4.69)	17.33 (4.28)	16.33 (4.16)	18.00 (4.35)	21.00 (4.69)
CD (P=0.05)		2.27	2.2	2.56	3.29	2.05	2.02	2.78	2.53

Figures in parentheses are square root transformed values

DA1S = days after 1st spray; DA2S = days after 2nd spray

3.2 Year 2023

Field evaluations repeated in 2023 confirmed the trends observed in the previous year. All insecticidal treatments significantly outperformed the untreated control. Leaf infestation percentages across treatments ranged from 0.00% to 68.00%, compared to 7.30% to 83.00% in the control (Table 3).

TABLE 3

EFFICACY OF DIFFERENT INSECTICIDES AGAINST LEAF MINER ON APPLE AT BAPORA ZAINAPORA DURING 2023

Treatments	Dosage (ml/liter of water)	Percent Leaf infestation*							
		10DA1S	20DA1S	30DA1S	40DA1S	10DA2S	20DA2S	30DA2S	40DA2S
Chlorpyrifos 50EC + Cypermethrin 5EC	1.25	1.00 (4.62)	6.00 (14.14)	14.33 (22.16)	24.00 (29.30)	32.00 (34.42)	43.00 (40.95)	55.00 (47.86)	57.67 (49.39)
Thiamethoxam 12.6% + Lambda-Cyhalothrin 9.5% ZC	0.5	0.33 (1.91)	0.67 (3.82)	0.67 (3.82)	1.00 (4.62)	0.67 (3.82)	1.00 (5.74)	2.33 (8.46)	3.33 (10.34)
Thiamethoxam 25WG	0.5	0.33 (1.91)	2.67 (9.26)	8.67 (17.07)	13.00 (21.09)	20.33 (26.75)	23.67 (29.07)	29.67 (32.97)	34.00 (35.62)
Quinalphos 25EC + Thiamethoxam 25WG	1ml + 0.2g	0.00 (0.00)	1.00 (4.62)	0.67 (3.82)	2.00 (7.94)	2.00 (7.94)	2.00 (7.94)	3.00 (9.88)	5.33 (13.26)
Thiacloprid 21.7 SC	0.6	1.33 (6.53)	4.33 (11.99)	7.33 (15.65)	14.00 (21.86)	25.00 (29.98)	35.67 (36.63)	42.33 (40.56)	45.33 (42.30)
Quinalphos 25EC + Thiacloprid 21.7 SC	1 + 0.4	0.33 (1.91)	2.00 (7.94)	5.33 (13.26)					

Figures in the parentheses are arc sine transformed values

DA1S=days after 1st spray; DA2S=days after 2nd spray

The most effective treatment was again Thiamethoxam 12.6% + Lambda-cyhalothrin 9.5% ZC, which showed leaf infestation rates of 0.33% to 3.33%. This was closely followed by Quinalphos 25EC + Thiamethoxam 25WG, which achieved 0.00% to 5.33% infestation. Both treatments exhibited maximum effectiveness 10 days after the first spray. In contrast, Quinalphos 25EC + Thiacloprid 21.7 SC showed a broader infestation range (0.33% to 29.00%) and was statistically less effective than the aforementioned treatments. Single applications of Quinalphos 25EC or Thiacloprid 21.7 SC were considerably less effective, with consistently higher infestation levels.

Live larval counts followed a similar pattern. The lowest larval densities were recorded in plots treated with Quinalphos 25EC + Thiamethoxam 25WG (2.00–2.67 larvae per 20 infested leaves), followed by Thiamethoxam + Lambda-cyhalothrin (2.33–3.00 larvae) and Quinalphos + Thiacloprid (3.33–6.00 larvae). The untreated control exhibited the highest larval counts, ranging from 15.00 to 24.00 larvae per 20 leaves (Table 4).

TABLE 4

EFFICACY OF DIFFERENT INSECTICIDES AGAINST LEAF MINER ON APPLE AT BAPORA ZAINAPORA DURING 2023

Treatments	Dosage (ml/liter of water)	Mean number of live larvae/20 infested leaves							
		10DA1S	20DA1S	30 DA1S	40DA1S	10DA2S	20DA2S	30DA2S	40DA2S
Cholorpyriphos 50EC + Cypermethrin 5EC	1.25	9.00 (3.15)	9.00 ((3.14)	13.00 (3.73)	16.67 (4.20)	11.33 (3.50)	11.67 (3.54)	11.33 (3.50)	12.00 (3.60)
Thiamethoxam 12.6% + Lambda-Cyhalothrin 9.5% ZC	0.5	2.33 (1.82)	2.33 (1.79)	2.00 (1.71)	1.67 (1.63)	1.00 (1.38)	2.00 (1.71)	3.00 (1.99)	3.00 (1.99)
Thiamethoxam 25Wg	0.5	5.00 (2.44)	7.00 (2.81)	9.33 (3.20)	11.00 (3.46)	6.33 (2.70)	7.33 (2.88)	10.67 (3.41)	8.00 (2.99)
Quinalphos 25EC+ Thiamethoxam 25Wg	1ml + 0.2g	2.00 (1.71)	3.00 (1.99)	3.00 (1.99)	3.00 (1.99)	2.33 (1.79)	3.00 (1.99)	3.00 (1.99)	2.67 (1.91)
Thiocloprid 21.7 SC	0.6	7.67 (2.94)	6.33 (2.70)	11.00 (3.46)	11.67 (3.55)	11.67 (3.55)	14.00 (3.87)	9.67 (3.26)	6.00 (3.15)
Quinalphos 25EC + Thiocloprid 21.7 SC	1 + 0.4ml	6.00 (2.64)	5.33 (2.50)	4.33 (2.29)	3.33 (2.06)	3.33 (2.06)	5.00 (2.44)	4.00 (2.23)	3.33 (2.08)
Quinalphos 25EC	1.25	12.00 (3.60)	16.00 (4.11)	17.33 (4.26)	21.67 (4.76)	15.00 (3.98)	17.33 (4.26)	15.67 (4.08)	13.67 (3.82)
Control	water	15.00 (3.99)	20.00 (4.57)	24.67 (5.06)	29.33 (5.50)	23.67 (4.96)	22.67 (4.86)	20.33 (4.61)	24.00 (4.99)
CD (P=0.05)		**2.39**	**4.00**	**4.29**	**3.63**	**3.78**	**3.89**	**3.51**	**3.08**

Figures in the parentheses are square root transformed values

DA1S=days after 1st spray; DA2S=days after 2nd spray

3.3 Overall Performance and Comparative Analysis

When comparing data across both years, three treatments—Thiamethoxam 12.6% + Lambda-cyhalothrin 9.5% ZC, Quinalphos 25EC + Thiamethoxam 25WG, and Quinalphos 25EC + Thiacloprid 21.7 SC—consistently demonstrated the highest efficacy. These treatments significantly reduced both leaf infestation and larval populations over multiple observation intervals. Among them, the Thiamethoxam + Lambda-cyhalothrin combination proved to be the most consistent and effective across all parameters. Conversely, individual applications of Quinalphos 25EC or Thiacloprid 21.7 SC offered limited protection and resulted in higher infestation and larval counts, highlighting the advantage of using combination formulations for managing *L. malifoliella*.

IV. DISCUSSION

Apples play a crucial role in Kashmir's agricultural landscape, serving as a commercially significant fruit crop and contributing approximately 65% of India's total apple production (Khursheed et al., 2024). The recent emergence of the invasive pest *Leucoptera malifoliella* has understandably raised serious concerns among apple producers. In this context, the dissemination of reliable and up-to-date information on the efficacy of available insecticides is imperative. When no other effective or economically viable options exist, pesticides become essential tools for managing invasive species.

In the present two-year field study, data revealed that leaf infestation by the apple blotch leaf miner was significantly reduced at 10 and 20 days after both spray intervals when treated with thiamethoxam 12.6% + lambda-cyhalothrin 9.5% ZC, quinalphos 25EC + thiamethoxam 25WG, and quinalphos 25EC + thiacloprid 21.7 SC, compared with untreated control trees. The same treatments consistently maintained lower larval populations and leaf infestation at 10, 20, 30, and 40 days post-treatment.

Among the evaluated insecticides, chlorpyrifos 50EC + cypermethrin 5EC and quinalphos 25EC (used individually) consistently showed high levels of leaf infestation and larval populations throughout the observation period. All insecticides, when used in combination (except chlorpyrifos + cypermethrin), demonstrated high efficacy against *L. malifoliella*. The

reduced performance of chlorpyrifos + cypermethrin may be due to their non-systemic and non-translaminar properties, which make them less effective against internal feeders like leaf miners. These insecticides primarily act on pests residing on the external surfaces of plant structures, rendering them inadequate for controlling pests that feed within leaf tissues.

Under the prevailing pest pressure and crop growth stages observed during the study, synthetic combination insecticides containing neonicotinoids provided the most satisfactory protection against the apple blotch leaf miner. Research supports the view that mixtures of two or more insecticides—especially those with differing or complementary modes of action—can yield additive or synergistic effects, even when used at low doses (Taillebois and Thany, 2016; Vidau et al., 2011; Yi et al., 2012). Commercial insecticide formulations that combine pyrethroids and neonicotinoids are frequently employed against pests resistant to pyrethroids. For example, mixtures such as cyhalothrin with thiamethoxam, cyfluthrin with imidacloprid, and bifenthrin with acetamiprid have demonstrated effective control of *Cimex lectularius* (Hemiptera: Cimicidae) (Wang et al., 2016).

The enhanced efficacy of such combinations can be explained by the complementary modes of action of neonicotinoids and pyrethroids. While pyrethroids target voltage-gated sodium channels and prolong their open state (Vais et al., 2000), neonicotinoids act as agonists at nicotinic acetylcholine receptors (nAChRs), causing overstimulation of the insect nervous system (Narahashi, 1992; Bodereau-Dubois et al., 2012). This neural overstimulation further facilitates pyrethroid binding by activating sodium channels, leading to lethal paralysis in insect pests. Literature strongly supports the use of such combinations, especially against pyrethroid-resistant populations.

Despite continuous oviposition and overlapping generations of *L. malifoliella*, which caused slight increases in infestation during the study, pest levels in treated plots remained significantly lower than in the control. The combined application of insecticides with distinct modes of action has gained widespread interest due to its potential to broaden the pest spectrum and mitigate resistance development (Daglish, 2008; Wakil et al., 2010; Athanassiou et al., 2013; Paudyal et al., 2017; Rumbos et al., 2018). Karanika et al. (2019) emphasized that combining insecticides with different toxicological mechanisms provides enhanced control efficacy compared to single compounds.

For instance, Athanassiou et al. (2013) demonstrated that a combination of betacyfluthrin and imidacloprid, which have entirely different mechanisms of action, significantly improved insecticidal activity, even in populations with known pyrethroid resistance. Similarly, in the present study, the combination of quinalphos (an organophosphate) and thiacloprid (a neonicotinoid) provided strong protection against the apple blotch leaf miner. When applied individually, both insecticides were considerably less effective. Their combination likely produced a synergistic effect: the organophosphate inhibits acetylcholinesterase, causing accumulation of acetylcholine at the synapse, while the neonicotinoid binds irreversibly to nAChRs, resulting in prolonged neural excitation (Taillebois and Thany, 2022). This interaction leads to severe overstimulation due to increased acetylcholine levels (Shao et al., 2013).

In this study, a slight resurgence in infestation and larval numbers was observed in neonicotinoid-treated trees later in the season. This slight resurgence likely reflects the emergence of new generations after the residual activity of the initial sprays began to decline, highlighting the need for careful timing of applications. However, the infestation remained low compared to untreated plots, suggesting that the long residual activity of neonicotinoids contributed to prolonged pest suppression. Previous studies have reported similar long-term effects. For instance, imidacloprid applied via irrigation maintained sufficient residue in grapevines throughout the growing season (Byrne and Toscano, 2006), and citrus trees treated with imidacloprid or thiamethoxam retained effective concentrations for up to five months (Castle et al., 2005). Likewise, a single application of thiamethoxam was shown to provide more than six months of protection in coffee plantations (de Souza et al., 2006).

In contrast, the mixture of chlorpyrifos and cypermethrin demonstrated poor efficacy against the apple blotch leaf miner, resulting in high leaf infestation and larval density even 10 days after application. This failure may be due to antagonistic interactions and potential resistance development from the frequent application of pyrethroids and organophosphates in fruit orchards. Such antagonism has previously been reported in several pest species, including *B. tabaci* from Pakistan (Ahmad, 2007), *Helicoverpa armigera* from Africa (Martin et al., 2003), and *Spodoptera littoralis* from Egypt (El-Guindy et al., 1983). However, in other species, synergistic effects of these combinations have also been observed—for instance in *B. tabaci* (Bryne and Devonshire, 1991), *Culex quinquefasciatus* (Corbel et al., 2004), *H. armigera* (Phokela et al., 1999; Ahmad, 2004), *Musca domestica* (Islam and Khalequzzaman, 2002), *Pectinophora gossypiella* (Keddis et al., 1986), *Plutella xylostella* (Attique et al., 2006), *Spodoptera litura* (Ahmad et al., 2009), *S. littoralis* (Ascher et al., 1986), and *Tetranychus*

urticae (Chapman and Penman, 1980). The current findings indicate that the toxicity of traditional pyrethroids and organophosphates could be enhanced when combined with novel insecticides such as thiamethoxam or thiacloprid.

Overall, the application of insecticides significantly reduced both leaf infestation and larval population during both growing seasons. A key factor in effective pest suppression was ensuring thorough spray coverage of the foliage. Two timely applications provided sufficient protection throughout the growing season, with noticeably lower infestation levels than untreated trees. While field scouting remains important to determine the need for intervention, this study offers valuable insights for managing *L. malifoliella* and supports broader pest management efforts in other regions.

V. CONCLUSION

Given the recent invasion of *L. malifoliella* in northern India, extensive chemical intervention has become necessary. Our findings provide evidence-based recommendations on the use of neonicotinoid and pyrethroid/organophosphate mixtures as effective chemical tools for leaf miner control. Specifically, Thiamethoxam 12.6% + Lambda-Cyhalothrin 9.5% ZC and Quinalphos 25EC + Thiamethoxam 25WG are recommended as the most effective treatments. Growers should rotate these combinations with other modes of action to delay resistance development and should base spray decisions on regular field scouting and economic thresholds.

However, long-term sustainability depends on an Integrated Pest Management (IPM) approach. A holistic strategy—including the use of natural enemies (once established), botanical compounds, semiochemicals, plant-based deterrents, burlapping, bark scraping, and rigorous orchard sanitation—will be essential to manage this pest in an ecologically sound and economically viable manner.

CONFLICT OF INTEREST

The authors declare that there is no conflict of interest regarding the publication of this research paper.

ACKNOWLEDGEMENTS

We extend our heartfelt appreciation to the university authorities for generously providing the essential facilities required to carry out the field trials. We are also immensely grateful to the field staff of AARC for their invaluable assistance in successfully conducting the field trials

REFERENCES

[1] Ahmad, M. (2004). Potentiation and antagonism of deltamethrin and cypermethrins with organophosphate insecticides in the cotton bollworm, *Helicoverpa armigera* (Lepidoptera: Noctuidae). *Pesticide Biochemistry and Physiology, 80*, 31–42.
[2] Ahmad, M. (2007). Potentiation and antagonism of pyrethroids with organophosphate insecticides in *Bemisia tabaci* (Homoptera: Aleyrodidae). *Journal of Economic Entomology, 100*, 886–893.
[3] Ahmad, M., Saleem, M. A., & Sayyed, A. H. (2009). Efficacy of insecticide mixtures against pyrethroid- and organophosphate-resistant populations of *Spodoptera litura* (Lepidoptera: Noctuidae). *Pest Management Science, 65*, 266–274.
[4] Ascher, K. R. S., Eliahu, M., Ishaaya, I., Zur, M., & Ben Moshe, E. (1986). Synergism of pyrethroid–organophosphorus insecticide mixtures in insects and their toxicity against *Spodoptera littoralis* larvae. *Phytoparasitica, 14*, 101–110.
[5] Athanassiou, C. G., Kavallieratos, N. G., Arthur, F. H., & Throne, J. E. (2013). Efficacy of a combination of beta-cyfluthrin and imidacloprid, and of beta-cyfluthrin alone, for control of stored-product insects on concrete. *Journal of Economic Entomology, 106*, 1064–1070.
[6] Attique, M. N. R., Khaliq, A., & Sayyed, A. H. (2006). Can resistance to insecticides in *Plutella xylostella* (Lepidoptera: Plutellidae) be overcome by insecticide mixtures? *Journal of Applied Entomology, 130*, 122–127.
[7] Baufeld, P., & Freier, B. (1991). Artificial injury experiments on the damaging effect of *Leucoptera malifoliella* on apple trees. *Entomologia Experimentalis et Applicata, 61*, 201–209.
[8] Biondi, A., Guedes, R. N. C., & Wan, F. (2018). Ecology, worldwide spread, and management of the invasive South American tomato pinworm, *Tuta absoluta*: Past, present, and future. *Annual Review of Entomology, 63*, 239–258. https://doi.org/10.1146/annurev-ento-031616-035524
[9] Bodereau Dubois, B., List, O., Calas List, D., Marques, O., Communal, P. Y., Thany, S. H., & Lapied, B. (2012). Transmembrane potential polarization, calcium influx, and receptor conformational state modulate the sensitivity of imidacloprid-insensitive neuronal insect nicotinic acetylcholine receptors to neonicotinoid insecticides. *Journal of Pharmacology and Experimental Therapeutics, 341*, 326–339. https://doi.org/10.1124/jpet.111.188060
[10] Byrne, F. J., & Devonshire, A. L. (1991). In vivo inhibition of esterase and acetylcholinesterase by profenofos treatment in the tobacco whitefly *Bemisia tabaci* (Genn.): Implications for routine biochemical monitoring. *Pesticide Biochemistry and Physiology, 40*, 198–204.
[11] Byrne, F. J., & Toscano, N. C. (2006). Uptake and persistence of imidacloprid in grapevines treated by chemigation. *Crop Protection, 25*, 831–834.

[12] Castle, S. J., Byrne, F. J., Bi, J. L., & Toscano, N. C. (2005). Spatial and temporal distribution of imidacloprid and thiamethoxam in citrus and impact on *Homalodisca coagulata* (Say) populations. *Pest Management Science, 61*, 75–84.
[13] Chapman, R. B., & Penman, D. R. (1980). The toxicity of mixtures of a pyrethroid with organophosphorus insecticides to *Tetranychus urticae* Koch. *Pesticide Science, 11*, 600–604.
[14] Corbel, V., Raymond, M., Chandre, F., Darriet, F., & Hougard, J. M. (2004). Efficacy of insecticide mixtures against larvae of *Culex quinquefasciatus* Say (Diptera: Culicidae) resistant to pyrethroids and carbamates. *Pest Management Science, 60*, 375–380.
[15] Daglish, G. J. (2008). Impact of resistance on the efficacy of binary combinations of spinosad, chlorpyrifos-methyl and s-methoprene against five stored grain beetles. *Journal of Stored Products Research, 44*, 71–76.
[16] de Souza, J. C., Reis, P. R., de Oliveira, R. L., & Junior, A. I. C. (2006). Eficiência de thiamethoxam no controle do bicho-mineiro do cafeeiro. II—Influência na época de aplicação via irrigação por gotejamento. *SBICafé*, Viçosa, Brazil.
[17] El Guindy, M. A., Rehman, A., El Refai, M., & Abdel Sattar, M. M. (1983). The joint action of mixtures of insecticides, or of insect growth regulators and insecticides, on susceptible and diflubenzuron resistant strains of *Spodoptera littoralis* Boisd. *Pesticide Science, 14*, 246–252.
[18] Forsline, P. L., Aldwinckle, H. S., Dickson, E. E., Luby, J. J., & Hokanson, S. C. (2010). Collection, maintenance, characterization, and utilization of wild apples of Central Asia. In J. Janick (Ed.), *Horticultural reviews*. John Wiley & Sons.
[19] Golawska, S., Krzyżanowski, R., & Łukasik, I. (2010). Relationship between aphid infestation and chlorophyll content in Fabaceae species. *Acta Biologica Cracoviensia Series Botanica, 52*(2), 76–80. https://doi.org/10.2478/v10182-010-0026-4
[20] Gomez, S. K., Oosterhuis, D. M., Rajguru, S. N., Johnson, D. R., & Gomez, S. (2004). Foliar antioxidant enzyme responses in cotton after aphid herbivory. *Journal of Cotton Science, 8*(2), 99–104.
[21] Guedes, R. N. C., Smagghe, G., Stark, J. D., & Desneux, N. (2016). Pesticide-induced stress in arthropod pests for optimized integrated pest management programs. *Annual Review of Entomology, 61*, 43–62.
[22] Islam, M. Z., & Khalequzzaman, M. (2002). Potentiation of malathion by other insecticides against adult housefly. *Pakistan Journal of Biological Sciences, 5*, 299–302.
[23] Karanika, C., Rumbos, C. I., Agrafioti, P., & Athanassiou, C. G. (2019). Insecticidal efficacy of a binary combination of cyphenothrin and prallethrin, applied as surface treatment against four major stored product insects. *Journal of Stored Products Research, 80*, 41–49.
[24] Keddis, M. E., Abdelsattar, M. M., Issa, Y. H., & El Guindy, M. A. (1986). The toxicity of certain insecticide mixtures to *Pectinophora gossypiella* Saund. *Bulletin of the Entomological Society of Egypt, 14*, 251–255.
[25] Kenis, M., Auger-Rozenberg, M.-A., Roques, A., Timms, L., Péré, C., Cock, M. J. W., Settele, J., Augustin, S., & Lopez-Vaamonde, C. (2009). Ecological effects of invasive alien insects. *Biological Invasions, 11*(1), 21–45. https://doi.org/10.1007/s10530-008-9318-y
[26] Khursheed, S., & Raj, D. (2013). Efficacy of insecticides and biopesticides against hadda beetle, *Henosepilachna vigintioctopunctata* (Fabricius) (Coleoptera: Coccinellidae) on bitter gourd. *Indian Journal of Entomology, 75*, 163–166.
[27] Khursheed, S., Bhat, Z. A., Mir, M., Rather, H. H., Itoo, H., Mir, M. A., Javeed, K., & Shah, R. A. (2024). Using bio pesticides to control the black-headed fireworm, *Rhopobota naevana* (Lepidoptera: Tortricidae), on apple, *Malus domestica*, in the mid hill Himalayas of Kashmir. *Journal of Eco-friendly Agriculture, 19*(1), 112–121. https://doi.org/10.48165/jefa.2024.19.01.20
[28] Martin, T., Ochou, O. G., Vaissayre, M., & Fournier, D. (2003). Organophosphorus insecticides synergise pyrethroids in the resistant strain of cotton bollworm, *Helicoverpa armigera* (Lepidoptera: Noctuidae) from West Africa. *Journal of Economic Entomology, 92*, 468–474.
[29] Musacchi, S., & Serra, S. (2018). Apple fruit quality: Overview of pre harvest factors. *Scientia Horticulturae, 234*, 409–430.
[30] Narahashi, T. (1992). Nerve membrane Na^+ channels as targets of insecticides. *Trends in Pharmacological Sciences, 13*, 236–241. https://doi.org/10.1016/0165-6147(92)90075-H
[31] Paudyal, S., Opit, G. P., Osekre, E. A., Arthur, F. H., Bingham, G. V., Payton, M. E., Danso, J. K., Manu, N., & Nsiah, E. P. (2017). Field evaluation of the long lasting treated storage bag, deltamethrin-incorporated (ZeroFly® Storage Bag), as a barrier to insect pest infestation. *Journal of Stored Products Research, 70*, 44–52.
[32] Phokela, A., Singh, S. P., & Mehrotra, K. N. (1999). Effect of synergists on pyrethroids toxicity in adults of *Helicoverpa armigera* (Hubner). *Pesticide Research Journal, 11*, 62–64.
[33] Rather, S., & Buhroo, A. A. (2015). Arrival sequence, abundance and host plant preference of the apple leaf miner *Lyonetia clerkella* Linn. (Lepidoptera: Lyonetiidae) in Kashmir. *Natural Sciences, 13*, 25–31.
[34] Rovesti, L., & Deseo, K. V. (1991). Effectiveness of neem seed kernel extract against *Leucoptera malifoliella* Costa (Lep., Lyonetiidae). *Journal of Applied Entomology, 111*, 231–236.
[35] Rumbos, C. I., Dutton, A. C., & Athanassiou, C. G. (2018). Insecticidal effect of spinetoram and thiamethoxam applied alone or in combination for the control of major stored product beetle species. *Journal of Stored Products Research, 75*, 56–63.
[36] Sammour, E. A., Kandil, M. A. H., Abdel Aziz, N. F., Agamy, E. A. M., El Bakry, A. M., & Abdelmaksoud, N. M. (2018). Field evaluation of new formulation types of essential oils against *Tuta absoluta* and their side effects on tomato plants. *Acta Scientific Agriculture, 2*(6), 15–22.
[37] Shao, X., Xia, S., Durkin, K. A., & Casida, J. E. (2013). Insect nicotinic receptor interactions in vivo with neonicotinoid, organophosphorus, and methylcarbamate insecticides and a synergist. *Proceedings of the National Academy of Sciences of the United States of America, 110*, 17273–17277. https://doi.org/10.1073/pnas.1316369110
[38] Subić, M. (2015). Mogućnosti i ogranicenja suzbijanja moljca kružnih mina (*Leucoptera malifoliella* Costa) (Lepidoptera: Lyonetiidae) u Međimurju. *Glasilo Biljne Zaštite, 15*, 195–206.
[39] Taillebois, E., & Thany, S. H. (2016). The differential effect of low dose mixtures of four pesticides on the pea aphid *Acyrthosiphon pisum*. *Insects, 7*(4), Article 53. https://doi.org/10.3390/insects7040053
[40] Taillebois, E., & Thany, S. H. (2022). The use of insecticide mixtures containing neonicotinoids as a strategy to limit insect pests: Efficiency and mode of action. *Pesticide Biochemistry and Physiology, 184*, Article 105126. https://doi.org/10.1016/j.pestbp.2022.105126
[41] Vais, H., Atkinson, S., Eldursi, N., Devonshire, A. L., Williamson, M. S., & Usherwood, P. N. R. (2000). A single amino acid change makes a rat neuronal sodium channel highly sensitive to pyrethroid insecticides. *FEBS Letters, 470*, 135–138.

[42] Vidau, C., Diogon, M., Aufauvre, J., Fontbonne, R., Viguès, B., Brunet, J. L., Texier, C., Biron, D. G., Blot, N., El Alaoui, H., Belzunces, L. P., & Delbac, F. (2011). Exposure to sublethal doses of fipronil and thiacloprid greatly increases mortality of honey bees previously infected by *Nosema ceranae*. *PLoS ONE, 6*(6), e21550. https://doi.org/10.1371/journal.pone.0021550

[43] Wakil, W., Ashfaq, M., Ghazanfar, M. U., & Riasat, T. (2010). Susceptibility of stored product insects to enhanced diatomaceous earth. *Journal of Stored Products Research, 46*, 248–249.

[44] Wang, C., Singh, N., Zha, C., & Cooper, R. (2016). Efficacy of selected insecticide sprays and aerosols against the common bed bug, *Cimex lectularius* (Hemiptera: Cimicidae). *Insects, 7*(1), Article 5. https://doi.org/10.3390/insects7010005

[45] Yi, F., Zou, C., Hu, Q., & Hu, M. (2012). The joint action of destruxins and botanical insecticides (rotenone, azadirachtin, and paeonolum) against the cotton aphid, *Aphis gossypii*. *Molecules, 17*(6), 7533–7543. https://doi.org/10.3390/molecules17067533.

International Journal of Environmental & Agriculture Research (IJOEAR)
ISSN: [2454-1850]
[Vol-12, Issue-4, April- 2026]
Website: www.ijoear.com
Journal DOI: 10.25125/agriculture-journal

Exploring the Molecular Variability of Diverse Black gram (*Vigna mungo* L. Hepper) Genotypes Using SSR Markers

Sudheer Naidu Balle[1*]; V. Roja[2]; D. Mohan Reddy[3]; B.V.Bhaskara Reddy[4]; B. Spandana[5]

[*1]Department of Molecular Biology and Biotechnology, Sri Venkateswara Agriculture College, Acharya N. G. Ranga Agricultural University, Andhra Pradesh, India.
[2]Department of Molecular Biology and Biotechnology, Regional Agricultural Research Station, Maruteru, Andhra Pradesh, India.
[3]Department of Genetics and Plant Breeding, Regional Agricultural Research Station, Lam, Guntur – 522034, Andhra Pradesh, India.
[4]Department of Plant Pathology, Agricultural Research Station, Kadiri – 515591, Andhra Pradesh, India.
[5]Department of Molecular Biology and Biotechnology, Agriculture College, Naira-532185, Andhra Pradesh, India
*Corresponding Author

Received:- 24 March 2026/ Revised:- 03 April 2026/ Accepted:- 12 April 2026/ Published: 30-04-2026

Abstract— *This investigation aimed to explore the molecular diversity of 117 black gram genotypes employing Simple Sequence Repeats (SSR) markers. Out of 43 SSR markers studied, 15 markers showed polymorphism. Polymorphic Information Content (PIC) values ranged from 0.4 to 0.7 with a mean of 0.6. A total of 52 alleles, ranging from three to four with a mean of 3.4 alleles per locus, were detected. Population structure analysis grouped the 117 genotypes into four sub-populations. UPGMA cluster analysis grouped the genotypes into three main clusters: Cluster I (51 genotypes), Cluster II (19 genotypes), and Cluster III (47 genotypes). Principal coordinate analysis indicated that the genotypes were distinctly separated from one another. The results of the unweighted neighbor-joining clustering tree and PCoA analysis were in close correspondence with the results of model-based STRUCTURE analysis. The findings provide valuable insights into the genetic diversity of black gram, which can assist plant breeders in developing improved cultivars.*

Keywords— Simple Sequence Repeats (SSR) Markers, Polymorphic Information Content, Genetic Diversity, Population Structure, Black gram.

I. INTRODUCTION

Black gram (Vigna mungo L. Hepper) is a short-duration, cleistogamous, self-pollinating, diploid species with a chromosome number (2n-2x-22) and a genomic size of 574 mega base pairs (Mbp). It is a member of the Leguminaceae family (Gupta et al., 2008). India is the world's largest user and producer of black gram. Black gram in India is cultivated extensively over an area of about 4.6 million hectares (Mha), with annual production and productivity of 24.5 lakh tonnes and 533 kg per hectare, respectively. In Andhra Pradesh, black gram is grown over an area of 3.93 lakh ha with 3.65 lakh tonnes production and 929 kg ha^{-1} productivity (2020-21) (www.agricoop.nic.in). According to El-Karamany (2006), most nutrients, including vitamins, minerals, and amino acids, are abundant in black gram, with proteins making up 25–26%, carbohydrates 60%, and fats 1.5%. It is high in vitamins A, B1, and B3, and contains trace amounts of riboflavin, niacin, and vitamin C.

As one of the most valued pulses in India and Pakistan, black gram is native to India and has been grown there since ancient times. Grown practically throughout India, this leguminous pulse has become the most renowned and is appropriately called the "king of the pulses." Asia, Pakistan, Myanmar, and other southern Asian nations are the main growing regions. Black gram is a member of the genus Vigna and the family Leguminaceae. There are only seven Vigna species that have been raised for their edible seeds: two African species of the subgenus Vigna, Vigna unguiculata (cowpea) and V. subterranea (the Bambara groundnut), and five Asian species of the subgenus Ceratotropis: Vigna mungo (black gram), Vigna radiata

(mungbean), Vigna aconitifolia (mothbean), Vigna angularis (adzuki bean), and Vigna umbellata (rice bean). Black gram belongs to the Asian Vigna group.

Black gram has been the subject of less investigation than cowpea and mung bean, particularly regarding molecular genetic diversity. It is essential to research and utilize the genetic variability of black gram in order to maximize its potential as a food and feed crop. Microsatellite or SSR markers are the preferred markers for molecular genetics research in crops due to their multi-allelic, co-dominant, and reliable characteristics. They are PCR-based, easy to score, and require only a tiny quantity of DNA for analysis. It is possible to employ SSR markers from related species. Although no SSR marker has been developed specifically from black gram, thousands of SSR markers have been developed in other Vigna crops, such as adzuki bean and cowpea.

SSR markers derived from cowpea and adzuki bean were utilized in the present study to investigate the genetic diversity and population structure of 117 diverse black gram accessions. The findings will provide valuable insights into domestication patterns and genetic diversity of black gram, which can assist plant breeders in developing enhanced cultivars.

II. MATERIALS AND METHODS

2.1 Genomic DNA Isolation

DNA was extracted from seedling leaves that were 20–25 days old using the Cetyltrimethylammonium bromide (CTAB) method (Murray and Thompson, 1980).

Stock solutions prepared for DNA extraction:

- **1M Tris Hydrochloric acid (HCl) (pH 8.0):** 30.285 g of Tris base was dissolved in distilled water, adjusted pH to 8.0 with HCl, and the final volume was brought to 250 mL.
- **0.5M Ethylenediaminetetraacetic acid (EDTA) (pH 8.0):** 46.53 g of EDTA was dissolved in distilled water, pH was adjusted to 8.0 with 4 g NaOH pellets, and made up to 250 mL.
- **5M Sodium chloride (NaCl):** 73.05 g of NaCl was dissolved in distilled water and made up to 250 mL.
- **1% Polyvinylpyrrolidone (PVP):** 1 g of PVP was dissolved in 100 mL of sterile distilled water.
- **2% CTAB:** 2 g of CTAB was dispersed in 100 mL of sterile distilled water.

The DNA extraction buffer (100 mL) was composed of 10 mL Tris HCl, 4 mL EDTA, 28 mL NaCl, 1 g PVP, and 2 g CTAB, supplemented with 50 µL β-Mercaptoethanol. Chloroform-isoamyl alcohol (24:1) and 70% ethanol were prepared for utilization in DNA extraction. RNase solution (25 mg) was prepared in 5 mL buffer (T10E1) and stored at -20°C for use.

Procedure for DNA isolation: 500 µl of extraction buffer was used to homogenize 2 g of fresh leaf samples. After adding another 300 µl of CTAB, the mixture was incubated for 45 minutes at 65°C. The supernatant was centrifuged again after being treated with chloroform-isoamyl alcohol (24:1). Ice-cold isopropanol was used to precipitate the DNA, which was then washed three times with 70% ethanol, allowed to air dry, and then dissolved in 100 µL of molecular biology-grade water.

DNA Quality and Quantity Estimation: The DNA purity and concentration were measured using a NanoDrop spectrophotometer (Jenway Genova Nano). A 260/280 ratio of 1.8-2.0 indicated DNA purity, while ratios closer to 2.0 suggested RNA contamination. DNA was diluted to 100 ng/µl for PCR reactions.

Agarose Gel Electrophoresis for DNA Quantification: For quality assessment, DNA samples were run in a 0.8% agarose gel in 1X Tris Acetate EDTA (TAE) buffer. The gels were stained with ethidium bromide, and bands were visible when exposed to ultraviolet (UV) light. By comparing the band intensity to a lambda DNA standard, the concentration of DNA was determined.

2.2 Genomic DNA Amplification by PCR Employing SSR Markers

Two µL of template DNA, 1 µL of each forward and reverse primer (10 pmol), 0.5 µl of dNTPs, 2 µL 10X buffer, 0.5 µL of $MgCl_2$, 0.1 µL of Taq polymerase, and 3.9 µL of molecular-grade water were used to set up PCR reactions (10 µL). Using an Eppendorf thermocycler, PCR amplification was performed as follows: 94°C for 5 minutes, followed by 35 cycles of denaturation at 94°C for 45 seconds, annealing at 55-60°C for 45 seconds, extension at 72°C for 1 minute, and final extension at 72°C for 7 minutes.

2.3 Agarose Gel Electrophoresis for SSR Marker Resolution

PCR products were electrophoresed at 100 V for one hour and 120 V for 30 minutes on 3% agarose gels prepared in 1X TAE buffer for SSR marker resolution. To confirm marker amplification, gels were stained with ethidium bromide and examined under a UV lamp.

2.4 Molecular Data Scoring

For every genotype and marker, marker allele data were created based on the presence or absence of bands and the size of the bands. These data were then sorted in various input formats (matrix form, HapMap format) for each genotype-marker pair.

2.5 Marker Polymorphism

The Polymorphic Information Content (PIC) for each marker was determined using the formula provided by Anderson et al. (1993) to estimate the markers' informativeness:

$$\mathbf{PIC = 1 - \Sigma(p_{ij})^2} \quad (1)$$

Where p_{ij} is the frequency of the jth allele for the ith marker, summed over n alleles. The calculation was based on the count of alleles per locus.

Using POPGENE (version 1.32) software, estimates of each polymorphic marker's utility information, number of alleles (Na*), number of effective alleles (Ne*), major allelic frequency (MAF), Shannon's information index (I*), Polymorphic Information Content (PIC), and genetic diversity index (Nei*) were made (Yeh et al., 1999).

2.6 Population Structure

As previously mentioned, 117 black gram genotypes were screened using SSR markers. The Q (population structure) model was utilized to report population structure and individual relatedness among 117 black gram genotypes to prevent any potential spurious relationships. The program STRUCTURE version 2.3.4 was employed to assess the genetic structure (Q) and cluster the population (Pritchard et al., 2000). The most likely K value for the examined data was determined using Structure Harvester version 0.6 and the Evanno et al. (2005) ΔK approach (Earl and Vonholdt, 2012). Following ten separate runs with a burn-in duration of 10,000 steps and 100,000 Monte Carlo Markov chain (MCMC) repeats, the optimal number of populations (K) was chosen. K = 1 to 10 was the range of genetic clusters. The posterior probability values (LnP(D) and ΔK) were employed to estimate the number of subpopulations (K).

2.7 Cluster Analysis

For dissimilarity analysis, the allelic data Excel file was fed into the DARwin (Dissimilarity Analysis and Representation) program version 6.0.12 (Perrier and Jacquemoud-Collet, 2006). Dissimilarity was computed using the allelic data as a simple matching dissimilarity index with a bootstrap value of 1000. To infer genetic links, the produced dissimilarity matrix was utilized to create a dendrogram using the Unweighted Pair Group Method with Arithmetic Means (UPGMA), which is based on the neighbor-joining approach.

2.8 Principal Coordinate Analysis (PCoA)

The first three components were utilized to represent the genotypes, and principal coordinate analysis was executed to highlight the resolving power. The dissimilarity matrix created with DARwin version 6.0 was used for PCoA.

III. RESULTS AND DISCUSSION

3.1 Genotyping of Black Gram Genotypes with Microsatellite Markers

A total of 117 black gram genotypes were screened using 43 SSR markers that were arbitrarily dispersed throughout the 11 chromosomes. Of these, 15 SSR markers (35.7%) were discovered to be polymorphic.

3.1.1 Allele Count at Each Locus

From 15 polymorphic microsatellite markers, 52 alleles were detected, ranging from three to four, with a mean of 3.4 alleles per locus. The markers CEDG 154, CEDG 116, CEDG 91, TWSSR 66, CEDG 180, CEDG 53, and CEDG 105 generated a maximum of four alleles, while CEDG 6, CEDG 97, CEDG 92, CEDG 44, CEDG 176, TWSSR 87, CEDG 128, and TWSSR 167 produced three alleles. In their analysis of genetic diversity in black gram using yellow mosaic virus-resistant SSR markers, Korattukudy et al. (2022) reported 60 alleles, with a mean of 4.2 alleles per locus and a range of two to seven alleles

per locus. Similarly, Mwangi et al. (2021) analysis of black gram genotypes revealed a total of 23 alleles from eight polymorphic SSR markers. The estimated genetic diversity within the genotypes being studied is depicted by this value. The average unique allele number for each marker was 2.8, with a range of 2 to 5. The number of alleles per locus for 15 polymorphic markers is represented in Table 1.

3.1.2 Effective Number of Alleles

The effective number of alleles is the count of equally frequent alleles needed to produce the same expected heterozygosity. The effective number of alleles should never exceed the observed number of alleles. The number of effective alleles in the current study ranged from 1.8 (CEDG 105) to 3.3 (CEDG 180), with a mean value of 2.6. CEDG 91 (3.2) and TWSSR 66 (3.3) displayed the greatest number of effective alleles, whilst CEDG 44 (2.1) and TWSSR 87 (2.1) displayed the fewest. The outcomes of the investigation regarding the count of effective alleles were higher than those of Korattukudy et al. (2022), who conducted an assessment of black gram genetic diversity analysis and reported a mean value of 2.4 with a range of 1.5 to 3.5. The effective number of alleles for 15 polymorphic markers is represented in Table 1.

3.1.3 Polymorphic Information Content (PIC)

PIC is a measure of diversity for SSR markers. PIC values assess a locus's discriminatory power by accounting for the extent of expressed alleles and their relative frequencies. With an average of 0.6, the PIC values of the 15 polymorphic markers varied from 0.4 to 0.7. The highest PIC value was noted for SSR markers CEDG 128 (0.7), followed by CEDG 44 (0.7), TWSSR 87 (0.7), CEDG 154 (0.7), CEDG 53 (0.7), CEDG 92 (0.7), and CEDG 91 (0.6). Markers with a PIC value ≥ 0.60 are more informative and can distinguish the genotypes effectively. The lowest PIC value was exhibited by CEDG 105 (0.4), followed by TWSSR 167 (0.5), depicting the less discriminatory power of these markers in differentiating the genotypes. Similarly, Santhees et al. (2014) reported that out of 42 SSR markers used, 15 SSR markers expressed polymorphism with PIC values varying from 0.3 for SSR marker (CEDG 024) to 0.7 (CEDG 154), with a mean of 0.6 in their study on screening of black gram varieties for yellow mosaic virus resistance employing SSR markers. According to Mwangi et al. (2021), with a mean of 0.3, the PIC values varied from 0.1 (CEDG 056) to 0.5 (CEDG 092). Of all the markers, CEDG 092 was the most informative, with a high PIC value of 0.8 reported by Prajapathi et al. (2022) in their study on molecular variability in MYMV-resistant and susceptible black gram using SSR markers. PIC values for 15 polymorphic markers are represented in Table 1.

3.1.4 Nei's Genetic Diversity Index

Nei's genetic diversity index is an estimate of the average genetic variation or diversity found at each locus. Based on Nei's genetic diversity index, the highest level of genetic diversity was recorded in the case of CEDG 180 (0.7) and TWSSR 66 (0.7), and the lowest was recorded by CEDG 105 (0.4), with a standard value of 0.6. Nei's genetic diversity was found to range from 0.2 to 0.7 with a mean value of 0.4 in Pyngrope et al. (2015) genetic diversity study of 30 black gram genotypes utilizing 12 SSR markers. Nei's genetic diversity index for 15 polymorphic markers is represented in Table 1.

3.1.5 Shannon's Information Index

Variation at various levels of genetic structure can be described using Shannon's information index, which is also used to quantify genetic diversity. Shannon's information index in the present investigation had a mean value of 1.0 and varied from 0.8 (CEDG 105) to 1.2 (TWSSR 66). The highest Shannon's information index was displayed by TWSSR 66 (1.2), CEDG 180 (1.2), and CEDG 91 (1.2), whereas the lowest was exhibited by CEDG 105 (0.8), TWSSR 87 (0.8), and CEDG 128 (0.9). Shannon's information index ranged from 0.6 to 1.2 with an average of 1.0 in the previous reports of Gangadhar et al. (2023). Shannon's information index for 15 polymorphic markers is represented in Table 1.

3.1.6 Major Allele Frequency

The major allele frequency in this study averaged 0.4 and varied from 0.3 (TWSSR 167) to 0.7 (CEDG 105). TWSSR 66 (0.3), CEDG 180 (0.3), and CEDG 91 (0.3) had the lowest major allele frequencies, whereas CEDG 105 (0.7) had the highest, followed by CEDG 44 (0.5), CEDG 176 (0.5), and TWSSR 87 (0.5). Among the 15 polymorphic markers studied, CEDG 180 followed by CEDG 128, CEDG 44, TWSSR 66, CEDG 91, and CEDG 154 recorded higher PIC values along with a high number of effective alleles, Nei's genetic diversity index, and Shannon's information index. Hence, these markers can be considered more effective for discriminating genotypes and are useful for genetic diversity studies. Major allele frequency for 15 polymorphic markers is represented in Table 1.

TABLE 1
SUMMARY OF STATISTICS OF GENETIC DIVERSITY ASPECTS AMONG 15 POLYMORPHIC MICROSATELLITE MARKERS EMPLOYED IN THE PRESENT INVESTIGATION

S. No.	SSR Marker	Linkage Group	Pos. (cM)	Na*	Ne*	MAF	I*	PIC	Nei*
1	CEDG 6	2	14.5	3	2.5	0.5	1	0.6	0.6
2	CEDG 97	10	37.1	3	2.6	0.4	1	0.5	0.6
3	CEDG 92	8	54.2	3	2.5	0.5	1	0.7	0.6
4	CEDG 44	11	18	3	2.1	0.5	0.8	0.7	0.5
5	CEDG 176	7	60.9	3	2.4	0.5	0.9	0.6	0.5
6	CEDG 154	4	23.5	4	2.8	0.4	1.1	0.7	0.6
7	CEDG 116	10	28	4	2.9	0.5	1.2	0.6	0.6
8	CEDG 128	15	5.3	3	2.3	0.5	0.9	0.7	0.5
9	CEDG 180	10	9.9	4	3.3	0.3	1.2	0.6	0.7
10	CEDG 91	4	25.5	4	3.2	0.3	1.2	0.6	0.6
11	TWSSR 87	—	—	3	2.1	0.5	0.8	0.7	0.5
12	CEDG 53	12	4.8	4	2.9	0.3	1.1	0.7	0.7
13	TWSSR 66	1	—	4	3.3	0.3	1.2	0.7	0.7
14	TWSSR 167	10	—	3	2.9	0.3	1	0.5	0.6
15	CEDG 105	—	—	4	1.8	0.7	0.8	0.4	0.4
Maximum				**4**	**3.3**	**0.7**	**1.2**	**0.7**	**0.7**
Minimum				**3**	**1.8**	**0.3**	**0.8**	**0.4**	**0.4**
Mean				**3.4**	**2.6**	**0.4**	**1**	**0.6**	**0.6**

Na = Number of alleles; Ne* = Number of effective alleles; MAF = Major allelic frequency; I* = Shannon's information index; PIC = Polymorphic information content; Nei* = Genetic diversity index*

3.2 Population Structure and Genetic Diversity Analysis of Black Gram Genotypes

3.2.1 Population Structure Analysis

Only after considering population structure is the true association revealed (Yu et al., 2006). The LnP(D) graph delineated with number of subpopulations (K) on the x-axis and logarithmic probability distribution on the y-axis did not give a vivid picture of the true value of K, so ΔK value was charted against number of subpopulations, displaying the highest peak at K = 4, which revealed that there are four subpopulations within the panel. Structure Harvester (Earl, 2012) was a web-based program used for the visualization of STRUCTURE output and implementation of the Evanno method for measuring maximum ΔK value. The summary plot of Q matrix estimates and clustering of 117 genotypes is represented in Fig. 1 and Table 2.

Based on the Q values that were obtained from the structure software, the genotypes were assigned to each subpopulation with consideration for the highest membership likelihood criterion. Based on the membership fractions, the genotypes with a Q value ≥ 75% were assigned to corresponding subgroups and those with ≤ 75% were defined as admixtures. The genotypes with a score > 0.75 were considered pure, while those with < 0.75 were considered admixtures.

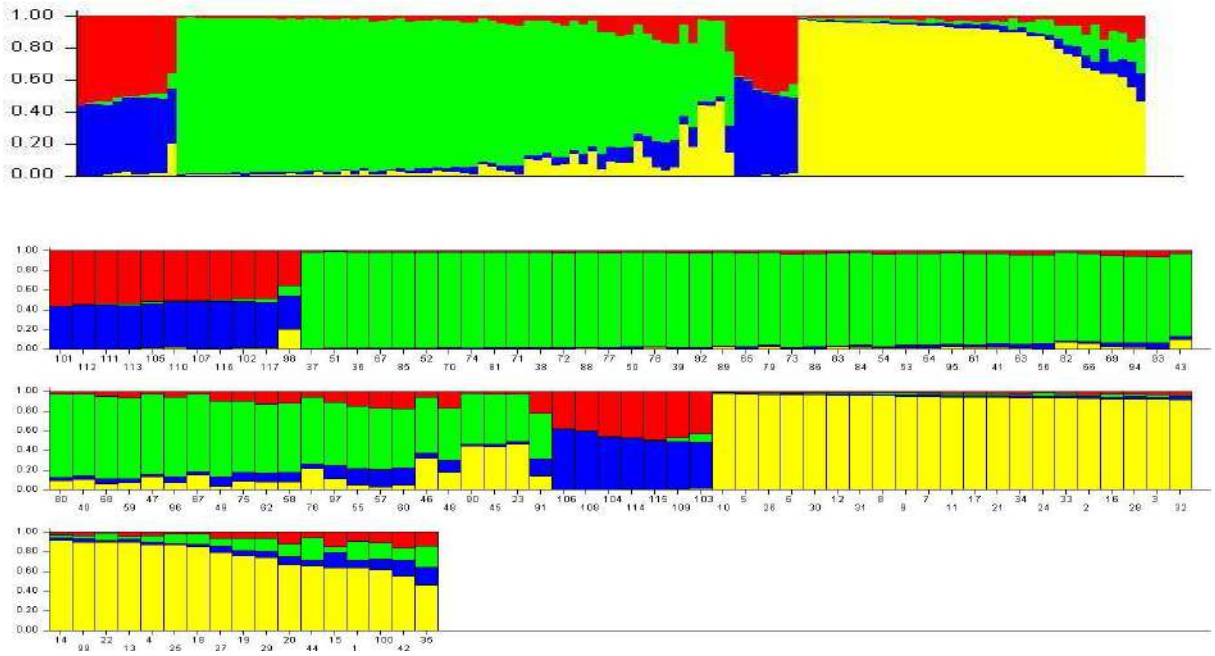

FIGURE 1: The summary plot of Q matrix estimates showing (a) cluster 1 (red), cluster 2 (green), cluster 3 (blue), and cluster 4 (yellow); (b) clustering of 117 genotypes representing membership fractions

TABLE 2
GROUPING OF 117 BLACK GRAM GENOTYPES INTO 4 SUB-POPULATIONS BASED ON POPULATION STRUCTURE

S. No.	Sub-Population	Number of Genotypes	Names of Genotypes
1	Sub-Population 1	9	VBN-10, GBG 92, PBG 272, GBG 5, PU 1537, LBG 685, LBG 1012, GBG 30, LBG 806
2	Sub-Population 2	58	KUG 898, 0BG 38, KUG 883, TBG 152, TJU 262, OBG 39, TBG 155, TBG 138, TBG 149, TBG 156, LBG 623, TBG 129, TU 94, TBG 145, OBG 102, TBG 146, LBG 645, VBG-13-003, UTTARA, TBG 142, TBG 147, TBG 141, TU 40, TJU 111, TJU 258, PANTU 19, OBG 43, TBG 104, VBG-17-026, SB-42-8, LBG 8282, SUE17-52, PBG 32-2, TBG 150, TBG 151, TBG 154, VBG-17-012, LBG 890, TBG 148, LBG 787, TU 94, PUSA 851, LBG 969, VBN-7, TU 67, OBG 101, TBG 143, SEKHAR-2, PU-31, TBG 144, VBN-6, PBG-1, PU 1527, RUB-15-04, LBG 965, MBG 1069, VBG-12-034
3	Sub-Population 3	9	ADT 5, KPU-12-1735, LBG 1064, LBG 1006, IPU-13-6, GBG 23, GBG 86, LBG 1013, PU 1805
4	Sub-Population 4	41	VAMBAN 7, LBG 938, KPU 405, GBG 1, COBG 653, KU-19-299, COBG-13-04, KU-21-162, GBG 111, KU-21-165, DKU-90, DKU-99, DKU-87, GBG 108, IPU-12-15, KPU-514-75, KU-21-170, ABFBG 4, IPU-11-16, KU-21-158, ABFBG 12, KU-21-167, IPU-12-22, KU-21-163, KPU-13-241, GBG 99, BDU-12, KU-21-160, IPU-16-09, KU-21-157, IPU-2-43, KU-21-159, KPU-520-69, LBG 907, IPU-11-16, ABFBG 3, LBG 826, LBG 852, KUG 479

Sub-population 1 (POP1), represented with red colour in the bar graph, comprises a total of 9 genotypes. Sub-population 2 (POP2), represented with green colour in the bar graph, consists of 58 genotypes. Sub-population 3 (POP3), represented with

blue colour in the bar graph, consists of 9 genotypes. Sub-population 4 (POP4), represented with yellow colour in the bar graph, consists of 41 genotypes. Singh et al. (2022) also reported four subpopulations in 117 diverse black gram germplasm in their study of genome-wide association studies for yield and yield-related traits in black gram germplasm.

3.3 Cluster Analysis Based on UPGMA

Genetic similarity ratings between the black gram genotypes under investigation were used to generate the dendrogram displayed in Figure 2. The UPGMA approach was employed to compute a similarity matrix utilizing SSR markers based on Jaccard's coefficient using DARwin 6.0 software. Cluster I, Cluster II, and Cluster III are the three crucial clusters into which the 117 genotypes used in this investigation were separated. With 51 genotypes, Cluster I was the largest, followed by Cluster II (19 genotypes) and Cluster III (47 genotypes). Further subdividing Cluster I resulted in two sub-clusters: IA (28 genotypes) and IB (23 genotypes). Cluster II was further sectioned into two sub-clusters: IIA (18 genotypes) and IIB (1 genotype). Cluster III was further categorized into two sub-clusters: IIIA (40 genotypes) and IIIB (7 genotypes). Additionally, as the similarity coefficient rose, the sub-clusters were further segmented into distinct sub-clusters. Table 3 shows the specifics of the DARwin software's grouping of 117 black gram genotypes. Similar to the present study, Kaewwongwal et al. (2015) constructed a phylogenetic tree using 534 black gram genotypes and 22 SSR markers. The phylogenetic tree developed consisted of three major clusters: C-I, C-II, and C-III. Furthermore, the results of the neighbor-joining tree coincide with the results of the model-based population structure analysis.

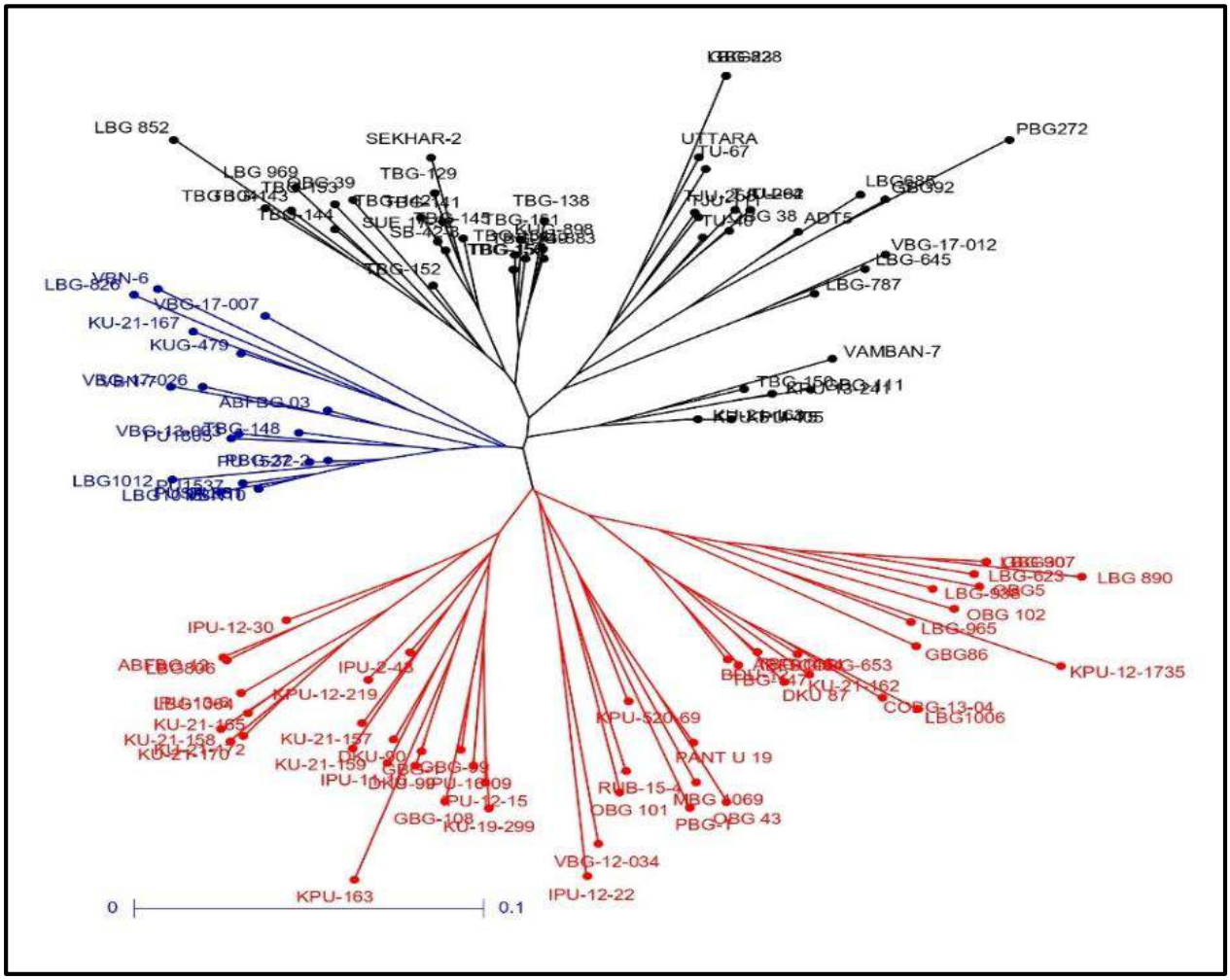

FIGURE 2: Neighbor-joining dendrogram depicting the genetic relationships among black gram genotypes based on SSR marker data. Colored branches indicate distinct genetic clusters: blue, black, and red. Scale bar represents genetic distance.

TABLE 3
GROUPING OF 117 BLACK GRAM GENOTYPES INTO DISTINCT CLUSTERS BASED ON JACCARD'S SIMILARITY COEFFICIENT USING UPGMA METHOD

S. No.	Cluster	Sub-Cluster	Number of Genotypes	Names of Genotypes
1	I	IA	28	GBG30, LBG907, LBG890, LBG623, GBG5, LBG938, OBG102, KPU-12-1735, LBG965, GBG86, LBG1006, COBG-13-04, COBG-653, KU-21-162, TBG146, ABFBG04, DKU87, TBG147, BDU12, PANTU19, OBG43, MBG1069, PBG1, KPU-520-69, RUB-15-4, OBG101, VBG-12-034, IPU-12-22
		IB	23	KU-19-299, IPU-12-15, IPU-16-09, GBG99, GBG108, GBG1, DKU99, KPU163, IPU-11-16, DKU90, KU-21-159, KU-21-157, IPU-2-43, KPU-12-219, KU-21-172, KU-21-170, KU-21-165, KU-21-158, LBG1064, IPU-13-6, LBG806, ABFBG12, IPU-12-30
2	II	IIA	18	VBN10, PU31, PUSA851, LBG1013, PU1537, LBG1012, PU1527, PBG32-2, PU-1805, VBG-13-003, TBG148, VBN7, VBG-17-026, ABFBG3, KUG479, KU-21-167, LBG826, VBN6
		IIB	1	VBG-17-007
3	III	IIIA	40	TBG104, LBG852, TBG143, TBG144, LBG969, TBG153, OBG39, TBG152, TBG142, SUE 17-52, SB-42-8, TBG141, TBG129, SEKHAR2, TBG145, TBG156, TBG155, TBG154, TBG151, TBG149, TBG138, KUG898, KUG883, GBG23, LBG828, UTTARA, TU67, TJU258, TJU111, TU40, TJU262, TU94, OBG38, ADT5, LBG685, GBG92, PBG272, VBG-17-012, LBG645, LBG787
		IIIB	7	VAMBAN7, TBG150, KPU-13-241, GBG111, KPU-21-163, KPU-514-75, KPU-405

3.4 Principal Coordinate Analysis (PCoA)

The principal coordinate analysis delineated that the 117 black gram genotypes were clearly separated from one another. The initial three principal coordinates explained 11.1%, 10.0%, and 8.2% of the total variation of 41.6%, as depicted in Table 4 and Figure 3.

The genotypes that are adjacent to the axis and clustered in one place are more strongly related to each other. Certain genotypes are extremely far from the axis, indicating a lack of a close relationship between them. The genotypes were sorted according to model-based analysis using PCoA analysis as well. The population STRUCTURE results were further validated by the outcomes of the model-based STRUCTURE analysis, which were almost correlated with the results of the PCoA and unweighted neighbor-joining clustering tree analyses. Principal Coordinate Analysis (PCoA) was used by Kaewwongwal et al. (2015) to determine genetic diversity among 534 genotypes of black gram. Of the total variation of 37.3%, the first coordinate explained 14.8% and the second coordinate explained 13.0% of the variation.

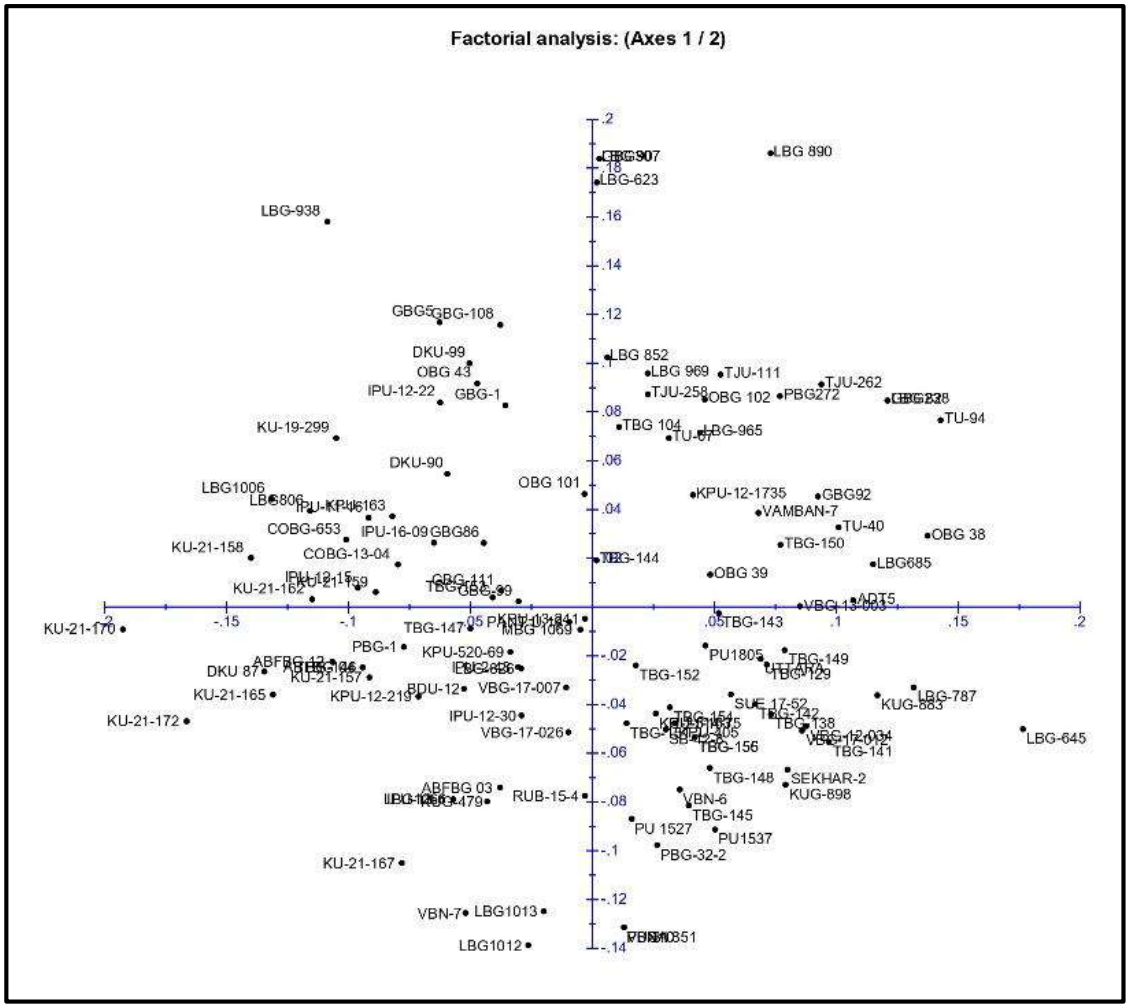

FIGURE 3: Principal Coordinate Analysis (PCoA) plot showing the distribution of black gram genotypes based on SSR marker data across the first two axes. The axes represent the major components of genetic variation among the accessions.

TABLE 4
FACTORIAL ANALYSIS BASED ON DISSIMILARITY

Axis	Eigenvalue	Inertia (%)
1	0.0056	11.1
2	0.005	10
3	0.0041	8.2
4	0.0032	6.5
5	0.0028	5.7

aCluster I generated through neighbor-joining analysis showed 13.4% similarity of genotypes with sub-population 1 and 2 generated through model-based analysis, whereas cluster I showed 32.6% correspondence with sub-population 4 and cluster II showed 18.7% correspondence with sub-population 4.

IV. CONCLUSION

From the results of population structure analysis, the maximum value for Evanno's measure of ΔK showed a clear peak at an optimal K value of four (K = 4), which indicated that the entire population can be grouped into four subgroups. Diversity analysis using DARwin based on the unweighted neighbor-joining method segregated black gram germplasm into three main clusters: Cluster I, Cluster II, and Cluster III. The grouping of genotypes based on UPGMA clustering and PCoA analysis was in close correspondence with the results of model-based STRUCTURE analysis, which further confirmed the population structure results. The identified polymorphic SSR markers, particularly those with high PIC values (CEDG 128, CEDG 44,

TWSSR 87, CEDG 154, CEDG 53, CEDG 92, and CEDG 91), can be effectively utilized for future genetic diversity studies and marker-assisted selection programs in black gram.

ACKNOWLEDGEMENTS

The authors sincerely thank Acharya N. G. Ranga Agricultural University for providing laboratory facilities and research materials throughout the course of this study.

CONFLICT OF INTEREST

The authors declare that they have no financial or non-financial competing interests related to the submitted work.

REFERENCES

[1] Earl, D. A., & Vonholdt, B. M. (2012). Structure Harvester: A website and program for visualizing STRUCTURE output and implementing the Evanno method. *Conservation Genetics Resources, 4*, 359–361.

[2] Evanno, G., Regnaut, S., & Goudet, J. (2005). Detecting the number of clusters of individuals using the software STRUCTURE: A simulation study. *Molecular Ecology, 14*, 2611–2620.

[3] Gangadhar, L., Nikhil, A., Rathore, M., Shanmugavadivel, P. S., Lal, G. M., & Gayathri, G. (2023). Morphological variability and molecular diversity in blackgram (*Vigna mungo* (L.) Hepper) genotypes using SSR markers. *International Journal of Plant & Soil Science, 35*, 2050–2062.

[4] Gupta, S. K., Souframanien, J., & Gopalakrishna, T. (2008). Construction of a genetic linkage map of black gram, *Vigna mungo* (L.) Hepper, based on molecular markers and comparative studies. *Genome, 51*, 628–637.

[5] Kaewwongwal, A., Kongjaimun, A., Somta, P., Chankaew, S., Yimram, T., & Srinives, P. (2015). Genetic diversity of the black gram [*Vigna mungo* (L.) Hepper] gene pool as revealed by SSR markers. *Breeding Science, 65*, 127–137.

[6] Korattukudy, C. A., Samy, A. P. L. M. A., Rengasamy, K., Devadhasan, S., Shunmugavel, S., Yasin, J. K., & Madhavan, A. P. (2022). Genetic diversity analysis in blackgram (*Vigna mungo*) genotypes using microsatellite markers for resistance to yellow mosaic virus. *Plant Protection Science, 58*, 110–124.

[7] Murray, M. G., & Thompson, W. F. (1980). Rapid isolation of high molecular weight plant DNA. *Nucleic Acids Research, 8*(19), 4321–4326.

[8] Mwangi, J. W., Okoth, O. R., Kariuki, M. P., & Piero, N. M. (2021). Genetic and phenotypic diversity of selected Kenyan mung bean (*Vigna radiata* L. Wilczek) genotypes. *Journal of Genetic Engineering and Biotechnology, 19*, 1–14.

[9] Perrier, X., & Jacquemoud-Collet, J. P. (2006). *DARwin software*. http://darwin.cirad.fr/darwin

[10] Prajapati, P. K., & Singh, A. P. (2022). Investigation of molecular variability on MYMV-resistant and susceptible blackgram species using SSR marker. *International Journal of Research and Analytical Reviews, 9*, 192–215.

[11] Pritchard, J. K., Stephens, M., & Donnelly, P. (2000). Inference of population structure using multi-locus genotype data. *Genetics, 155*, 945–959.

[12] Pyngrope, A. H., Noren, S. K., Wricha, T., Sen, D., Khanna, V. K., & Pattanayak, A. (2015). Genetic diversity analysis of blackgram [*Vigna mungo* (L.) Hepper] using morphological and molecular markers. *International Journal of Applied and Pure Science and Agriculture, 1*, 104–113.

[13] Sathees, N., Shoba, D., Mani, N., Saravanan, S., Kumari, M. P., & Pillai, M. A. (2022). Tagging of SSR markers associated with yellow mosaic virus resistance in black gram (*Vigna mungo* (L.) Hepper). *Euphytica, 218*, Article 23.

[14] Singh, L., Dhillon, G. S., Kaur, S., Dhaliwal, S. K., Kaur, A., Malik, P., Kumar, A., Gill, R. K., & Kaur, S. (2022). Genome-wide association study for yield and yield-related traits in diverse blackgram panel (*Vigna mungo* L. Hepper) reveals novel putative alleles for future breeding programs. *Frontiers in Genetics, 13*, Article 849016.

[15] Yeh, F. C., Boyle, R., Yang, R. C., Ye, Z., Mao, J. X., & Yeh, D. (1999). *POPGENE*. http://www.ualberta.ca/~fyeh/popgene.html.

International Journal of Environmental & Agriculture Research (IJOEAR)
ISSN: [2454-1850]
[Vol-12, Issue-4, April- 2026]
Website: www.ijoear.com
Journal DOI: 10.25125/agriculture-journal

Quantification of Environmental Reactive Oxygen Species (ROS) by Chromo-Stoichiometry: Development and Validation of the Monagas Variant

García Raurich, Josep[1*]; Torres Lerma, Jose Antonio[2]; Monagas Asensio, Pedro[3]; Monagas Borredà, Àlex[4]; Crespiera Portabella, Judith[5]; Monagas Borredà, Èric[6]

[1,3,4,5]Centre de Recerca en Seguretat i Control Alimentari de la UPC (CRESCA).
[2]Composites and Advanced Materials for Multifunctional Structures UPC (CAMMS)
[6]Nanoscience and Nanotechnology Program, Department of Physics, UAB
*Corresponding Author

Received:- 01 April 2026/ Revised:- 10 April 2026/ Accepted:- 16 April 2026/ Published: 30-04-2026

Abstract— *This research develops a quantitative model for estimating reactive oxygen species (ROS) in ambient air using a chromo-stoichiometric approach applied to the traditional Schönbein scale. Starting from the stoichiometric relationship between ozone (O_3) and water vapor as precursors of hydroxyl radicals (OH·), and considering ozone as the limiting reagent, a direct conversion is established between the Schönbein number and the OH· emission rate expressed in $mol \cdot cm^{-3} \cdot s^{-1}$. This transformation results in the so-called "Monagas Variant," which converts a qualitative tool based on the colorimetric change of potassium iodide reagent strips into a quantitative method for radical estimation.*

The model integrates the conversion of ozone concentrations (ppb) to amount of substance, the calculation of absolute humidity, and the application of stoichiometric relationships to determine the theoretical production of OH· during a standard 8-hour exposure period. The results allow for the classification of ambient oxidation into three levels (LOW, MIDDLE, and HIGH), defined by ranges of radical emission. Experimental validation, performed in a 1 m^3 tank with an Open Air Factor (OAF) generator and through comparative tests with 17.5% hydrogen peroxide, showed consistent agreement between the observed color change and the values calculated by the model.

The data obtained, on the order of 10^6–10^7 $mol \cdot cm^{-3} \cdot s^{-1}$, are consistent with values reported in the literature on ozone photolysis at air-water interfaces and atmospheric OH· production. Furthermore, it is shown that reliable determinations can be made in just 90 minutes, significantly reducing the evaluation time compared to the full 8-hour cycle. The Monagas Variant thus constitutes an accessible, reproducible, and low-cost tool for monitoring environmental oxidative capacity and assessing OAF in indoor spaces, offering a practical solution for the rapid control of advanced oxidation processes and indoor air quality.

Keywords— Hydroxyl radicals (OH·), Reactive oxygen species (ROS), Monagas Variant, Schönbein scale, Open Air Factor (OAF), Chromo-stoichiometry, Indoor Air Quality (IAQ), Advanced Oxidation Processes (AOPs), Atmospheric environmental chemistry.

I. INTRODUCTION

1.1 Current Situation and Reason for the Study:

The recent COVID-19 pandemic has highlighted and accelerated, in just over three years, a large number of new trends, behaviors, regulations, and requirements surrounding indoor disinfection. The need to meet these disinfection requirements in public places, such as supermarkets, businesses, hospitals, and hotels, to maintain a pathogen-free environment as much as possible, has led to the reappearance and uncontrolled use of a multitude of existing products and substances, as well as new

ones, mostly oxidizers. Some of these are already part of our daily lives, such as bleach, alcohols, peroxides, chlorinated compounds, ozone, etc.

Therefore, it is increasingly necessary to be able to quantify the role of oxidants in indoor environments, both for the air and for the surfaces where they are applied, since they all have a direct and indirect relationship with health: direct through dispersion in the environment through breathing and contact with these substances, and indirect through evaporation or methods of application that can end up in food and all kinds of consumer products.

TABLE 1
PERMISSIBLE EXPOSURE LIMITS FOR OZONE AND HYDROGEN PEROXIDE

Agency	Ozone (O_3)	Hydrogen Peroxide (H_2O_2)	Regulatory Context
WHO	100 µg/m³ (~0.05 ppm)	No specific ambient air limit	8-hour daily average. WHO Global Air Quality Guidelines (2021)
OSHA	0.1 ppm (0.2 mg/m³)	1 ppm (1.4 mg/m³)	Permissible Exposure Limit (PEL) - 8-hour TWA. 29 CFR 1910.1000
FDA	0.05 ppm	GRAS (Generally Recognized as Safe)	Max. for medical devices in occupied spaces / Food additive safety

Source: Own elaboration

The Open Air Factor (OAF) is well-known in nature and has an environmental sanitizing effect. In Garcia Raurich et al. (2023), it was theoretically demonstrated that, artificially, with the appropriate proportion and combination of reactants, it is possible to achieve, in indoor environments, the same level of hydroxyl radical molecules generated as in nature, using only two reactants: hydrogen peroxide and almost negligible amounts of ozone, without ever exceeding the maximum recommended emission levels established by WHO, OSHA, and FDA.

The immediate, involuntary, and vital need to breathe and move about in a safe, sanitized environment makes it practically impossible to quickly and easily determine whether these required safety parameters are being met. Therefore, the need arises to be able to detect the presence of oxidants in a given environment in near real-time, without sophisticated laboratory equipment.

1.2 Reactive Oxygen Species (ROS):

Reactive oxygen species (ROS) refer to a group of reactive molecules and free radicals derived from molecular oxygen (O_2). Recent work (Held, P., 2015) demonstrates that ROS are responsible for activating cell signaling cascades, in addition to serving as cellular messengers. Most ROS are produced as byproducts of mitochondrial electron transport, such as the reactions that occur during the reduction of atomic oxygen. In fact, because atomic oxygen has two unpaired electrons in separate orbits, its structure is susceptible to radical formation.

The effect of ROS on cellular processes, oxidative stress, depends on the concentration, duration, and context of exposure. The typical cellular response to stress is the detoxification of reactive intermediates to repair the corresponding damage. Peroxides and free radicals that emerge from molecular oxygen can cause toxic effects on all components of the cell. However, it has been shown that some ROS, such as hydroxyl radicals (OH·), have a short half-life of ~10^{-9} s, thus inhibiting this effect in humans, animals, and plants.

Furthermore, these ROS are always present in the natural environment. Therefore, it is evident that these ROS could be measured by monitoring oxidation processes in the air. In a first approach, presented in Garcia Raurich et al. (2023), an estimate of ROS concentration can be correlated by monitoring OH·, as they have the second highest oxidation potential. However, a complete correlation between the OH· concentration and the absolute ROS concentration will never be achieved.

One of the most common processes that produces hydroxyl radicals is the reaction between hydrogen peroxide and ozone, both in the gas phase. The maximum reaction efficiency is achieved with the stoichiometric ratio of the reactants. Therefore, the maximum oxidative efficiency also corresponds to the maximum concentration of OH· and the minimization of waste, which is achieved at different ambient volumes depending on the purity of the hydrogen peroxide and considering an initial ozone concentration of 0.05 ppm. Specifically, the volume required to obtain maximum efficiency increases with the purity of the

peroxide. In any case, an OH· emission of ~4.4 × 10^7 mol·cm^{-3}·s^{-1} is obtained, consistent with experimental results obtained in other studies (Anglada et al., 2014).

$O_3 + H_2O_2 \rightarrow OH\cdot + O_2 + O_2H\cdot$ **(R1)**

The quickest and simplest qualitative methods available, used in a wide variety of studies, including those conducted at environmental monitoring stations and in academic settings, employ the Schönbein reagent strip to analyze ambient ozone present in nature (UCAR, [online]). The reaction between potassium iodide (KI), ozone (O_3), and water (H_2O) produces corresponding color scales, which represent different ozone concentrations under varying relative humidity.

$2KI + O_3 + H_2O \rightarrow 2KOH + O_2 + I_2$ **(R2)**

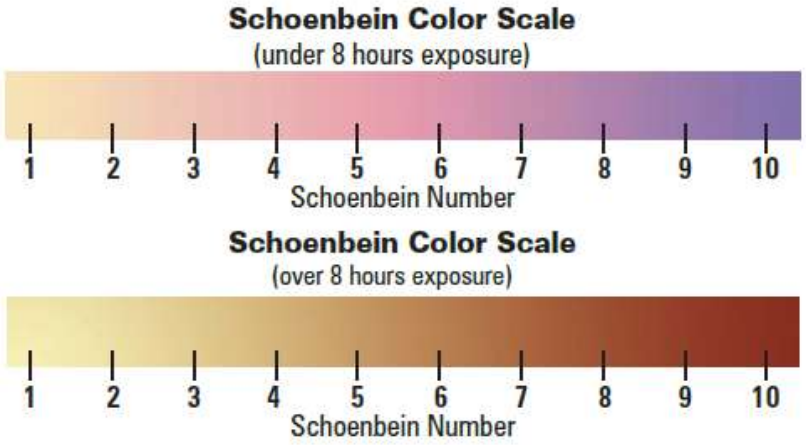

GRAPHIC 1: Schönbein chart values for colors. Workman and Frye (JoVE Journal, Science Education Collection, Measuring Tropospheric Ozone)

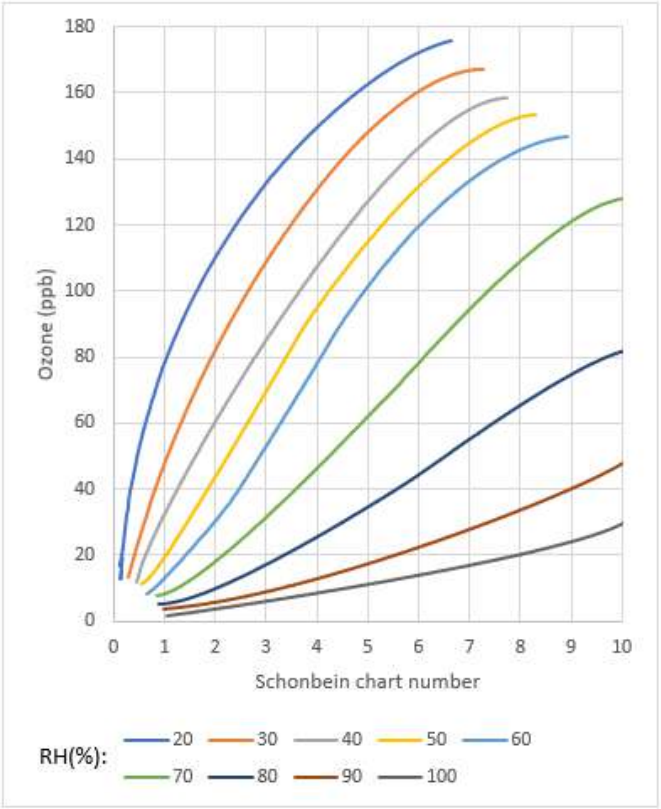

GRAPHIC 2: Schönbein chart for different ambient humidity values. Several Departments of Environmental Quality employ this Schönbein chart to measure ozone concentration in air. Workman and Frye (JoVE Journal, Science Education Collection, Measuring Tropospheric Ozone)

Given a specific relative humidity (RH) value, as the concentration of ozone in the air increases, the Schönbein number also increases, implying a decrease in color brightness. Furthermore, as the presence of water vapor in the air (relative humidity) increases, the ozone concentration corresponding to a given color decreases. Thus, due to the presence of ozone and moisture in the air, the well-known Schönbein number table also demonstrates that the scales represented are influenced by the presence of oxidizing reactive oxygen species (ROS), such as hydroxyl radicals (OH·).

$$2O_3 + H_2O \longrightarrow 2OH\cdot + 2O_2 + O_2H\cdot \quad \textbf{(R3)}$$

Given that other oxidants besides ozone and molecular oxygen exist in nature, such as the hydroxyl radical (OH·), produced by ozone photolysis as the main source of these radicals (Stone et al., 2012; Carslaw et al., 2017), it seems logical to consider measuring this oxidizing molecule, considered the most important "cleaner" of the troposphere (George, C. et al., 2015; Ruiz-Lopez et al., 2020). It is called the "detergent of the atmosphere" due to its high reactivity, and despite this high reactivity, it remains at appreciable concentrations because it is regenerated in several of the chain processes in which it participates.

Therefore, by taking advantage of the Schönbein color chart and carefully analyzing the ozone concentration values that make up this internationally accepted color scale and the ozone chart for different relative humidity levels, the corresponding hydroxyl radical emission is obtained by calculating the required stoichiometry. This reveals the amount of OH· associated with each color shown on each scale and allows for the creation of another variant of the same chart and scale, this time to determine the number of OH· molecules needed for that equivalent oxidation.

II. THEORETICAL DERIVATION OF THE MONAGAS VARIANT

2.1 Conversion of Ozone Concentration to Amount of Substance:

The first step is to express each reactant data point as the amount of substance in moles. Ozone concentration information is expressed in parts per billion (ppb). Consequently, the amount of substance is calculated considering the molar volume under standard conditions for an ideal gas (1 atm of ambient pressure, which is 22.4 L/mol). The required conversion is shown below:

$$ppb_{O_3}[ppb].\frac{1\left[\frac{L_{O_3}}{L}\right]}{10^9[ppb]}.\frac{1\ mol_{O_3}}{22.4\ L_{O_3}} = 4.464.ppb_{O_3}.10^{-11}.\left[\frac{mol\ O_3}{L}\right] \quad \textbf{(R4)}$$

2.2 Calculation of Absolute Humidity:

On the other hand, the absolute amount of water in the reaction can be obtained from the Relative Humidity (RH) values in %. This value is due to the ratio between the water vapor pressure in the air and the corresponding vapor pressure under saturation conditions. Relative humidity should never be understood as the ratio of the volume of water to the volume of air, or anything similar. Therefore, the Absolute Humidity (AH), which is the actual ratio of the mass of water to the volume of air in kg/m³, can be obtained using the following expressions:

$$AH = \frac{m_w}{V} = \frac{e_w\cdot(RH/100)}{R_vT} \quad \textbf{(R5)}$$

Where $R_v = 461.5\frac{J}{kg\cdot K}$ is the gas constant for water vapor, T is the ambient temperature in Kelvin, and e_w is the saturation pressure of water vapor in Pascals, which is calculated as follows:

$$e_w(p,t) = (1.0016 + 3.15\cdot 10^{-6}p - 0.074\cdot p^{-1})\cdot 6.112\cdot exp\ exp\left(\frac{17.62t}{243.12+t}\right) \quad \textbf{(R6)}$$

Where p is the ambient pressure in hPa and t is the ambient temperature in °C. The value of e_w obtained with this last equation is expressed in hPa, so the value used in the Absolute Humidity equation will first be converted to Pa.

Finally, the amount of water substance per unit volume is obtained as follows:

$$AH\ \left[\frac{kg}{m^3}\right]\cdot\frac{1000\ g}{1\ kg}\cdot\frac{1\ m^3}{1000\ L}\cdot\frac{1\ mol\ H_2O}{18\ g} = \frac{AH}{18}\left[\frac{mol\ H_2O}{L}\right] \quad \textbf{(R7)}$$

2.3 Identification of the Limiting Reactant:

At this point, the next step is to identify which of the reactants is the limiting one. Therefore, a range of values for both ozone concentration and relative humidity is compared in terms of the amount of the related substance.

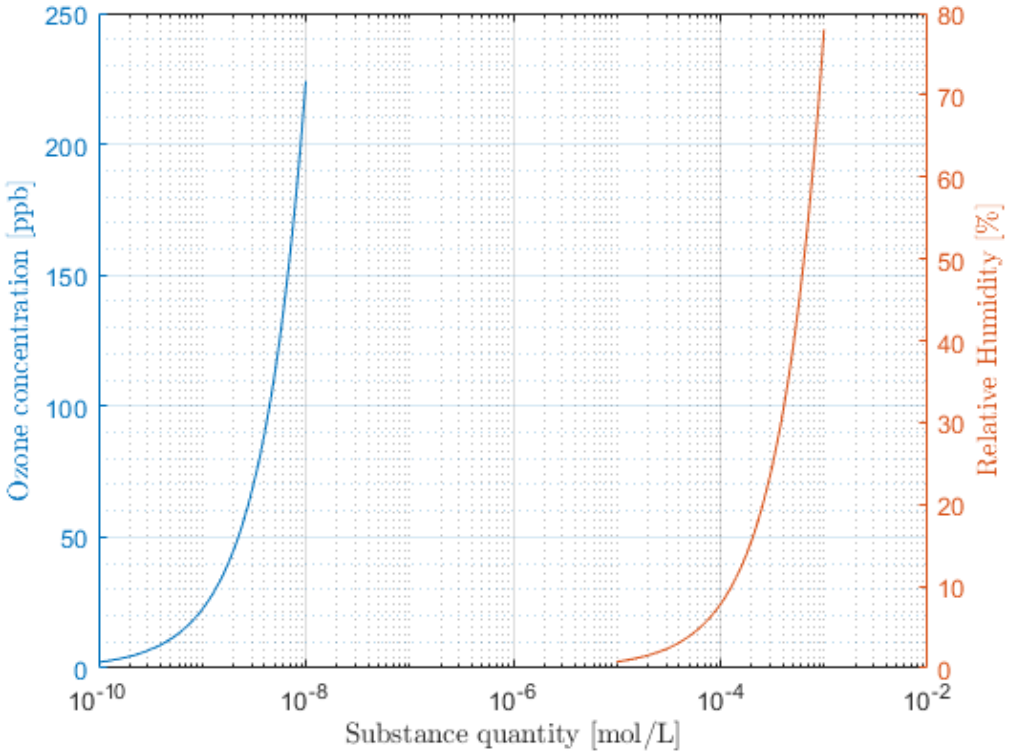

GRAPHIC 3: Comparison of ozone concentration with relative air humidity in terms of the amount of related substance (Own elaboration)

It can be observed that, in any case, the amount of ozone participating in the reaction is between four and five orders of magnitude lower than the corresponding amount of water vapor. Therefore, it is concluded that ozone is always the limiting reactant, again justifying the direct correspondence between the Schönbein color scale defined by ozone and the emission of hydroxyl radicals, which are directly related to the luminosity of that color.

2.4 Calculation of Hydroxyl Radical Generation:

Once ozone is identified as the limiting reactant, the amount of OH· generated from the reaction of ozone with water vapor is calculated as shown below:

$$n_{OH\cdot} = 4.464 \cdot ppb_{O_3} \cdot 10^{-11} \left[\frac{mol\ O_3}{L}\right] \cdot \frac{2\ mol\ OH\cdot}{2\ mol\ O_3} = 4.464 \cdot ppb_{O_3} \cdot 10^{-11} \left[\frac{mol\ OH\cdot}{L}\right] \quad \textbf{(R8)}$$

$$molec_{OH\cdot} = n_{OH\cdot} \left[\frac{mol\ OH\cdot}{L}\right] \cdot \frac{6{,}022\cdot 10^{23}\ molec\ OH\cdot}{1\ mol\ OH\cdot} = 26.8822 ppb_{O_3} 10^{12} \left[\frac{molec\ OH\cdot}{L}\right] \quad \textbf{(R9)}$$

$$molec_{OH\cdot} = 26.8822 ppb_{O_3} 10^{9} \left[\frac{molec\ OH\cdot}{cm^3}\right] \quad \textbf{(R10)}$$

2.5 Calculation of OH· Emission Rate:

Finally, the OH· emission rate is obtained by dividing the previous expression by the exposure time, which in this case is considered to be 8 hours, since the Schönbein strip color scales are defined around this exposure value. Therefore,

$$[OH\cdot] = \frac{26.8822 ppb_{O_3} 10^{9}}{8\cdot 3600} = 9.3341 ppb_{O_3} 10^{5} \left[\frac{molec}{cm^3\cdot s}\right] \quad \textbf{(R11)}$$

Thus, with the complete equivalence between ozone and OH· defined, the table of paired Schönbein numbers is obtained in terms of the emission of hydroxyl radicals OH· emitted per unit volume and time, which will be called the "Monagas Variant."

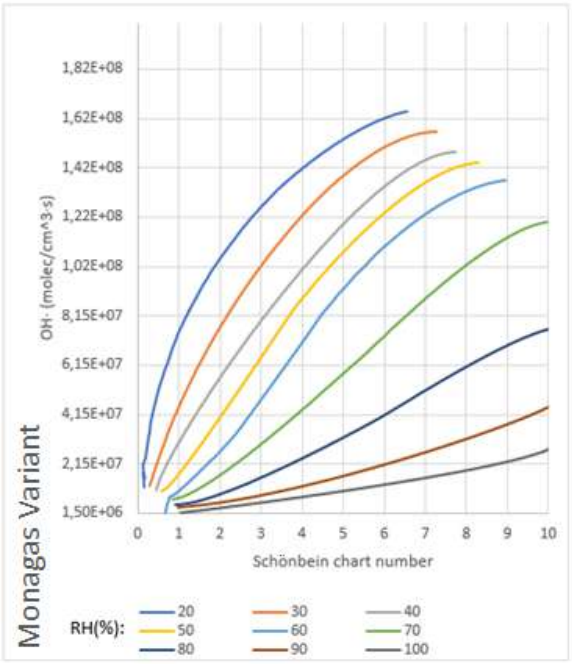

GRAPHIC 4: Proposed new Monagas chart for Environmental Quality Departments based on Schönbein chart to measure OH· concentration in air (Own elaboration)

2.6 Comparison with Literature Values:

With all the information presented above, the results obtained provide a starting point for applying chromo-stoichiometric techniques to the quantification of ROS and show consistency with real environmental values measured in air (Anglada et al., 2014). This is achieved by comparing the behavior of ozone (O_3) under sunlight in two very different environments: air (gaseous phase) and the water surface (air-water interface). The table demonstrates that ozone decomposes much faster and produces many more hydroxyl radicals (OH·) when in contact with water than when it is alone in air.

TABLE 2

OZONE PHOTOLYSIS RATE CONSTANTS (J) AND OH· PRODUCTION RATES (νOH·) IN THE GAS PHASE AND AT THE AIR-WATER INTERFACE (ANGLADA ET AL., 2014)

Category	Gas Phase – J (s^{-1})	Gas Phase – νOH· (molec·cm^{-3}·s^{-1})	Air–Water Interface – J (s^{-1})	Air–Water Interface – νOH· (molec·cm^{-3}·s^{-1})
Calculated (this work)	3.2×10^{-5}	0.7×10^{6}	7.6×10^{-4}*	1.5×10^{10}
Calculated (this work)†	—	—	1.1×10^{-4}	0.21×10^{10}
Measured (literature)‡	3.8×10^{-5}	$0.7–10 \times 10^{6}$	—	—

The table validates the article's main thesis: water is not a passive medium. Furthermore, it generates a spectral shift. The authors discovered that when ozone is in a humid environment, due to the proximity of the water molecule, its structure changes slightly, allowing it to absorb sunlight much more efficiently (a "redshift" in its absorption spectrum). This suggests that in places with high humidity, clouds, or over the ocean, atmospheric chemistry is much more active than previously thought, as very high levels of OH· (the main reagent for degrading pollutants) are being generated right at the water's surface.

III. EXPERIMENTAL DESIGN FOR THE DETERMINATION OF ENVIRONMENTAL OXIDANTS

3.1 Test Strips:

Airborne oxidants can be detected using specially prepared paper strips moistened with a reagent, known as Schönbein paper. The Schönbein reagent strips consist of cellulose paper wipes arranged in a plastic reservoir. The strips change color in the

presence of oxidizing species in the environment, with the color providing a qualitative indicator of the concentration of these oxidants.

To validate the paper wipe as a reagent carrier, it is necessary to evaluate its behavior with different concentrations of a known oxidant, such as hydrogen peroxide of a known purity. This is done by applying a couple of drops of reagent to each wipe fragment. First, the wipe is exposed to a selected control environment free of other oxidants. Then, a couple of drops of the corresponding known concentration of hydrogen peroxide are applied, and finally, the wipe is left to act for 8 hours (considering that the reactant liquid is applied directly to the reactive wipe and that an instantaneous reaction occurs, a high level of humidity is interpreted in the Monagas Variant table).

FIGURE 1: Reactive wipe (strip) with different concentrations of peroxide (Own elaboration)

On the other hand, to simultaneously ensure and rule out the possibility that the material itself (cellulose paper) from which the wipe is made reacted with the reagent and changed color in the absence of oxidants in the environment, an additional sample was added to the test as a "control." This was done by placing a reactive wipe in a container with no oxidants present and sealing it. The control wipe was then stored in a light-protected container. As can be seen in the following image, after almost a month since the test, the reactive wipe has not undergone any alteration.

FIGURE 2: Control wipe (strip) with reagent and closed in an environment without any oxidizing agent, after one month (Own elaboration)

3.2 Validation Steps:

The tests have been validated through the following steps:

1. Environmental conditions were verified to be suitable and reproducible for the required measurements. It was also verified that no other oxidizing sources were present in the environment.
2. Schönbein reagent wipes were used as easily accessible and manageable sensing elements. These were placed in the study area and then qualitatively verified (by checking the color) after 30 minutes and 8 hours.
3. Control Schönbein reagent wipes were also placed.
4. Oxidizing agent production, under controlled conditions, was evaluated for various purity ranges using the colorimetric reaction that developed and was observed on the surface of the Schönbein reagent wipes.
5. Once the results were obtained, a qualitative evaluation (by observing the color change) was performed in three ranges: Low, Medium, and High. For a rapid test of the presence of ambient oxidation of the OAF (Open Air Factor), the test wipe is placed in the environment and left for 90 minutes; for a more comprehensive test, 8 hours are allowed. The 90-minute rapid oxidation test will provide the reference results for quantitative calibration of the color techniques.

3.3 OAF Generator Validation:

Finally, to allow for future comparison with other oxidants, a study is conducted to examine the oxidative influence of hydroxyl radicals on Schönbein reagent wipes using a device that generates hydroxyl radicals from the OAF. The study is performed in a 1 m³ chamber. The status is monitored at the same time points as the previous exposures: 90 minutes and 8 hours.

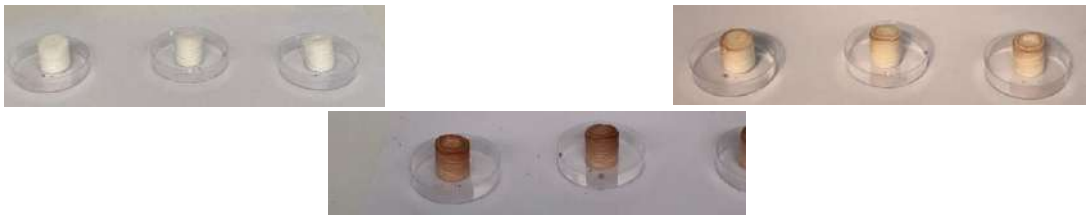

FIGURE 3: Results of the qualitative study. From left to right: test at start time, 90 min, and 8 h (Own elaboration)

The oxidation reactions are shown by the resulting color, providing percentage equivalencies for the purity of a known oxidant, such as hydrogen peroxide. The similarity in color and tone produced by different hydrogen peroxide purities coincides with the tones of the oxidations obtained under the influence of the OAF generating device.

The cellulose paper towel support, like a conventional test strip, can be used to quickly and qualitatively validate the presence of oxidants in the environment, as well as in the vicinity of devices or products that generate oxidants. Establishing this relationship allows for grouping by levels.

FIGURE 4: Result of the quantitative association of oxidation by OH· as a function of the color of the transition (Own elaboration)

The qualitative results obtained from the strips with colorimetric comparisons allow for the construction of a chromo-stoichiometry based on the average oxidative capacity observed in the different color ranges. This is equivalent to the oxidative capacity provided by this quantitative method, with a tolerance of approximately ±500 Kelvin. The numerical value associated with radical emission as a function of the degree of oxidation is then indicated.

3.4 Example with 17.5% Hydrogen Peroxide:

As a particular case, a photograph is shown taken for a wipe test after 90 minutes in an intrinsically humid environment, using hydrogen peroxide of 17.5% purity:

FIGURE 5: Qualitative result of the color change of a reagent strip with application of H_2O_2 at 17.5% (Own elaboration)

The quantitative value, according to the Monagas Variant, corresponding to the color obtained belongs to the HIGH oxidation level. Therefore, it is equivalent to a radical emission greater than 1.83×10^7 molec·cm^{-3}·s^{-1}.

IV. NUMERICAL COMPARISON AND RESULTS

4.1 Theoretical Model Results:

The relationship between the color change of potassium iodide test strips and the concentration of oxidizing species is based on a rigorous chromo-stoichiometric approach. This analysis uses the Schönbein Scale, which qualitatively correlates the observed color with the ozone (O_3) concentration in ppb under different relative humidity conditions. The quantification process begins with converting these concentrations to moles of substance and calculating the absolute humidity, essential factors for identifying O_3 as the limiting reactant in the reaction.

Based on this, the stoichiometric calculation is performed to determine the generation of hydroxyl radicals (OH·), thus obtaining an emission rate expressed in mol·cm^{-3}·s^{-1} after considering an eight-hour exposure period:

$$[OH\cdot] = \frac{26.8822 ppb_{O_3} 10^9}{8 \cdot 3600} = 9.3341 ppb_{O_3} 10^5 \left[\frac{molec}{cm^3 \cdot s}\right] \quad \textbf{(R12)}$$

*****Based on this equivalence, the Monagas Variant was constructed, which transforms a qualitative color scale into a quantitative scale of radiative emission.

In this way:

$$\text{Color (qualitative)} \rightarrow \text{Schönbein number} \rightarrow \text{OH· emission (quantitative)}$$

The chromaticity observed in the reactive wipes under exposure to OAF generators showed a direct correspondence with the values calculated using the Monagas Variant.

4.2 Oxidation Degree Classification:

Applying the Monagas Variant, a three-level classification was established based on OH· emission ranges:

TABLE 3
DEGREE OF OXIDATION BASED ON OH· EMISSION RANGE

Oxidation Degree	OH· Emission Range (molec·cm^{-3}·s^{-1})
HIGH	$> 1.8304 \times 10^7$
MIDDLE	$1.6762 \times 10^6 – 1.8304 \times 10^7$
LOW	$< 1.6762 \times 10^6$

Source: Own elaboration

4.3 Experimental Results:

Experiments conducted in a 1 m³ tank using the OAF generator demonstrated the system's remarkable responsiveness. In just 90 minutes, the color change reached a range equivalent to MIDDLE-HIGH, finally stabilizing at the HIGH level after 8 hours

of exposure. Additionally, tests performed with 17.5% H_2O_2 yielded similar results, with a change in the HIGH range that allowed for an estimated equivalent emission exceeding 1.83×10^7 molec·cm^{-3}·s^{-1}.

In contrast to the activity observed in the presence of oxidizing agents, tests conducted in control environments without these elements showed no color variation, even after a 30-day period, placing its equivalent emission at the LOW level. This data confirms the robustness of the Monagas Variant, as the model allows for rapid determinations in just 90 minutes with complete technical agreement with the measurements of the extended 8-hour model. Essentially, it confirms that it is not necessary to wait for the complete cycle to obtain a reliable reading of the oxidative potential.

V. DISCUSSION

The Monagas Variant proposal transcends the purely qualitative nature of traditional tools to establish itself as a quantitative method for estimating environmental radicals. When this approach is compared with the qualitative experimental design, it is observed that the intensity of the color change on the reagent strips fully coincides with the expected theoretical emission ranges. Furthermore, the color response obtained in just 90 minutes maintains a constant proportionality with the results after 8 hours of exposure, while the stability of the reagent support is confirmed by the absence of changes in oxidant-free environments, thus guaranteeing the sensor's reliability.

From a strictly quantitative perspective, the values achieved, which are on the order of 10^7 molec·cm^{-3}·s^{-1}, are closely related to the production of hydroxyl radicals (OH·) documented in the scientific literature. Specifically, these data align with the ozone photolysis at air-water interfaces described by Anglada et al. (2014) and with the values reported under natural high Open Air Factor (OAF) conditions. This strong consistency between the stoichiometric model, experimental results, and scientific precedents reinforces the validity of the proposal. In this context, the fact that ozone always acts as the limiting reactant technically justifies the direct reinterpretation of Schönbein's original chromatic scale in terms of radical emission.

The practical implications of this work are significant. The Monagas Variant provides an accessible, low-cost tool for monitoring environmental oxidative capacity and assessing OAF in indoor spaces. The ability to obtain reliable readings in just 90 minutes, rather than the traditional 8 hours, makes this method particularly valuable for rapid assessments in healthcare facilities, commercial buildings, and other indoor environments where air quality is critical.

VI. CONCLUSIONS AND FUTURE PROSPECTS

In conclusion, this research has successfully developed a robust chromo-stoichiometric model that transforms the traditional Schönbein Scale into a quantitative analytical tool. Thanks to the Monagas Variant, it is now possible to estimate OH· emission (expressed in molec·cm^{-3}·s^{-1}) by simply observing a color change, allowing for efficient classification into three intensity levels (LOW, MIDDLE, and HIGH) with a response time of only 90 minutes. This advancement translates the complexity of stoichiometry to a visual scale, offering an accessible protocol for maintenance and monitoring teams without the need for expensive laboratory equipment.

The results obtained demonstrate consistency with the scientific literature on atmospheric radical production, positioning this system as an extraordinary bridge between qualitative observation and quantitative estimation. Its accessibility, reproducibility, and low cost make it an ideal solution for monitoring ambient oxidation and assessing the Open Air Factor in indoor spaces, where accuracy and speed are crucial.

Finally, this work lays the groundwork for future research. The scientific community is encouraged to continue refining the methodology using more precise photometric and colorimetric sensors. This technical evolution would allow a shift from visual to digital interpretation, paving the way for the development of portable tools and mobile applications. Integrating this methodology into everyday devices would bring radical monitoring to an unprecedented level of ubiquity and accuracy in the field of environmental health.

ACKNOWLEDGEMENTS

The authors express their sincere gratitude to the institutional facilities and support provided for carrying out this research work.

CONFLICT OF INTEREST

The authors declare that there is no conflict of interest regarding the publication of this paper.

REFERENCES

[1] Anglada, J. M., Martins-Costa, M. T. C., Ruiz-López, M. F., & Francisco, J. S. (2014). Spectroscopic signatures of ozone at the air-water interface and photochemistry implications. *Proceedings of the National Academy of Sciences of the United States of America, 111*(32), 11618–11623. https://doi.org/10.1073/pnas.1411727111

[2] Carslaw, N., Fletcher, L., Heard, D., Ingham, T., & Walker, H. (2017). Significant OH production under surface cleaning and air cleaning conditions: Impact on indoor air quality. *Indoor Air, 27*(6), 1091–1100. https://doi.org/10.1111/ina.12394

[3] García Raurich, J., Torres Lerma, A., Monagas Asensio, P., Martínez Vimbert, R., Arañó Loyo, M., & Martínez Roldán, T. (2023). Stoichiometry and kinetics of hydroxyl radicals in air quality. *IJOEAR, 9*(6). https://doi.org/10.5281/zenodo.8094725

[4] George, C., Ammann, M., D'Anna, B., Donaldson, D. J., & Nizkorodov, S. A. (2015). Heterogeneous photochemistry in the atmosphere. *Chemical Reviews, 115*(10), 4218–4258. https://doi.org/10.1021/cr500648z

[5] Held, P. (2015). *An introduction to reactive oxygen species: Measurement of ROS in cells* (TechNote). BioTek Instruments, Inc. https://www.biotek.com/resources/white-papers/an-introduction-to-reactive-oxygen-species-measurement-of-ros-in-cells/

[6] Ruiz-Lopez, M. F., Francisco, J. S., Martins-Costa, M. T. C., & Anglada, J. M. (2020). Molecular reactions at aqueous interfaces. *Nature Reviews Chemistry, 4*(9), 459–475. https://doi.org/10.1038/s41570-020-0203-2

[7] Stone, D., Whalley, L. K., & Heard, D. E. (2012). Tropospheric OH and HO2 radicals: Field measurements and model comparisons. *Chemical Society Reviews, 41*(19), 6348–6404. https://doi.org/10.1039/c2cs35140d

[8] University Consortium for Atmospheric Research. (2025, March 15). *Making and using ozone indicators*. UCAR Center for Science Education. http://www.ucar.edu/learn/1_7_2_29t.htm

[9] Workman, M., & Frye, K. (2025, March 10). *Measuring tropospheric ozone*. JoVE Journal (Science Education Collection), DePaul University. https://web.unica.it/static/resources/cms/documents/joveprotocol10024measuringtroposphericozone.pdf

[10] Domènech, X., Jardim, W. F., & Litter, M. (2025, March 20). *Procesos avanzados de oxidación para la eliminación de contaminantes*. https://www.researchgate.net/publication/237764122_Procesos_avanzados_de_oxidacion_para_la_eliminacion_de_contaminantes

[11] World Health Organization. (2021). *WHO global air quality guidelines: Particulate matter (PM2.5 and PM10), ozone, nitrogen dioxide, sulfur dioxide and carbon monoxide*. https://www.who.int/publications/i/item/9789240034228

[12] Occupational Safety and Health Administration. (n.d.). *Table Z-1 limits for air contaminants - 1910.1000*. Retrieved March 12, 2025, from https://www.osha.gov/annotated-pels/table-z-1

[13] U.S. Food and Drug Administration. (n.d.). *Substances added to food (formerly EAFUS): Hydrogen peroxide*. Retrieved March 12, 2025, from https://hfpappexternal.fda.gov/scripts/fdcc/index.cfm?set=FoodSubstances&id=HYDROGENPEROXIDE

[14] U.S. Food and Drug Administration. (n.d.). *Substances added to food (formerly EAFUS): Ozone*. Retrieved March 12, 2025, from https://hfpappexternal.fda.gov/scripts/fdcc/index.cfm?set=FoodSubstances&id=OZON.

International Journal of Environmental & Agriculture Research (IJOEAR)
ISSN: [2454-1850]
[Vol-12, Issue-4, April- 2026]
Website: www.ijoear.com
Journal DOI: 10.25125/agriculture-journal

Integration of GPS-enabled Smart Telematics for Monitoring Subsidized Agricultural Machinery via Government FARMS Platform: A Framework for Manufacturers

Mr. Dhruvil Vasava[1*]; Mr. Saurav Sangada[2]; Dr. Mayur V. Jalu[3]

[*1]MBA in International Agribusiness Management, Anand Agricultural University, Anand
[2]International Agribusiness Management, Anand Agricultural University, Anand
[3]Department of Agricultural Engineering, Junagadh Agricultural University. Junagadh
*Corresponding Author

Received:- 02 April 2026/ Revised:- 14 April 2026/ Accepted:- 21 April 2026/ Published: 30-04-2026

Abstract— *Mechanization improves productivity, reduces labour dependence, and increases operational efficiency. Government subsidy programs aim to accelerate the adoption of agricultural machinery, but verifying proper utilization and ensuring compliance remain challenges. This study presents an industry-driven, pilot-tested framework developed by Agricultural Farm Machinery Manufacturer, integrating GPS-enabled smart telematics with the Indian FARMS (Farmer Assisted Remote Monitoring System) application. The framework focuses on Round Balers deployed under Crop Residue Management (CRM) subsidy programs. Pilot deployment demonstrates real-time monitoring, operational analytics, and compliance verification. Farmers also have access to VIN-based monitoring of their machines. Full integration with the FARMS platform is pending government approval. Key outcomes include transparency in subsidy utilization, optimized machine deployment, predictive maintenance, and evidence-based policy support. The study also addresses technical, economic, connectivity, and legal considerations for implementation.*

Keywords— Agricultural mechanization, GPS telematics, subsidy compliance, FARMS platform, machine utilization, digital agriculture, public–private collaboration.

I. INTRODUCTION

1.1 Need

Subsidized agricultural machinery, such as Round Balers under Crop Residue Management (CRM) programs, often suffers from under-utilization or misuse, limiting the effectiveness of government investment. There is a clear need for a systematic monitoring solution that:

- Tracks actual machine deployment and usage
- Ensures subsidy compliance and accountability
- Provides data-driven insights to manufacturers, policymakers, and farmers

1.2 Problem

Despite substantial subsidies, machinery usage is difficult to monitor due to lack of real-time visibility. Traditional monitoring methods are manual, error-prone, and non-scalable, reducing program effectiveness and limiting evidence-based policy decisions.

1.3 Objective

This study presents a pilot-tested framework developed by Agricultural Farm Machinery Manufacturer, using GPS-enabled smart telematics on Round Balers. The framework is designed to:

- Enable real-time monitoring of subsidized machines
- Support compliance verification and predictive maintenance
- Empower farmers with VIN-based performance tracking
- Prepare for future integration with the FARMS (Farmer Assisted Remote Monitoring System) platform, once government approval is obtained

II. LITERATURE REVIEW

2.1 Telematics in Agricultural Machinery

GPS-enabled telematics capture location, bale size, bale location, moisture content, and other operational parameters. Benefits observed in the pilot include optimized fuel use, reduced downtime, enhanced machine life, and quantification of field work. The pilot focus is on Round Balers due to their high subsidy value and operational traceability requirements.

2.2 Government Initiatives

Pilot projects in Punjab and Tamil Nadu have demonstrated reduced under-utilization of subsidized machinery using GPS monitoring. The manufacturer's pilot confirms the feasibility of real-time monitoring and compliance verification.

2.3 Technology Providers, Subscription, and Connectivity

Provider: Blackbox GPS Technology (an Indian GPS manufacturer)

Subscription Models:

- SIM subscription for data transmission
- Platform fees for dashboards, analytics, and VIN-based monitoring

Connectivity and Reliability:

- Single SIM with GPRS/2G fallback
- Edge buffering ensures offline data collection during connectivity loss
- FOTA (Firmware Over-The-Air) updates available for device maintenance

Impact on Monitoring:

- Minor delays may occur in real-time dashboards during connectivity issues
- Historical telemetry and compliance data remain intact due to edge buffering

2.4 Legal Aspect

Monitoring is limited to subsidized machinery. Explicit farmer consent is required; the practice is legal and compliant with the Digital Personal Data Protection (DPDP) Act, 2023.

III. CONCEPTUAL FRAMEWORK

The framework presented in this study has been developed by Agricultural Farm Machinery Manufacturer, leveraging insights from a pilot implementation of GPS-enabled telematics on Round Balers. It is an industry-driven solution, designed to be practical, secure, and compatible with government platforms such as FARMS, while remaining generalizable to other machinery categories in the future.

3.1 System Architecture

The proposed telematics framework for agricultural machinery monitoring is designed as a four-layer interoperable architecture, as shown in Figure 1, ensuring end-to-end data integrity and compliance with government integration standards.

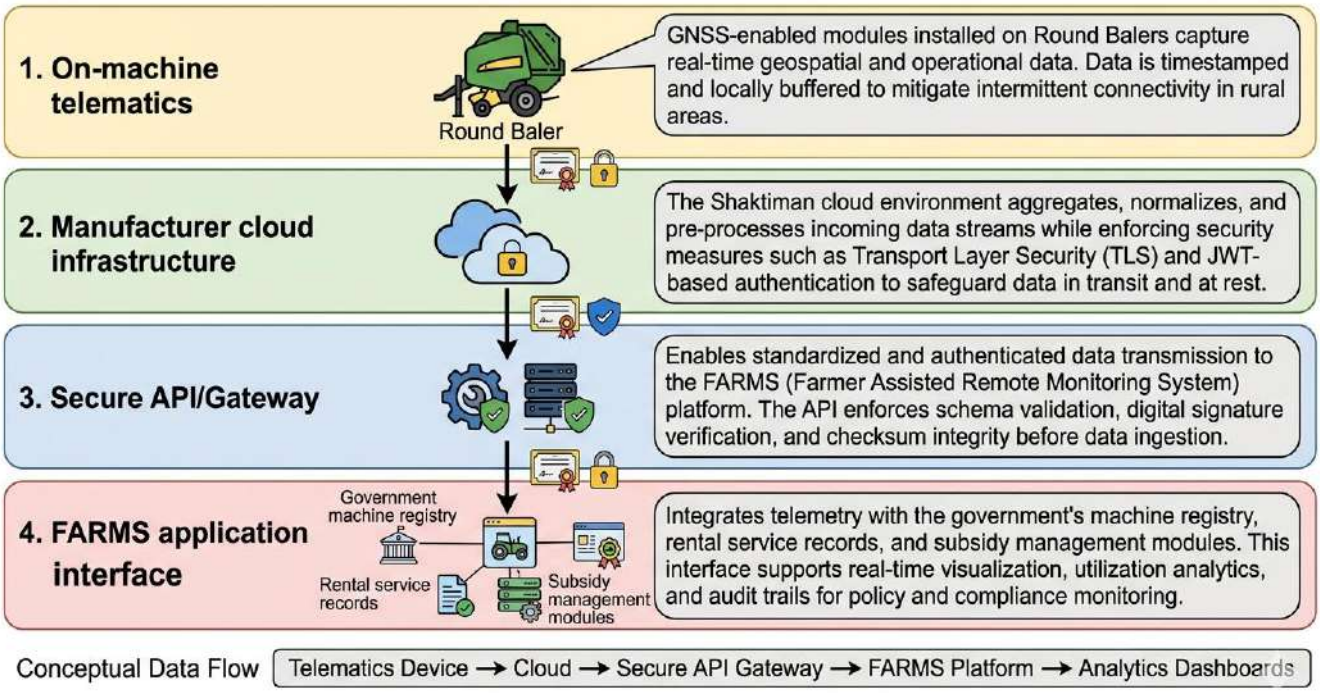

FIGURE 1: Four-layer architecture of the proposed telematics framework

1. **On-machine telematics** – GNSS-enabled modules installed on Round Balers capture real-time geospatial and operational data. Data is timestamped and locally buffered to mitigate intermittent connectivity in rural areas.
2. **Manufacturer cloud infrastructure** – The cloud environment aggregates, normalizes, and pre-processes incoming data streams while enforcing security measures such as Transport Layer Security (TLS) and JWT-based authentication to safeguard data in transit and at rest.
3. **Secure API/Gateway** – Enables standardized and authenticated data transmission to the FARMS (Farmer Assisted Remote Monitoring System) platform. The API enforces schema validation, digital signature verification, and checksum integrity before data ingestion.
4. **FARMS application interface** – Integrates telemetry with the government's machine registry, rental service records, and subsidy management modules. This interface supports real-time visualization, utilization analytics, and audit trails for policy and compliance monitoring.

Conceptual Data Flow:

Telematics Device → Cloud → Secure API Gateway → FARMS Platform → Analytics Dashboards

3.2 Data Schema and Security

The minimum required telemetry dataset includes:

- Unique Device ID
- Machine VIN/Serial Number
- Subsidy Scheme ID
- Timestamp (UTC)
- GPS Coordinates (Latitude, Longitude)
- Engine Hours
- Operation Mode / PTO Status
- Firmware Version

Data governance and security protocols ensure that:

- Access is restricted through role-based authentication
- Retention follows minimal and purpose-bound retention policies
- Farmer data is processed only under explicit consent, in full alignment with the Digital Personal Data Protection (DPDP) Act
- All transactions are logged and auditable to maintain accountability across stakeholders

3.3 Industry-driven Integration Rationale

- **Manufacturer Leadership:** Agricultural Farm Machinery Manufacturers are best positioned to deploy GPS-enabled telematics because they understand machine specifications, operational patterns, and maintenance needs.
- **Standardization:** Industry-led deployment ensures uniform data formats, device certification, and compliance with government standards.
- **Data Accuracy and Reliability:** Manufacturers can ensure proper installation, calibration, and firmware updates (FOTA), minimizing errors in telemetry and ensuring actionable insights.
- **Farmer Engagement:** Providing VIN-based monitoring dashboards directly from manufacturers builds trust, operational transparency, and incentive for proper machine usage.
- **Policy Alignment:** Close collaboration with government platforms, such as FARMS, enables manufacturers to support compliance verification, subsidy accountability, and evidence-based mechanization policies.
- **Scalability:** Manufacturer-led integration facilitates wider deployment across multiple machine types, starting with high-value subsidized equipment like Round Balers.

IV. METHODOLOGICAL APPROACH FOR MANUFACTURERS

The following six-step approach is recommended for manufacturers seeking to implement similar telematics-based monitoring systems:

1. **Device deployment** – Retrofit or embed telematics units, ensuring edge processing to classify field-work versus transport activity.
2. **Data normalization** – Incorporate subsidy identifier and standardize telemetry payload for government APIs.
3. **API integration** – Implement REST/MQTT endpoints or push mechanisms, enforcing message signing and replay protection.
4. **Certification and compliance** – Collaborate with government testing centers (FMTTIs) to ensure acceptance in subsidy programs.
5. **Farmer engagement** – Provide dashboards and advisory services to demonstrate benefits and increase trust.
6. **Analytics and reporting** – Enable utilization heatmaps, compliance dashboards, and anomaly detection for policymakers.

V. RESULTS FROM PILOT IMPLEMENTATION

The pilot deployment conducted by Round Balers under CRM subsidy programs yielded the following key results:

- **Real-time monitoring:** Successful tracking of machine location, operational status, and bale production metrics was achieved across the pilot deployment area.
- **Compliance verification:** The system enabled verification that subsidized machines were being used for intended agricultural purposes within designated operational zones.
- **Operational analytics:** Data on engine hours, field vs. transport activity, and bale production provided actionable insights for both farmers and manufacturers.

- **Connectivity resilience:** Edge buffering functionality ensured no data loss during temporary network outages, with seamless data synchronization upon reconnection.
- **Farmer engagement:** VIN-based monitoring dashboards were well-received by farmers, who reported increased confidence in machine utilization tracking.
- **Maintenance optimization:** Predictive maintenance alerts enabled timely service interventions, reducing unplanned downtime.

Pending government approval for full API integration with the FARMS platform, the pilot demonstrated that the technical framework is fully functional and ready for scaled deployment.

VI. Observed Outcomes and Policy Implications

- **Transparency and compliance:** The system ensures machines are used for intended purposes, reducing subsidy leakage and improving accountability.
- **Operational efficiency:** Rental hubs and individual farmers can optimize machine utilization based on real-time usage data.
- **Predictive maintenance:** Manufacturers can deliver data-driven service interventions, reducing downtime and extending machine life.
- **Evidence-based policymaking:** Aggregated anonymized data can inform allocation strategies, mechanization priorities, and subsidy redesign for government agencies.

VII. Challenges and Mitigation Strategies

Table 1
Challenges and Mitigation Strategies for Telematics Implementation

Challenge	Mitigation Strategy
Rural connectivity	Edge buffering, dual-SIM, LPWAN (Low-Power Wide-Area Network) fallback
Data privacy concerns	Explicit farmer consent, limited retention periods, audit logs
Device heterogeneity	Standardized data schema, certified telematics modules
Cost	Subsidized telematics or public–private partnerships to reduce farmer burden

VIII. Limitations and Future Directions

8.1 Limitations

- Full integration with the FARMS platform is pending government approval, limiting real-time data sharing with policy dashboards at present.
- The pilot was conducted on a single machine type (Round Balers) and may require adaptation for other agricultural equipment categories.
- Connectivity dependency remains a challenge in very remote rural areas despite edge buffering solutions.
- The pilot scale and duration were limited; larger-scale validation is recommended.

8.2 Future Directions

- Expand deployment to additional subsidized machinery types (e.g., tractors, harvesters, seeders).
- Integrate with state-level and national-level agricultural databases for comprehensive policy monitoring.
- Develop farmer-facing mobile applications for enhanced transparency and service booking.

- Explore integration with soil health and crop yield data to correlate mechanization with productivity outcomes.

IX. CONCLUSION

GPS-enabled smart telematics provide a transformative solution for monitoring subsidized agricultural machinery. The pilot demonstrates that even a single-machine focus, such as Round Balers, can yield real-time operational insights, ensure subsidy compliance, and reduce misuse.

Integration with the FARMS platform not only enhances transparency but also enables data-driven governance, allowing policymakers to allocate resources efficiently, optimize mechanization programs, and design evidence-based subsidy strategies.

For manufacturers, adopting secure, standardized telematics systems opens opportunities for predictive maintenance, improved operational efficiency, and stronger engagement with farmers, while ensuring regulatory compliance.

Ultimately, the combination of technology, policy integration, and farmer participation creates a sustainable model for mechanized agriculture, bridging the gap between subsidy intent and real-world utilization, and setting a precedent for scalable, accountable, and efficient agricultural mechanization across India.

CONFLICT OF INTEREST

The authors declare that there is no conflict of interest regarding the publication of this research paper.

REFERENCES

[1] Mehta, C. R., & Singh, R. (2020). GPS applications in precision agriculture and farm machinery. *Journal of Agricultural Engineering, 57*(2), 45–52.

[2] Food and Agriculture Organization of the United Nations. (2021). *Digital agriculture: Data-driven mechanization*. FAO.

[3] Tamil Nadu Department of Agriculture. (2023). *Pilot project on GPS-based subsidy monitoring*. Government of Tamil Nadu.

[4] Ministry of Agriculture & Farmers Welfare. (2023). *FARMS app guidelines*. Government of India.

[5] Singh, G., & Sharma, A. (2022). ICT-enabled solutions for farm machinery management. *Agricultural Engineering Today, 46*(3), 15–22.

[6] Indian Council of Agricultural Research. (2023). *Annual report on farm mechanization in India*. ICAR.

[7] Bureau of Indian Standards. (2022). *Standards for telematics devices in agricultural machinery*. BIS.

[8] Narayanan, P., & Jha, K. (2019). IoT-enabled farm mechanization: Opportunities and challenges. *Agricultural Reviews, 40*(4), 276–283.

International Journal of Environmental & Agriculture Research (IJOEAR)
ISSN: [2454-1850]
[Vol-12, Issue-4, April- 2026]
Website: www.ijoear.com
Journal DOI: 10.25125/agriculture-journal

Surgical Intervention for Dystocia in a Mehsana Buffalo in Chhattisgarh

Dr. Shailesh Vishal[1*]; Dr. Govina Dewangan[2]; Dr. Shraddha Diwan[3]

[*1]Teaching Assistant at Dau Shri Vasudev Chandrakar Kamdhenu Vishwavidyalaya, Durg, Chhattisgarh, India, 491001
[2]Assistant Professor at Dau Shri Vasudev Chandrakar Kamdhenu Vishwavidyalaya, Durg, Chhattisgarh, India, 491001
[3]Doctor at MVU Sakti, Chhattisgarh, India, 495689
*Corresponding Author

Received:- 02 April 2026/ Revised:- 11 April 2026/ Accepted:- 18 April 2026/ Published: 30-04-2026

Abstract— *The present case involved a 6-year-old Mehsana buffalo presented in Chitapadariya village, Jaijaipur block, Sakti district of Chhattisgarh, with a history of prolonged second stage of labor lasting more than 12 hours, with rupture of the water bag 6 hours prior to examination. The animal was restrained in left lateral recumbency, sedated with low-dose xylazine (0.05 mg/kg IM), and administered epidural anesthesia with 2% lignocaine. A ventrolateral approach was adopted. The uterus was sutured with Vicryl No. 2 in an inverting suture pattern before being replaced into the abdominal cavity after thorough lavage with normal saline and metronidazole solution. Muscle and peritoneal layers were closed with Vicryl No. 2 in a lockstitch pattern, and the skin with Silk No. 2 in a simple interrupted pattern. Postoperative care included administration of Intacef-Tazo (10 mg/kg IM for 7 days), meloxicam (0.5 mg/kg for 5 days), and Tribivet (15 ml IM for 5 days). The surgical site was cleaned daily with povidone-iodine, and skin sutures were removed after 10 days. The buffalo recovered uneventfully with no postoperative complications.*

Keywords— Dystocia, Cesarean section, Field surgery, Mehsana Buffalo, Chhattisgarh.

I. INTRODUCTION

n buffaloes (*Bubalus bubalis*), dystocia occurs more frequently than in cattle, primarily due to factors like a narrow pelvic canal, weak uterine contractions, oversized fetuses, abnormal fetal presentations, and various management shortcomings. The condition is observed more often in first-calving heifers than in multiparous buffaloes. The occurrence of dystocia is generally higher in buffaloes compared to other domestic animals [1]. The causes of dystocia are broadly categorized into maternal and fetal factors. In buffaloes, maternal dystocia has been reported to occur more frequently [2], although some studies have indicated a greater prevalence of fetal dystocia in this species [3]. A cesarean section is considered a suitable option in cases of dystocia when delivery of the calf through fetal manipulation and extraction is not possible. In bovines, eight surgical approaches are available for performing a cesarean section: standing left paralumbar celiotomy, standing right paralumbar celiotomy, recumbent left paralumbar celiotomy, recumbent right paralumbar celiotomy, recumbent ventral midline celiotomy, recumbent ventral paramedian celiotomy, ventrolateral celiotomy, and standing left oblique celiotomy [4].

The Mehsana buffalo is an important dairy breed in India, and dystocia in this breed can result in significant economic losses if not managed promptly. This case report describes the successful management of dystocia in a Mehsana buffalo via cesarean section under field conditions.

II. MATERIALS AND METHODS

A 6-year-old Mehsana buffalo from Chitapadariya village, Jaijaipur block, Sakti district of Chhattisgarh was presented with a history of prolonged second stage of labor lasting more than 12 hours. The owner reported rupture of the fetal membranes

approximately 6 hours prior to presentation, followed by repeated but unsuccessful attempts to deliver the fetus manually. There was no history of systemic illness, anorexia, or abnormal behavior before the onset of parturition. The parity of the animal was not specified by the owner.

A thorough clinical examination was carried out, including assessment of general health parameters such as rectal temperature, heart rate, respiratory rate, hydration status, and mucous membrane color, which were found to be within normal physiological limits. The per-vaginal examination revealed an abnormal fetal disposition (posterior presentation with bilateral hip flexion) with no likelihood of successful correction through manual manipulation or traction, indicating dystocia unsuitable for vaginal delivery. The fetus was determined to be stillborn based on absence of fetal reflexes and putrefactive changes. Based on the clinical findings and prolonged duration of labor, a decision was made to perform a cesarean section. The animal was properly restrained in lateral recumbency, and the surgical site was prepared following standard aseptic procedures. The cesarean operation was carried out using established obstetrical and surgical techniques under appropriate anesthesia.

III. RESULTS

3.1 Anesthesia and Restraint

The animal was sedated with xylazine at a low dose of 0.05 mg/kg administered intramuscularly. Xylazine administration causes bradycardia and reduction in salivary secretions [5]. Epidural anesthesia was performed with 60 ml of 2% lignocaine [6]. The animal was restrained in left lateral recumbency with both forelimbs and hind limbs tied separately. Adequate fluid replacement was administered with dextrose normal saline.

3.2 Surgical Site Preparation

The incision site was prepared on the ventrolateral aspect. Hair was clipped from a wide area around the intended incision site, and the area was scrubbed with antiseptic solution povidone-iodine (Fig. 1).

FIGURE 1: Site preparation

3.3 Surgical Procedure

The operative site was prepared by thoroughly shaving and scrubbing, followed by local infiltration anesthesia at the surgical site using 2% lignocaine. A skin incision was made, and the skin was carefully separated from the subcutaneous tissue. The underlying muscles were incised with care to avoid major blood vessels. Muscle layers were separated by blunt dissection to expose the peritoneum.

The uterus, usually covered by omental fat, was identified and an incision was gently made along the greater curvature of the uterus, avoiding the cotyledons. The fetus was removed promptly (Fig. 2). The uterine margins were rinsed with sterile normal saline. The placenta was removed.

FIGURE 2: Fetal extraction from the uterus

FIGURE 3: After completion of suturing

Closure of the uterus was performed using absorbable suture material (Vicryl No. 2) in a Cushing inverting pattern. The uterus was then replaced into the abdominal cavity after thorough lavage with normal saline and metronidazole solution. Any contaminants in the peritoneal cavity were removed by flushing with sterile normal saline and Metrogyl, and by manually scooping out debris. Before final closure, antibiotic pessaries were placed inside the uterus.

The muscle and peritoneal layers were sutured together using Vicryl No. 2 in a lockstitch pattern, and antibiotic powder was applied between suture layers to prevent infection. The skin was closed with Silk No. 2 in a simple interrupted pattern (Fig. 3).

3.4 Postoperative Care

The success of the operation depends on postoperative care. Antibiotics and anti-inflammatory drugs were administered postoperatively to combat toxemia. The following regimen was administered:

- Intacef-Tazo: 10 mg/kg bodyweight intramuscularly for 7 days
- Meloxicam: 0.5 mg/kg bodyweight intramuscularly for 5 days to prevent inflammation and adhesion formation
- Tribivet (15 ml): intramuscularly for 5 days

Owners were advised to clean the operative site daily with betadine for 2 weeks. The surgical site healed without any signs of infection or complications. The buffalo recovered uneventfully, with normal appetite and activity resumed within 5 days post-surgery. Sutures were removed 10 days postoperatively.

IV. DISCUSSION

Dystocia in buffaloes is a critical condition requiring prompt diagnosis and intervention. In the present case, the prolonged second stage of labor (>12 hours) with unsuccessful manual attempts necessitated surgical intervention. The choice of the ventrolateral approach was based on the animal's recumbent positioning and the need for adequate exposure of the reproductive tract.

The use of low-dose xylazine (0.05 mg/kg IM) provided adequate sedation while minimizing the risk of adverse effects such as bradycardia and reduced salivary secretions, as previously documented [5]. Epidural anesthesia with 2% lignocaine provided effective regional analgesia for the surgical procedure [6].

The ventrolateral approach adopted in this case allowed good access to the uterus while avoiding major blood vessels. The use of Vicryl No. 2 (an absorbable suture material) for uterine and muscle layer closure minimized the need for future suture removal and reduced the risk of adhesion formation. The Cushing inverting pattern used for uterine closure is considered standard for preventing leakage of uterine contents into the peritoneal cavity.

Postoperative management is crucial for successful outcomes. The administration of Intacef-Tazo (a combination of ceftriaxone and tazobactam) provided broad-spectrum antimicrobial coverage, while meloxicam effectively controlled inflammation and pain. Tribivet, a multivitamin preparation, supported recovery by addressing nutritional deficiencies that may arise during the stress of surgery and recovery.

The absence of postoperative complications in this case highlights the importance of aseptic technique, appropriate antibiotic therapy, and diligent wound care. The successful outcome demonstrates that cesarean section can be performed effectively under field conditions with proper planning and execution.

V. CONCLUSION

Dystocia in buffaloes is a critical condition requiring prompt diagnosis and intervention. When vaginal delivery is not feasible, cesarean section is an effective life-saving procedure. In the present case, the buffalo recovered uneventfully with no postoperative complications. Successful outcomes depend on proper surgical technique, aseptic management, and adequate postoperative care, which collectively ensure recovery and improved reproductive performance. Field veterinarians should be trained in basic cesarean section techniques, as timely surgical intervention can save both the dam and calf.

CONFLICT OF INTEREST

The authors have no conflict of interest.

AUTHOR'S CONTRIBUTION

SV, GD, and SD carried out the diagnosis, treatment, and post-operative care. SV and GD outlined the draft manuscript and were involved in the revision of the manuscript.

DATA AVAILABILITY STATEMENT

All essential data related to this study are contained within the article. Additional raw data can be obtained from the corresponding author upon request.

ACKNOWLEDGEMENT

The authors are thankful to the Veterinary Hospital In-charge, Sakti for support and the veterinary field officer, Malakharoda

REFERENCES

[1] Purohit, G. N., Barolia, Y., Shekhar, C., & Kumar, P. (2011). Maternal dystocia in cows and buffaloes: A review. *Open Journal of Animal Sciences, 1*(2), 41–53. https://doi.org/10.4236/ojas.2011.12006

[2] Roberts, S. J. (1986). Diseases and accidents during the gestation period. In S. J. Roberts (Ed.), *Veterinary obstetrics and genital diseases (Theriogenology)* (pp. 230–233). Woodstock, VT.

[3] Singla, V. K., Gandotra, V. K., Prabhakar, S., & Sharma, R. D. (1990). Incidence of various types of dystocia in cows. *Indian Veterinary Journal, 67*, 283–284.

[4] Schultz, G., Tyler, W., Moll, D., & Constantinescu, M. (2008). Surgical approaches for cesarean section in cattle. *Canadian Veterinary Journal, 49*(6), 565–568.

[5] Peshin, P. K., & Kumar, A. (1983). Haemocytological and biochemical effects of xylazine in buffaloes. *Indian Veterinary Journal, 60*, 981–986.

[6] Khurma, J., Choudhary, C. R., Sharma, V., Deeksha, & Singh, K. P. (2017). Cesarean section in Murrah buffaloes. *Indian Journal of Animal Research*, Article B-3370. https://doi.org/10.18805/ijar.B-3370.

International Journal of Environmental & Agriculture Research (IJOEAR)
ISSN: [2454-1850]
[Vol-12, Issue-4, April- 2026]
Website: www.ijoear.com
Journal DOI: 10.25125/agriculture-journal

Effect of Different Levels of Nitrogen and Biofertilizers on Growth and Yield of Cauliflower (*Brassica oleracea var. botrytis L.*)

Shrutika Bajpai[1], Deepti Srivastava[2*]; L.P. Yadav[3]; J.K. Singh[4]

[1]Department of Horticulture, C B G Ag PG College, BKT, Lucknow
[2-4]Assistant Professor, Department of Horticulture, Chandra Bhanu Gupt Agriculture PG College, BKT, Lucknow 226201
*Corresponding Author

Received:- 04 April 2026/ Revised:- 15 April 2026/ Accepted:- 20 April 2026/ Published: 30-04-2026

Abstract— *This study explores the effect of different nitrogen levels and biofertilizer on enhancing growth and yield of cauliflower. To evaluate the results, a field experiment was carried out at Agriculture Research Farm, C B G Ag PG College, BKT during 2024-25. The experiment was laid out in a factorial randomized block design with two factors in which the first factor contains three levels of nitrogen (0, 60, and 90 kg N ha⁻¹) and the second factor consists of two levels of biofertilizer i.e., Azotobacter (0 and 2 kg ha⁻¹), applied in different combinations with three replications, resulting in six treatment combinations: T_1 - Absolute control (0 kg N ha⁻¹ + no biofertilizer), T_2 - 0 kg N ha⁻¹ + Azotobacter @ 2 kg ha⁻¹, T_3 - 60 kg N ha⁻¹ + no biofertilizer, T_4 - 60 kg N ha⁻¹ + Azotobacter @ 2 kg ha⁻¹, T_5 - 90 kg N ha⁻¹ + no biofertilizer, and T_6 - 90 kg N ha⁻¹ + Azotobacter @ 2 kg ha⁻¹. The interaction effect results revealed that the yield parameters increased with certain levels of nitrogen along with Azotobacter inoculation. Maximum number of curds per plot (27.78), curd diameter (26.63 cm), fresh and dry weight of curd (159.83 g and 62.90 g), yield per plot (270.74 g) and yield per hectare (21.52 Q) were found with T_6 (90 kg N ha⁻¹ + Azotobacter @ 2 kg ha⁻¹), which was followed by T_5 (90 kg N ha⁻¹ + no biofertilizer). However, treatment T_1 (no nitrogen and without Azotobacter) resulted in the lowest yield significantly. It was observed that the optimum dose of nitrogen with biofertilizer can reduce the need for extra nitrogen application, as nitrogen is also received through organic source (Azotobacter @ 2 kg ha⁻¹). Therefore, biofertilizer has been identified as an alternative to chemical fertilizer that increases soil fertility and crop production in sustainable farming.*

Keywords— Nitrogen levels, Biofertilizers, Azotobacter, Interaction effect, Cauliflower.

I. INTRODUCTION

Cauliflower (*Brassica oleracea var. botrytis L.*) is one of the most important winter vegetable crops in the family Brassicaceae, with a chromosome number of 2n=18. It is grown throughout the country for its tender curd (aborted floral meristem), which is used for culinary purposes and processing for vegetable soup and pickling. Being a heavy feeder, cauliflower demands a constant supply of large amounts of nutrients for its luxuriant growth. Its productivity depends upon the use of balanced fertilizer; if not adequately fertilized, yield losses become apparent (Bashyal, 2013). The indiscriminate use of chemical fertilizer increases soil acidity, impairs soil physical conditions, reduces organic matter, and creates micronutrient deficiencies (Kashyap et al., 2017).

Nutritionally, cauliflower contains a good amount of vitamin B and a fair amount of protein in comparison to other vegetables, which may help protect against diseases like heart problems and cholesterol imbalances. Fresh curd of cauliflower contains 2.6 g protein, 0.4 g fat, 1 g minerals, 4 g carbohydrates, fiber, and 56 mg vitamin C per 100 g. Nitrogen is an essential plant nutrient involved in physiological processes and enzyme activities. Farmers are using urea extensively to enhance flowering, curd set, and increase curd size. Nitrogen affects crop productivity through controlling the synthesis of

several key products such as nucleic acids, proteins, and phospholipids. The optimum supply of nitrogen enhances plant growth and productivity. Moreover, the excessive and overuse of nitrogen may increase the accumulation of compounds such as nitrates and non-protein compounds in edible parts (Giri et al., 2023).

The application of biofertilizers in vegetable crops has been found very effective. However, biofertilizer i.e., Azotobacter might fix nitrogen fertilizer by 10-20% as it is capable of fixing atmospheric nitrogen and also converting insoluble phosphorus into soluble phosphorus for uptake by plants (Kumar et al., 2020). Therefore, an experiment entitled "Effect of different levels of nitrogen and biofertilizers on growth and yield of cauliflower" was conducted to assess the response of different levels of nitrogen, biofertilizers, and their interaction on cauliflower growth and yield.

II. MATERIALS AND METHODS

The present investigation entitled "Effect of different levels of nitrogen and Biofertilizer on yield of cauliflower (*Brassica oleracea var. botrytis*)" was carried out at the Agricultural Research Farm, Hajipur, Chandra Bhanu Gupt Krishi Mahavidyalaya, B.K.T., Lucknow (U.P.) during the Rabi season 2024-25. An area of 11 × 21 m size was separated into 18 plots having the size of 3 × 3.5 m, arranged in three replications. The experiment was laid out in a Factorial Randomized Block Design (FRBD) under 6 treatments.

2.1 Field Preparation

Field preparation was done by mold board plough once, followed by leveling and weeding manually. The soil of the seedbed was prepared to obtain good tilth. Well-decomposed FYM was mixed equally in each plot at 20 t ha^{-1} at final land preparation. Nitrogen-fixing biofertilizer Azotobacter (1% w/w) was applied at 2 kg ha^{-1}. Biofertilizer was mixed with 10 kg FYM and left overnight. This mixture was applied in the soil in the root zone of plants. The agro-meteorological data for the crop growing period were obtained from IISR. The mean maximum and minimum temperatures (34.5°C and 14.4°C) and relative humidity (98% and 64%) were recorded per week for the crop growing season.

2.2 Seed Preparation and Transplanting

The seeds of cauliflower cultivar PSB K-1 were sown in well-prepared nursery beds of 3 m × 1 m × 0.15 m dimension, in lines, and covered with a mixture of sand, soil, and farmyard manure, then covered with a thin layer of dried grass mulch and watered with the help of a rose can. Four-week-old healthy uniform seedlings were transplanted with a spacing of 45 cm from row to row and 60 cm from plant to plant, accommodating 10 seedlings per plot.

2.3 Fertilizer Application

Phosphorus (as Single Super Phosphate) and potash (as Muriate of Potash) were applied at 75 kg per hectare during land preparation. Nitrogen fertilizer (urea) at the rate of 100 kg per hectare was applied in two split doses (20 and 40 days) after transplanting as top dressing. Half the dose of nitrogen as specified in the treatment was applied through urea at final land preparation as a basal dose.

A solution of 1:10 biofertilizer was prepared by taking a bucket of adequate quantity of water and adding 100 g of biofertilizer, mixing properly. To allow the roots to receive the inoculum, 25-day-old seedlings were plucked from the nursery bed and immersed in this solution for approximately 25-30 minutes. Application of 80-120 kg N, 60-100 kg P_2O_5, and 60-120 kg K_2O is recommended for optimum yield. Half the dose of N and the entire amount of P and K were given at the time of transplanting. The balance N was given six weeks after transplanting or at the time of earthing up. Top dressing was applied in bands, and after each application, earthing up of plants was done. Bavistin at the rate of 1% was applied to overcome the problem of damping off disease.

Yield parameters of centrally tagged plants viz., number of curds per plot, curd diameter, fresh weight of curd, dry weight of curd, yield per plot, and yield per hectare were recorded. The mean values of triplicate data of different parameters were analyzed statistically. Data were subjected to ANOVA to evaluate the significance of treatment effects.

III. RESULTS AND DISCUSSION

The effect of different levels of nitrogen and biofertilizers on growth and yield parameters is presented in Table 1.

TABLE 1
EFFECT OF DIFFERENT LEVELS OF NITROGEN AND BIOFERTILIZERS ON YIELD PARAMETERS OF CAULIFLOWER

Factor/Level	No. of curd per plot	Curd diameter (cm)	Fresh wt. of curd (g)	Dry wt. of curd (g)	Yield per plot (g)	Yield per ha (Q)
Nitrogen Levels (A)						
A_1 (0 kg N ha^{-1})	17.61	17.47	135.09	50.94	266.99	14.8
A_2 (60 kg N ha^{-1})	24.12	22.52	152.23	58	319.16	23.46
A_3 (90 kg N ha^{-1})	27.07	25.86	172.41	64.07	379.82	28.03
SEM	0.344	0.28	0.442	0.508	0.6	0.332
CD at 5% level	1.098	0.895	1.412	1.621	1.916	1.061
Biofertilizer Levels (B)						
B_1 (No Azotobacter)	21.7	20.83	146.41	56.11	303.35	15.9
B_2 (Azotobacter @ 2 kg ha^{-1})	24.28	23.06	160.07	59.23	340.62	18.7
SEM	0.281	0.229	0.361	0.414	0.49	0.271
CD at 5% level	0.896	0.731	1.153	1.323	1.565	0.866
Interaction Effects (T)						
T_1 (0 kg N, no biofertilizer)	16.25	16.11	136.11	48.83	256.31	14.42
T_2 (0 kg N + Azotobacter)	18.97	18.83	143.2	51.37	259	15.34
T_3 (60 kg N, no biofertilizer)	22.63	21.3	148.17	54.2	262.82	20.01
T_4 (60 kg N + Azotobacter)	25.6	24.73	155.84	57.4	267.61	19.58
T_5 (90 kg N, no biofertilizer)	26.22	25.08	157.06	59.43	268.11	20.05
T_6 (90 kg N + Azotobacter)	27.78	26.63	159.83	62.9	270.74	21.52
SEM	0.78	0.78	1.996	6.38	6.31	3.876
CD at 5% level	0.486	6.397	7.625	1.233	3.998	8.47

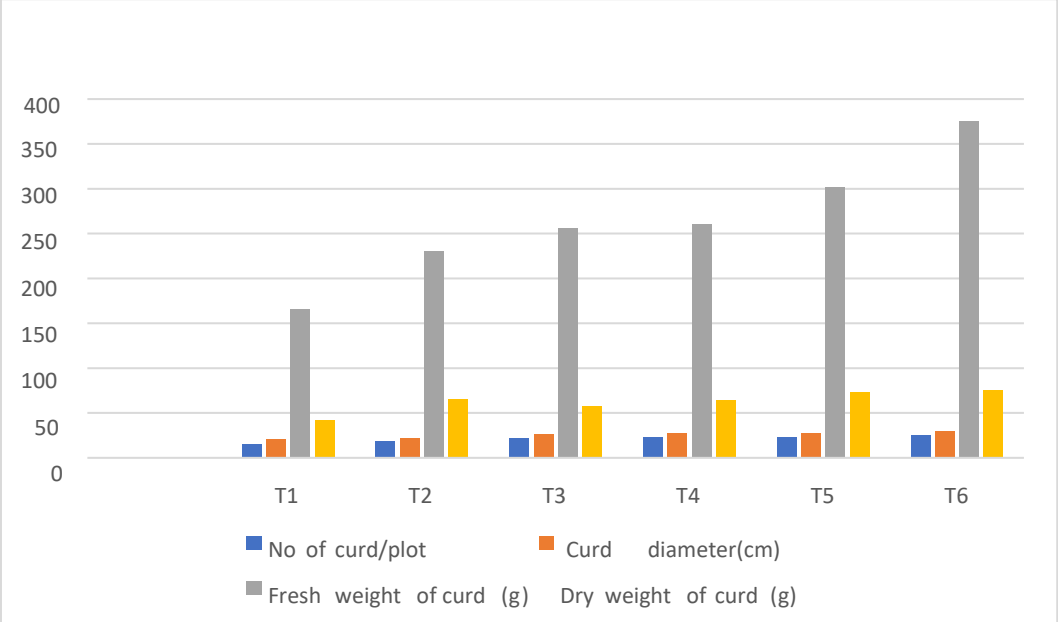

FIGURE 1: Interaction Effect of Biofertilizers and levels of Nitrogen on, No. of curd/plot Curd of diameter (cm), Fresh weight of curd (g) Dry weight of curd (g), Yield per plot and Yield per ha.

3.1 Nitrogen Effect

The main effects of nitrogen on number of curds per plot (27.07), curd diameter (25.86 cm), fresh and dry weight of curd (172.41 g and 64.07 g) were found maximum with treatment A_3 (90 kg N ha^{-1}), which was significantly higher than those recorded with A_2 (60 kg N ha^{-1}). Similar findings were reported by Kashyap et al. (2017) that fertilization with increasing levels of chemical nitrogen recorded a significant increase in yield parameters. Jat et al. (2015) reported in an experiment on cauliflower that crop fertilized with 200 kg N ha^{-1} recorded the highest plant height, diameter, and average weight of curd of cauliflower (*Brassica oleracea var. botrytis* L.). The results obtained in the present study are similar in line with Shrestha et al. (2022) on cauliflower variety Snowball-16.

3.2 Biofertilizer Effect

Application of biofertilizers on growth and yield parameters of cauliflower showed a significant increase in morphological and yield parameters as compared to control (nitrogen application without biofertilizer) treatment. However, maximum yield parameters i.e., number of curds per plot (24.28), curd diameter (23.06 cm), fresh and dry weight (160.07 g and 59.23 g), yield per plot (340.62 g), yield per hectare (18.70 Q) were produced under treatment B_2 (Azotobacter @ 2 kg ha^{-1}), which was significantly superior over treatment B_1 (without biofertilizer), where the number of curds per plot (21.70), curd diameter (20.83 cm), fresh and dry weight (146.41 g and 56.11 g), yield per plot (303.35 g) and yield per hectare (15.90 Q) were found significantly lower.

Kamdi et al. (2014) stated the significant effect of biofertilizers on growth, nodulation, and nitrogen fixation in legumes. Sharma et al. (2020) found that biofertilizer application in conjunction with nitrogen fertilizer improved net returns in cauliflower production. Singh and Singh (2005) evaluated the response of cauliflower cv. Snowball-16 to four biofertilizers (Azospirillum, Azotobacter, PSB and VAM) and two levels of nitrogen and phosphorus (75 and 100% of the recommended NPK dose of 120:60:60 kg/ha). Azospirillum + 100% of the recommended NPK recorded the highest values for growth, yield, and quality parameters. The increased supply of N and P and their higher uptake by plants might have stimulated the rate of various physiological processes in the plant and led to increased growth and yield parameters, resulting in increased pod and haulm yields in groundnut as reported by Bharathi et al. (2021). Similar results were recorded by Yamgar et al. (2001).

3.3 Interaction Effect

The interaction between different nitrogen levels and Azotobacter inoculation significantly impacted cauliflower yield. The main effects of nitrogen, biofertilizer, and their interaction were highly significant ($P < 0.01$) on curd yield (Table 1). The recommended dose of fertilizer (RDF) for cauliflower varies by region and soil but commonly ranges around 120:80:40 NPK kg ha^{-1}, particularly in regional studies.

Based on the results of Table 1, various yield parameters such as number of curds per plot, curd diameter, fresh weight of curd, dry weight of curd, yield per plot, and yield per hectare were observed statistically. The maximum number of curds per plot (27.78) was observed with treatment T_6 (90 kg N ha^{-1} + Azotobacter @ 2 kg ha^{-1}), which was significantly followed by 25.60 with treatment T_4 (60 kg N ha^{-1} + Azotobacter @ 2 kg ha^{-1}). Whereas, the minimum count of curds (16.25) was recorded with T_1 (Control). The significant difference between the treatments was found statistically.

However, treatment T_6 was found to be the best combination among all the treatments as it gave the maximum curd diameter (26.63 cm), which was followed by 25.08 cm with treatment T_5 (90 kg N ha^{-1} + no biofertilizer). The mean difference was found statistically significant among all the treatments. In the present investigation, observations showed the value 25.60 cm (T_4 - 60 kg N ha^{-1} + Azotobacter @ 2 kg ha^{-1}) was found at par with the value 24.73 cm with treatment T_3 (60 kg N ha^{-1} + no biofertilizer) significantly. This might be due to the prolonged availability of nutrients from biofertilizer-treated plots, which resulted in an increase in the diameter of the curd and ultimately the volume of the curd. The present findings are in line with those of Sanober et al. (2023) in broccoli. The minimum curd diameter (16.11 cm) was recorded with T_1 (control). Data presented on curd diameter showed a non-significant difference between treatment T_4 and T_5. The mean values are found at par with each other between T_4 and T_5.

The results revealed that yield parameters increased with an optimum dose of nitrogen along with Azotobacter inoculation. Based on the research investigation, it was found that optimum levels of nitrogen and biofertilizers had a significant effect on yield and yield-attributing characters. The observations recorded on gross curd weight clearly indicated that there was a significant difference among all the treatments on gross curd weight in cauliflower. Maximum values of fresh curd weight

(159.83 g) and dry weight of curd (62.90 g) were observed with treatment T_6 (90 kg N ha^{-1} + Azotobacter @ 2 kg ha^{-1}) significantly, which was followed by fresh weight (157.06 g) and dry weight (59.43 g) with treatment T_5 (90 kg N ha^{-1} + no biofertilizer). This might be due to the application of chemical fertilizers along with biofertilizers that increase the fresh and dry weight of plants, as reported by Srivastava and Ahlawat (1993). Kachari and Korla (2009) stated that the more gross plant weight could be attributed to optimum soil moisture in cauliflower.

In the present investigation, maximum yield per plot (270.74 g) and yield per hectare (21.52 Q ha^{-1}) was recorded with T_6 (90 kg N ha^{-1} + Azotobacter @ 2 kg ha^{-1}) significantly, which was followed by yield per plot (268.11 g) and yield per hectare (20.05 Q ha^{-1}) with treatment T_5 (90 kg N ha^{-1} + no biofertilizer). The values obtained by T4 and T5 showed all yield parameters i.e. No of curd (25.6 and 26.22).curd diameter (24.73 and 25.08 cm), Fresh weight of curd (155.84 and 157.06g) curd yield per plot (267.61 and 268.11kg) and yield per ha (20.05 and 21.52 Qha^{-1}) were found at par to each other which are found Non-significant to each other statistically. Zaki et al. (2012) concluded that in order to improve yield and reduce the use of N fertilizer, producing high yield of broccoli with high quality heads of broccoli plants of cv. Southern Star could be cultivated with a mixture of 75% organic + 25% mineral nitrogen and receiving biofertilizer containing a mixture of *Bacillus circulans*, *Bacillus megaterium*, and *Azotobacter*. Similar results were also recorded by Akanksha et al. (2023) that the yield was also found to be greatest with the treatment of Azotobacter along with the full dose of nitrogen. Hence, it was revealed that the application of biofertilizer i.e., Azotobacter with an optimum level of nitrogen fertilizer application resulted in higher yield parameters and yield, as application of biofertilizer increased the uptake and effective utilization of nutrients to enhance synthesis of carbohydrates, leading to the recombination of accumulated assimilates towards developing curds (Khedkar, 2023).

IV. CONCLUSION

On the basis of the results obtained in the present investigation, it was concluded that the yield parameters i.e., number of curds per plot (27.78), curd diameter (26.63 cm), fresh weight of curd (159.83 g), dry weight of curd (62.90 g), curd yield per plot (270.74 g), and curd yield per hectare (21.52 Q) obtained under treatment T_6 (application of 90 kg N ha^{-1} + Azotobacter @ 2 kg ha^{-1}) performed exceptionally well in all yield parameters. This was followed by treatment T_5 (90 kg N ha^{-1} + no biofertilizer). Thapa et al. (2022) reported that an adequate supply of co-limiting nutrients synergistically improves nitrogen uptake and assimilation efficiency within the plant. An integrated approach using biofertilizers to supplement a balanced nutrient value to the plant potentially reduces nitrogen application, which provides a cost-effective and environment-friendly way to achieve high yield in cauliflower.

CONFLICT OF INTEREST

The authors declare no conflict of interest.

REFERENCES

[1] Bashyal, L. N. (2013). Response of cauliflower to nitrogen fixing biofertilizer and graded levels of nitrogen. *Journal of Agriculture and Environment, 12*, 41–50. https://doi.org/10.3126/aej.v12i0.756
[2] Giri, B., Kumar, J., Thapa, P., Lal, M., & Chaudhary, R. P. (2023). The effect of different rates of nitrogen fertilizer application on the growth, yield and postharvest life of cauliflower. *The Pharma Innovation Journal, 12*(7), 307–309.
[3] Jat, M. L., Patel, M. M., & Bana, M. L. (2015). Effect of different spacing and nitrogen levels on growth and yield of cauliflower (*Brassica oleracea* var. *botrytis* L.) under north Gujarat condition. *Annals of Agriculture Research, 36*(1), 72–76.
[4] Kachari, M., & Korla, B. (2009). Effect of biofertilizers on growth and yield of cauliflower cv. PSB K-1. *Indian Journal of Horticulture, 66*(4), 496–501.
[5] Kale, T. S., Ghawade, S. M., Sonkamble, A. M., Paslawar, A. N., Gahukar, S. J., & Hadole, S. S. (2026). Effect of integrated nitrogen management on growth and yield contributing characters in turmeric (*Curcuma longa* L.). *International Journal of Advanced Biochemistry Research, 8*(10S), 281–286.
[6] Kamdi, T. S., Sonkamble, P., & Joshi, S. (2014). Effect of organic manure and biofertilizers on seed quality of groundnut (*Arachis hypogaea* L.). *The Bioscan, 9*(3), 1011–1013.
[7] Kashyap, L., Challa, V. R. P., & Tiwari, A. (2017). Effect of integrated nutrient management practices on carbon sequestration, carbon stock, plant growth parameters and economics of cauliflower. *International Journal of Current Microbiology and Applied Sciences, 6*(7), 1407–1415.
[8] Kashyap, S., Sandhu, S. K., & Biswa, B. (2025). Effect of growing environment and meteorological parameters on development of anthracnose disease of blackgram. *Journal of Food Legumes, 38*(2), 307–311.
[9] Khedkar, S. P., Mali, P. C., Khandekar, R. G., Salvi, V. G., Salvi, B. R., & Malshe, K. V. (2023). Influence of bio-fertilizers and organic manures on growth and yield of turmeric. *The Pharma Innovation Journal, 12*(8), 2825–2830.

[10] Kumar, A., Singh, G., Dhillon, N. S., & Verma, L. K. (2017). Impact of nitrogen on growth and yield of broccoli (*Brassica oleracea* L. var. *italica*) under open and protected environment. *International Journal of Current Microbiology and Applied Sciences, 6*(7), 1407–1415.
[11] Kumar, R., Verma, S., Singh, V., & Sharma, A. (2020). Effect of integrated use of nitrogen and biofertilizers on growth, yield and economics of cauliflower (*Brassica oleracea* var. *botrytis*). *Journal of Pharmacognosy and Phytochemistry, 9*(5), 2041–2044. https://doi.org/10.20546/ijcmas.2017.607.168
[12] Sanober Ali, Sapkal, D. R., Pandey, S., Kumar, C., & Sanyal, S. (2023). Effect of bio-fertilizers with chemical fertilizers on growth, yield, and quality of cauliflower (*Brassica oleracea* var. *botrytis*). *International Journal of Novel Research and Development, 8*(5). (ISSN: 2456-4184)
[13] Sharma, M., Gupta, R., & Thakur, A. (2020). Effect of biofertilizer and nitrogen levels on growth and yield of cauliflower. *Vegetable Science, 47*(1), 68–72.
[14] Shreshtha, S., Devkota, D., & Paudel, B. (2022). Effect of biofertilizer (*Azotobacter chroococum*) on growth and yield of cauliflower in Palung. *Plant Physiology and Soil Chemistry, 2*(1), 46–51.
[15] Singh, V. N., & Singh, S. S. (2005). Effect of inorganic and bio-fertilization production of cauliflower. *Vegetable Science, 32*(2), 146–149.
[16] Thapa, C., Pandey, S., Kumar, V., & Kumar, M. (2022). Effect of integrated nutrient management on growth and yield characteristics of cauliflower (*Brassica oleracea* var. *botrytis* cv. Snow Crown). *Biological Forum – An International Journal, 14*(4), 31–39.
[17] Yamgar, V. T., Kathmale, D. K., Belhekar, P. S., Patil, R. C., & Patil, P. S. (2001). Effect of different level of nitrogen, phosphorous and potassium and split application of N on growth and yield of turmeric (*Curcuma longa* L.). *Indian Journal of Agronomy, 46*(2), 372–374.
[18] Zaki, M. F., Tantawy, A. S., Saleh, S. A., & Helmy, Y. I. (2012). [Title missing]. *Environment and Ecology, 41*(4D), 3049–3053.

International Journal of Environmental & Agriculture Research (IJOEAR)
ISSN: [2454-1850]
[Vol-12, Issue-4, April- 2026]
Website: www.ijoear.com
Journal DOI: 10.25125/agriculture-journal

Global Fertilizer Supply Chain Disruptions during a Hypothetical Iran Conflict and Their Agricultural Impacts: A Scenario Analysis

Sanjeet Kumar Singh[1]; Abhay Singh[2*]

[1]Assistant Professor, Department of Entomology, Shri Murli Manohar Town Post Graduate College, Ballia, Uttar Pradesh, India - 277001

[*2]M.Sc. Scholar, Department of Agricultural Extension Education, Acharya Narendra Deva University of Agriculture & Technology (ANDUAT), Kumarganj, Ayodhya, Uttar Pradesh, India – 224229

*Corresponding Author

ORCID: 0009-0006-2891-2783

Received:- 06 April 2026/ Revised:- 13 April 2026/ Accepted:- 22 April 2026/ Published: 30-04-2026

Abstract— *The global fertilizer industry sustains more than eight billion people and represents one of the most geopolitically sensitive commodity systems on Earth. This comprehensive review systematically examines fertilizer production, consumption, import dependence, and trade dynamics across the United States of America, Israel, Gulf Cooperation Council (GCC) nations, and India – four geopolitically and agriculturally critical actors representing diverse positions on the fertilizer supply-demand spectrum. Against this backdrop, the paper analyses the potential cascading impacts of a hypothetical Iran-United States-Israel military conflict, which if it were to occur, would fundamentally disrupt Strait of Hormuz transit, elevate global urea prices by an estimated 19–28%, increase insurance premiums by over 50%, and reduce tanker traffic through the strait by approximately 75%. Drawing upon recent data from the International Fertilizer Association (IFA), Food and Agriculture Organization (FAO), World Bank, S&P Global Platts, and peer-reviewed agronomic literature, the study quantifies production capacity, consumption intensity, import vulnerability, and price transmission mechanisms for each examined country or region. The review further evaluates the historical precedent of the 2022 Russia-Ukraine conflict's fertilizer disruption, develops a multi-dimensional crisis-impact framework, and proposes evidence-based policy recommendations encompassing strategic reserves, supply diversification, biological input integration, and regional cooperation agreements. The findings reveal that India would face the most acute vulnerability among reviewed nations, with annual fertilizer import expenditure exceeding USD 12 billion and strategic reserve margins of less than 45 days. Gulf nations would simultaneously face market dislocation despite being major exporters, while the United States would confront price shock transmission affecting domestic agricultural competitiveness. The paper concludes that such a conflict would represent a structural stress test exposing systemic fragilities in global fertilizer architecture and would catalyse urgently needed diversification of supply chains, input substitution technologies, and international governance frameworks.*

Keywords— Nitrogen fertilizer, Strait of Hormuz disruption, Iran conflict scenario, Food security geopolitics, India fertilizer import, Biofertilizer, Strategic fertilizer reserves.

I. INTRODUCTION

The global fertilizer industry constitutes one of the most critical yet chronically underappreciated pillars of modern civilisation. Without the sustained application of nitrogen (N), phosphorus (P), and potassium (K) fertilizers, contemporary agricultural systems could support at most half the current global population at prevailing dietary standards. Since Fritz Haber and Carl Bosch demonstrated industrial ammonia synthesis in 1909, synthetic fertilizers have enabled a roughly

fourfold expansion of agricultural productivity per unit land area, fundamentally altering the relationship between population growth and food production capacity. Today, approximately 190 million metric tonnes (Mt) of fertilizer nutrients are applied globally each year, sustaining crop yields that feed roughly 4.1 billion people who could not otherwise be fed from available arable land under organic management regimes alone (IFA, 2025; Smil, 2004).

Yet this extraordinary productive achievement rests upon a supply chain architecture characterised by stark geographic concentration, substantial energy intensity, and deep sensitivity to geopolitical disruption. Nitrogen fertilizers – which comprise approximately 59% of total nutrient consumption – are synthesised primarily from ammonia produced via the Haber-Bosch process, which requires natural gas as both feedstock and energy source. Phosphate fertilizers derive from mined phosphate rock, concentrated in Morocco (which holds approximately 70% of identified global reserves), China, and a small number of other producing nations. Potash originates almost exclusively from Canada (Saskatchewan), Belarus, and Russia, with these three sources historically supplying over 70% of global muriate of potash (MOP) exports. This triple concentration in nitrogen energy sourcing, phosphate geology, and potash geography means that agricultural systems worldwide are perpetually vulnerable to supply shocks emanating from geopolitical developments far removed from the fields they ultimately serve.

A hypothetical full-scale military conflict between the United States, Israel, and Iran would dramatically crystallise this vulnerability. The Strait of Hormuz – through which approximately 30% of globally traded fertilizers pass, alongside 20% of world LNG trade essential for nitrogen fertilizer production – would become the epicentre of naval blockade, shipping insurance crisis, and route diversion. Within weeks of such a conflict, Middle Eastern granular urea would likely rise 19%, Egyptian urea 28%, DAP prices would surge, and freight rates for vessels transiting alternative routes would increase 35–45%. Nations heavily dependent on fertilizer imports would face immediate threats to their imminent planting seasons, with cascading risks to food availability, rural incomes, and national food security extending through the affected growing seasons and potentially beyond.

Against this backdrop, the present review pursues four interconnected objectives. First, it establishes a rigorous baseline of fertilizer production, consumption, and trade data for the United States, Israel, Gulf Cooperation Council (GCC) nations, and India – four actors selected for their significance in the global fertilizer system and their differential positioning as major producers, major consumers, or both. Second, it analyses the potential mechanisms through which such a conflict would transmit economic and physical disruption through the fertilizer supply chain to agricultural systems globally. Third, it examines historical analogues – particularly the 2022 Russia-Ukraine conflict – to contextualise potential disruptions within a broader pattern of fertilizer market fragility. Fourth, it proposes actionable policy frameworks for enhancing agricultural resilience through supply diversification, strategic reserve development, and accelerated adoption of alternative biological inputs.

The review synthesises data from the International Fertilizer Association (IFA), Food and Agriculture Organization (FAO), United States Geological Survey (USGS), World Bank commodity markets, S&P Global Platts fertilizer price indices, national statistics agencies, and peer-reviewed academic literature. The paper is structured to address each country-region systematically before analysing cross-cutting themes of crisis impact, historical precedent, and policy response.

II. FERTILIZER SUPPLY SYSTEMS AND EXTENSION LINKAGES

2.1 Global Production Landscape

Total global fertilizer production reached approximately 223 million metric tonnes (Mt) of product (or roughly 190 Mt of plant nutrients) in 2024, representing a recovery from the 2022–2023 disruption cycle triggered by the Russia-Ukraine war, European energy crisis, and associated price spikes. China remains the dominant producer across all three primary nutrient categories, producing approximately 49% of global nitrogen fertilizers, 27% of phosphate fertilizers, and 13% of potash. Russia, despite Western sanctions following its 2022 invasion of Ukraine, remained a leading fertilizer exporter throughout 2023–2025, with many developing nations – India, Brazil, and various African states – continuing to source Russian products given limited alternatives. The global fertilizer market reached a combined value of approximately USD 175 billion in 2024, down from the unprecedented USD 230 billion peak of 2022 but substantially above the 2019–2020 baseline of approximately USD 130 billion.

The supply structure exhibits critical concentration across each nutrient category. For nitrogen fertilizers, six countries – China, Russia, India, the United States, Indonesia, and Canada – account for approximately 68% of total production. For phosphates, Morocco/Western Sahara's OCP Group and Chinese producers together control over 55% of tradable phosphate

rock and finished fertilizer supply. For potash, Canada, Russia, and Belarus historically controlled approximately 70% of global export capacity, though Belarus-Russia sanctions following 2022 created temporary market dislocations since largely resolved through new supply agreements and substitution. These concentration patterns mean that any significant production disruption, export restriction, or transit route blockade in a small number of geographic locations would immediately create global market tension.

Table 1 presents the global production summary for major fertilizer types as of 2024, establishing the baseline against which subsequent country-specific analyses should be read.

TABLE 1
GLOBAL FERTILIZER PRODUCTION BY MAJOR TYPE AND LEADING PRODUCERS (2024, MT PRODUCT)

Fertilizer Type	Global Production (Mt)	Top Producer	% Share	2nd Producer	% Share
Urea (N)	189.4	China	47%	Russia	14%
Ammonium Nitrate	22.3	Russia	31%	Ukraine/EU	18%
DAP/MAP (P)	71.2	China	48%	Morocco	19%
TSP (P)	9.8	Morocco	39%	China	28%
MOP/Potash (K)	73.5	Canada	34%	Russia	22%
SOP (K)	7.6	Chile	28%	Germany	18%
Compound NPK	64.8	China	38%	Russia	11%

Source: IFA, 2025; USGS Mineral Commodity Summaries 2025; FAO, 2025

2.2 Global Consumption Patterns

Global fertilizer consumption distribution reflects both agricultural intensity and economic development. Asia – dominated by China, India, and Southeast Asia – accounts for approximately 60% of global nutrient consumption, driven by intensive rice, wheat, maize, and vegetable cultivation. The Americas, led by the United States and Brazil, account for approximately 22%. Europe, despite relatively high application rates per hectare, represents only about 12% given its smaller agricultural land base. Sub-Saharan Africa, despite vast agricultural land, contributes only approximately 3% of global consumption – reflecting both low application rates (often less than 20 kg nutrients/ha versus global averages of 135 kg/ha) and affordability constraints that such a crisis would dramatically exacerbate.

Consumption intensity varies widely even within regions. In East Asia, application rates of 300–400 kg nutrients/ha are common for intensive vegetable and rice cultivation, while large portions of Sub-Saharan Africa and South Asia's smallholder sectors apply less than 30 kg/ha. These differences reflect not only agronomic optimization but also market access, affordability, extension service reach, credit availability, and subsidy architecture. The political economy of fertilizer subsidies – prevalent across India, Indonesia, Egypt, Nigeria, and numerous other nations – creates both consumption incentives and fiscal vulnerabilities that would amplify the economic impact of supply disruptions.

III. FERTILIZER USE AND EXTENSION SUPPORT SYSTEMS IN THE UNITED STATES

3.1 Production Capacity and Industry Structure

The United States ranks as the world's third-largest nitrogen fertilizer producer and a significant manufacturer of phosphate fertilizers, though its domestic production capacity has evolved substantially over the past three decades. In 2024, the United States produced approximately 12.8 Mt of ammonia (anhydrous), generating roughly 8.5 Mt of urea, 6.7 Mt of ammonium nitrate, and 7.2 Mt of UAN (urea ammonium nitrate solution). The U.S. phosphate industry, centered in Florida and North Carolina, produced approximately 11.2 Mt of phosphate rock, generating around 4.8 Mt of DAP and 1.9 Mt of MAP. The United States is not a significant potash producer, possessing limited commercially viable reserves concentrated in New Mexico.

The domestic nitrogen industry is heavily concentrated in the Midwest and Gulf Coast, leveraging access to abundant and historically affordable natural gas from domestic shale production. Major producers include CF Industries (the world's largest nitrogen fertilizer producer by capacity), Nutrien (Canadian-owned with U.S. operations), OCI N.V., and Koch Fertilizer. The Florida phosphate industry is dominated by The Mosaic Company, which operates the world's largest integrated phosphate mining and fertilizer production complex, and Nutrien's phosphate operations. Collectively, U.S. fertilizer industry capacity represents a critical backstop for North American agricultural systems, though its competitiveness has been periodically challenged by lower-cost global producers in the Middle East, China, and Russia.

3.2 Consumption and Agricultural Demand

Total fertilizer consumption in the United States reached approximately 22.4 Mt of nutrients in 2024, representing application to approximately 340 million acres (137 million ha) of harvested cropland. Per-hectare application intensity averages approximately 163 kg nutrients/ha, reflecting intensive corn, soybean, wheat, and specialty crop cultivation systems. Nitrogen accounts for the largest share of consumption at approximately 12.7 Mt (as N), followed by phosphate at 4.8 Mt (as P_2O_5) and potash at 4.9 Mt (as K_2O).

The U.S. corn belt – encompassing Iowa, Illinois, Indiana, Minnesota, Nebraska, and surrounding states – represents the primary demand center, with corn requiring 150–200 kg N/ha and the crop's 95+ million acres driving enormous nitrogen market volumes. The shift in cropping patterns toward soybeans (which biologically fix nitrogen, reducing fertilizer demand) versus corn creates annual demand fluctuations of 8–12% based on planted acreage decisions. Cotton production in the South, winter wheat in the Great Plains, and vegetables and fruits in California and Florida generate substantial additional demand across all nutrient categories.

3.3 Trade Position and Import Dependence

Despite substantial domestic production, the United States maintains significant fertilizer trade flows in both directions. For potash – the fertilizer nutrient with the least domestic production capacity – the United States imports approximately 85–90% of consumption requirements, primarily from Canada (Nutrien, Mosaic) and, to a lesser extent, Russia and Belarus. These imports total approximately 5.5–6.0 Mt annually and would likely remain relatively stable given Canadian production reliability and proximity during a Gulf crisis. For urea, the United States has historically been a net importer of approximately 4–6 Mt annually (primarily from the Middle East, Russia, and Egypt), though domestic production expansion following the 2022 energy price shock has reduced import dependency modestly. For phosphate, the United States is a net exporter, selling approximately 3.5–4.0 Mt of DAP and MAP to global markets, primarily in South America and South and Southeast Asia.

Table 2 summarises the U.S. fertilizer trade balance by key product category, illustrating the country's complex dual position as both exporter and importer depending on nutrient type.

TABLE 2
UNITED STATES FERTILIZER TRADE BALANCE BY NUTRIENT CATEGORY (2024, MT)

Category	Domestic Production	Exports	Imports	Net Position
Nitrogen (N)	12.8 Mt NH_3 eq.	2.1 Mt	5.4 Mt	Net Importer
Phosphate (P_2O_5)	4.8 Mt	3.6 Mt	0.4 Mt	Net Exporter
Potash (K_2O)	0.4 Mt	0.1 Mt	5.6 Mt	Net Importer
Urea (finished)	8.5 Mt	1.2 Mt	4.8 Mt	Net Importer
DAP/MAP	6.7 Mt	3.9 Mt	0.5 Mt	Net Exporter

Source: USDA ERS, 2025; U.S. International Trade Commission, 2025; IFA, 2025

3.4 Potential Impact of a Hypothetical Conflict on U.S. Markets

A hypothetical Iran-U.S. conflict would create paradoxical effects on American fertilizer markets. While the United States would be one of the conflict's protagonists, its agricultural sector would face significant collateral economic damage. The disruption of Middle Eastern urea exports – particularly from Saudi Arabia's SABIC and Ma'aden, Qatari producers, and

Iranian facilities – would remove approximately 8–12 Mt of annual urea export capacity from accessible global markets, creating supply tightness that would drive domestic U.S. urea prices upward even as domestic production continued uninterrupted. Under such a scenario, the NOLA (New Orleans Louisiana) urea barge price index would likely surge from approximately USD 320/tonne (January 2026 baseline) to USD 425/tonne by early April of the crisis year – a 33% increase representing the steepest quarterly rise since 2022.

Elevated natural gas prices, with crude oil potentially crossing USD 100/barrel driving natural gas prices to USD 6.50–7.00/MMBtu, would simultaneously increase domestic production costs, compressing margins for U.S. producers despite higher selling prices. The net effect on U.S. corn farmers would be an estimated increase in per-hectare nitrogen cost of approximately USD 35–55, representing a 20–28% increase from baseline levels. For a typical 500-acre Iowa corn farm, this would translate to approximately USD 8,000–14,000 in additional input costs for the growing season – a material impact given prevailing corn price levels and farm profitability margins.

IV. ISRAEL: FERTILIZER PRODUCTION, CONSUMPTION, AND TRADE

4.1 ICL Group and the Dead Sea Potash Industry

Israel occupies a unique and strategically significant position in the global fertilizer industry disproportionate to its small geographic and population size. The Israel Chemicals Limited (ICL) Group – a diversified mining and specialty chemicals conglomerate – operates one of the world's major potash mining operations at the Dead Sea Works facility in Sdom, Israel. The Dead Sea, with its extraordinary mineral-rich brine, represents a remarkable geological endowment: the site produces potash through solar evaporation of Dead Sea brine, a process pioneered in Israel since the 1930s. Annual potash production capacity at the Dead Sea Works exceeds 3.5 Mt of MOP (muriate of potash), making Israel one of the world's top five potash producers and ICL among the four largest potash companies globally alongside Nutrien, Mosaic, and Belaruskali.

Beyond potash, ICL produces significant quantities of phosphate fertilizers. The Rotem Israel Phosphates subsidiary mines phosphate rock from the Negev Desert, extracting from the Zin and Oron deposits which represent part of the broader Tethys Sea phosphate belt extending from Morocco through Egypt, Jordan, and Syria. Israeli phosphate production reached approximately 3.1 Mt of rock in 2024, processed into approximately 1.1 Mt of phosphoric acid and 0.9 Mt of SSP (single superphosphate) and other downstream fertilizer products. ICL's integrated operations span mining, processing, specialty fertilizer manufacturing, and distribution, making it one of the few vertically integrated global fertilizer enterprises.

4.2 Domestic Consumption and Agricultural System

Israel's domestic fertilizer consumption, while small in absolute terms at approximately 0.26 Mt of nutrients annually (2024), is characterised by exceptionally high efficiency and technological sophistication. Israeli agriculture – particularly the intensive vegetable, flower, and orchard operations of the Negev Desert and Jordan Valley – pioneered and continues to refine fertigation (fertilizer application through drip irrigation systems), which achieves nutrient use efficiency of 85–95% versus the global average of approximately 50% for broadcast applications. Israel's application intensity of approximately 120 kg nutrients/ha of irrigated land reflects high-value crop intensity, while the fertigation approach dramatically reduces total input requirements relative to equivalent production systems in other countries.

Nitrogen represents the largest component of Israeli agricultural demand at approximately 110,000 tonnes annually, sourced primarily from domestically produced or imported ammonium nitrate and urea. Phosphate demand of approximately 60,000 tonnes is substantially met by domestic ICL production. Potash demand of approximately 90,000 tonnes is easily met by the massive Dead Sea Works output, with the vast majority of Israeli potash production exported globally. Israel maintains significant capability in advanced fertilizer formulations – coated release, nano-fertilizers, and biostimulant combinations – reflecting the country's research and development investment in precision agriculture.

4.3 Export Position and Global Market Role

Israel's significance in global fertilizer markets far exceeds its modest size through ICL's export operations. Approximately 3.2 Mt of potash is exported annually from the Dead Sea Works, reaching markets in Europe, Brazil, India, Southeast Asia, and China. Phosphate exports – including specialty phosphates, phosphoric acid, and downstream derivatives – add another 0.5–0.8 Mt annually, generating combined ICL fertilizer export revenues of approximately USD 4.5–5.5 billion per year depending on potash prices. ICL represents approximately 10% of global tradable potash supply, a market position sufficient to influence price formation during periods of supply tightness.

Under a hypothetical conflict scenario, ICL would face complex operational challenges despite Israel being a military participant. Geopolitical instability would elevate ICL's insurance and shipping costs, complicate logistics through regional ports, and deter some customers from placing new long-term purchase agreements given uncertainty about the conflict's duration and escalation risk. However, ICL's production operations themselves would likely remain largely unaffected, and global potash demand driven by spring planting seasons in the Northern Hemisphere would provide revenue resilience despite elevated operating costs.

V. GULF COOPERATION COUNCIL (GCC) NATIONS: THE FERTILIZER EXPORT POWERHOUSES

5.1 Saudi Arabia: SABIC, Ma'aden, and Nitrogen Fertilizer Leadership

Saudi Arabia has emerged over the past two decades as one of the world's most significant nitrogen fertilizer producers, leveraging its extraordinary natural gas endowment to manufacture urea and ammonia at globally competitive costs. The primary production entities are SABIC (Saudi Basic Industries Corporation) and Ma'aden (Saudi Arabian Mining Company), operating state-of-the-art gas-based nitrogen fertilizer complexes at Jubail and Ras Al-Khair. Combined, these facilities produce approximately 6.8 Mt of urea annually and 3.2 Mt of ammonia, representing approximately 4.5% of global urea supply. Saudi Arabia's natural gas feedstock cost advantage – historically USD 0.75–1.00/MMBtu versus USD 4–8/MMBtu in the U.S. and Europe – enables production at full cash costs of approximately USD 100–130/tonne urea, against global market prices of USD 250–450/tonne in recent years, generating extraordinary profit margins for state-linked producers.

Ma'aden's integrated phosphate project at Ras Al-Khair, fully operational since 2017, processes phosphate rock mined in the Al-Jalamid region of northern Saudi Arabia and manufactures approximately 3.0 Mt of DAP annually. This makes Ma'aden the world's third-largest DAP producer, with substantially all output exported to India, Pakistan, Australia, and other Asian markets. Saudi Arabia's combined fertilizer export revenues reached approximately USD 5.8 billion in 2024, representing a major non-oil revenue stream as part of Vision 2030's economic diversification agenda.

5.2 Qatar: Ammonia and Urea Giant

Qatar occupies a structurally distinct position in global fertilizer markets through its extraordinary natural gas reserves – the world's third-largest – and its Mesaieed Industrial City fertilizer complex. Qatar Fertiliser Company (QAFCO), the world's largest single-site nitrogen fertilizer producer until recently, operates six production trains generating approximately 3.8 Mt of urea and 1.6 Mt of ammonia annually. Qatar's competitive advantage derives from associated gas at essentially zero feedstock cost (as a byproduct of LNG production), creating the world's lowest-cost urea production economics. Qatar exports approximately 95% of its fertilizer output, making it almost entirely dependent on continued access to global shipping routes – a dependence that would be acutely compromised by a Strait of Hormuz disruption.

Under a hypothetical conflict scenario, the impact on Qatari fertilizer operations would be severe. While Qatar would likely maintain political neutrality in an Iran-U.S.-Israel conflict, an effective naval blockade and shipping insurance crisis would drastically reduce tanker departures from Mesaieed Port. Estimates suggest Qatari urea exports would decline by approximately 60–70% within the first month of such a conflict, with departures uncertain pending conflict resolution. The lost export volumes – representing approximately 150,000–200,000 tonnes/month – would be immediately reflected in global urea price spikes affecting India, Brazil, Europe, and East Asia simultaneously.

5.3 UAE, Oman, Kuwait, and Bahrain

The UAE operates FERTIL (Fertilisers & Chemicals Ltd.) at the Ruwais Industrial Complex, producing approximately 1.1 Mt of urea annually from associated gas. The Abu Dhabi National Oil Company (ADNOC) has invested substantially in expanding fertilizer production as part of the UAE's diversification strategy, with new capacity planned through 2027. Oman operates the Oman India Fertiliser Company (OMIFCO) plant in Sur, a joint venture with Indian entities, producing approximately 1.65 Mt of urea annually primarily destined for India under long-term offtake agreements. Kuwait Petrochemical Industries Company (KPIC) and Gulf Petrochemical Industries Company (GPIC) in Bahrain add further nitrogen fertilizer production capacity to the GCC total.

Aggregated across all GCC producers, the region produces approximately 14.5–16 Mt of urea annually and 4–5 Mt of ammonia designated for export. **Table 3** summarises GCC fertilizer production and export capacity by country, providing the quantitative foundation for assessing potential conflict-related disruption impacts.

TABLE 3
GCC FERTILIZER PRODUCTION AND EXPORT CAPACITY (2024 ESTIMATES)

Country	Annual Urea (Mt)	Ammonia (Mt)	DAP (Mt)	Export Share	Key Producer
Saudi Arabia	6.8	3.2	3	92%	SABIC / Ma'aden
Qatar	3.8	1.6	—	95%	QAFCO
UAE	1.1	0.5	—	85%	FERTIL / ADNOC
Oman	1.65	0.4	—	90%	OMIFCO
Kuwait	0.6	0.2	—	75%	KPIC
Bahrain	0.5	0.15	—	70%	GPIC
GCC Total	**~14.5**	**~6.0**	**~3.0**	**91%**	State-linked entities

Source: IFA, 2025; Company annual reports; GPCA (Gulf Petrochemicals and Chemicals Association), 2025

VI. INDIA: CONSUMPTION GIANT, PRODUCTION GAP, AND EXTREME IMPORT VULNERABILITY

6.1 Fertilizer Production Infrastructure

India operates one of the world's largest fertilizer manufacturing sectors in absolute output terms, yet its production capacity has chronically failed to keep pace with the demands of its vast agricultural system. The domestic fertilizer industry comprises approximately 30 large ammonia-urea units, 20 complex fertilizer units, and numerous small-scale straight fertilizer manufacturers, with a combined installed capacity of approximately 22.5 Mt of urea, 8.2 Mt of DAP/MAP, and 4.5 Mt of NPK compounds. In practice, effective production reached approximately 26.4 Mt of urea in 2024–25 (FY25), falling short of the approximately 35–36 Mt consumed domestically, requiring imports to bridge the gap. Production of DAP – the most widely used phosphatic fertilizer in Indian agriculture – reached only approximately 4.5 Mt domestically, against consumption of approximately 10–11 Mt, necessitating massive imports.

India's nitrogen fertilizer industry relies predominantly on natural gas as feedstock. The transition from naphtha-based (historically dominant) to gas-based production, supported by the government's New Investment Policy for urea (2012) and subsequent gas pooling mechanisms, has improved energy efficiency substantially. However, India's domestic natural gas production at approximately 90 MMscmd remains insufficient for both power sector and fertilizer sector demand, requiring LNG imports that now account for approximately 45% of gas supply to the fertilizer sector. This LNG dependency would create a direct channel through which Gulf-region disruptions – particularly blockades affecting Qatar's LNG exports – would translate into Indian fertilizer production cost increases, even before considering the impacts on finished fertilizer imports.

6.2 Consumption Scale and Agricultural Dependency

India is the world's second-largest fertilizer consumer, with total nutrient consumption of approximately 32.5 Mt in 2024–25. This demand is driven by intensive cultivation of rice, wheat, sugarcane, and cotton across approximately 140 million ha of net sown area, with an estimated 200 million ha of total cropped area including multiple cropping. Per-hectare fertilizer use averaging approximately 163 kg nutrients/ha belies enormous variation: irrigated wheat and rice areas in Punjab and Haryana may receive 300–400 kg/ha while dryland crops in Rajasthan, Madhya Pradesh, and Maharashtra receive 50–80 kg/ha. The Green Revolution's legacy, combined with the Nutrient Based Subsidy (NBS) scheme for P and K fertilizers and price control for urea, has shaped Indian fertilizer consumption patterns toward heavy nitrogen and relatively underweight phosphate and potassium, creating agronomic imbalances that reduce overall productivity.

Urea consumption alone represents approximately 33–35 Mt annually (product weight), making India the world's single largest urea consumer. The Government of India heavily subsidises urea, maintaining the Maximum Retail Price (MRP) at INR 242/45 kg bag (approximately USD 5.40/bag or USD 120/tonne) regardless of import cost, with the government bearing the difference as subsidy expenditure. In 2024–25, total fertilizer subsidy expenditure reached approximately INR 1.8 lakh crore (USD 21.6 billion), representing approximately 4.5% of total government expenditure and a substantial fiscal burden that would constrain the government's capacity to respond to price shocks through additional subsidy support.

6.3 Import Dependence and Trade Flows

India's fertilizer import dependence across key product categories represents perhaps the most acute supply chain vulnerability of any major economy. In 2024–25, India imported approximately 8.1 Mt of urea (meeting approximately 23% of urea demand), 6.0 Mt of DAP (meeting approximately 55% of DAP demand), 4.5 Mt of MOP (meeting approximately 90% of potash requirements, as India produces virtually no potash domestically), 1.8 Mt of NPK compounds, and approximately 1.1 Mt of ammonia. Combined, these imports represent total expenditure of approximately USD 12–14 billion annually – a substantial foreign exchange outflow and source of geopolitical vulnerability.

India's fertilizer import sources reflect pragmatic diversification within structural constraints. For urea, major sources include Russia (approximately 22%), China (approximately 18%), Saudi Arabia/Oman (approximately 28%), and Egypt/North Africa (approximately 15%). For DAP, China provides approximately 35%, Saudi Arabia/Ma'aden approximately 30%, Morocco approximately 12%, and Jordan approximately 8%. For MOP, Canada provides approximately 45%, Russia/Belarus approximately 30%, and Israel (ICL) approximately 15%. The geographic diversification of sources reduces but does not eliminate vulnerability to regional disruptions, as a Gulf conflict would simultaneously affect multiple major source regions.

Table 4 summarises India's fertilizer import dependence by nutrient category.

TABLE 4
INDIA FERTILIZER IMPORT DEPENDENCE BY NUTRIENT (2024–25)

Nutrient/Product	Domestic Production	Consumption	Import Volume	Import Share	Est. Import Value
Urea (N)	26.4 Mt	34.7 Mt	8.1 Mt	23%	USD 2.8 Bn
DAP (P)	4.5 Mt	10.4 Mt	6.0 Mt	58%	USD 3.5 Bn
MOP (K)	Negligible	4.8 Mt	4.5 Mt	94%	USD 2.1 Bn
NPK Compounds	4.8 Mt	6.9 Mt	1.8 Mt	26%	USD 0.9 Bn
Ammonia	12.1 Mt	13.2 Mt	1.1 Mt	8%	USD 0.5 Bn
TOTAL (all types)	**~47.8 Mt**	**~70.0 Mt**	**~21.5 Mt**	**~31%**	**~USD 9.8 Bn**

Source: Fertiliser Association of India (FAI), 2025; Department of Fertilizers GoI, 2025; Compiled from trade data

6.4 Potential Impact of a Hypothetical Conflict on Indian Agriculture

Under a hypothetical Gulf conflict scenario, India would face a multi-dimensional crisis that would be fundamentally more severe than that experienced by the United States or Israel given its extreme import dependence and limited financial cushion. The disruption would affect India through four simultaneous channels. First, physical supply disruption: approximately 50% of India's fertilizer imports – specifically Middle Eastern urea and Saudi DAP – would face shipping constraints due to Strait of Hormuz restrictions. Second, price transmission: import prices for urea would rise an estimated 22–28% in the first two months of such a crisis, generating significant subsidy cost increases threatening fiscal stability. Third, LNG price transmission into domestic production costs: Qatari LNG disruption would elevate Indian spot LNG prices, increasing domestic urea production costs by approximately USD 25–40/tonne. Fourth, farmer confidence effects: uncertainty about fertilizer availability ahead of the Kharif season (sowing begins May–June) would threaten planting decisions for approximately 140 million ha of summer crops.

Under such a scenario, the government's response would need to include emergency procurement through diplomatic channels (accelerating purchases from Russia and Egypt), activation of strategic buffer stocks maintained by the Fertiliser Coordination Committee, activation of emergency price-support measures for phosphate and potash products under the NBS scheme, and diplomatic overtures to alternative suppliers in Indonesia, Malaysia, and North Africa. However, the current buffer stock position remains tight: as of early 2026, urea stocks at approximately 8.5 Mt represent approximately 30–35 days of consumption, while DAP stocks of approximately 2.8 Mt represent only 25–30 days – a dangerously thin margin given the 45-day shipping transit time for alternative supply to reach Indian ports.

VII. FERTILIZER USE, PEST DYNAMICS, AND INTEGRATED MANAGEMENT

Fertilizer use has a direct influence on pest incidence in crops. High nitrogen application often increases the population of sucking pests such as aphids and leafhoppers. Imbalanced nutrient use can weaken plant resistance, making crops more vulnerable to insect attack. Therefore, proper nutrient management is important not only for yield but also for pest control.

Integrated Nutrient and Pest Management (INPM) combines the use of fertilizers with proper pest control methods. Instead of depending only on chemical inputs, farmers can use biofertilizers along with biopesticides to improve soil health and reduce pest pressure. This approach helps in maintaining crop yield while reducing input cost. It is especially useful during times when fertilizer supply is uncertain. INPM also supports sustainable agriculture by reducing environmental damage.

Agricultural extension plays an important role when there is a shortage of inputs like fertilizers. Extension workers guide farmers on how to use available resources more efficiently. They also provide information about alternative options such as organic manure and biofertilizers. During a potential supply crisis, extension services would help farmers adjust their practices and reduce risk. Timely advice from extension officers can prevent crop loss and improve decision-making at the farm level.

Farmer awareness is a key factor in improving fertilizer use efficiency. Many farmers still apply fertilizers based on habit rather than actual crop requirement. This leads to wastage and imbalance in soil nutrients. Through training programs and demonstrations, farmers can learn better practices such as soil testing and balanced fertilization. Increased awareness also helps in adopting integrated pest management practices, which reduce both fertilizer and pesticide use.

To reduce dependence on chemical fertilizers, extension systems need to promote practical and low-cost solutions. These include the use of compost, green manuring, and biofertilizers. Farmer field schools and village-level training can help in spreading these practices. In addition, digital advisory services can be used to reach more farmers quickly. Such strategies can reduce input costs and improve sustainability in the long run.

VIII. THE HYPOTHETICAL 2026 IRAN CONFLICT: MECHANISMS OF POTENTIAL FERTILIZER MARKET DISRUPTION

8.1 The Strait of Hormuz as a Critical Fertilizer Transit Chokepoint

The Strait of Hormuz – the narrow waterway between the Iranian coast and the Omani peninsula of Musandam – represents the single most consequential chokepoint for global commodity flows. Approximately 20 million barrels of crude oil pass through daily, alongside 20% of global LNG, 15% of petroleum products, and approximately 30% of global fertilizer trade. The strait's vulnerability derives not merely from its physical narrowness (approximately 33 km at its narrowest navigable width) but from the combination of Iranian coastal geography giving Iranian forces ideal positioning for anti-ship missile and drone operations, and from the limited alternative routing options for vessels otherwise transiting between Gulf ports and the Indian Ocean.

For fertilizer specifically, the Strait of Hormuz's criticality reflects the geographic concentration of GCC production capacity – all Saudi, Qatari, UAE, and Omani fertilizer production departs via ports accessible only through Hormuz transit. Unlike energy commodity disruptions (where pipeline alternatives exist for some volumes), fertilizer bulk carriers have no practical alternative route. Diversion via the Cape of Good Hope would add approximately 25–30 days to voyages from the Gulf to India, 15–18 days to Europe, and 20–22 days to Brazil, while dramatically increasing fuel and charter costs. These route extensions, combined with insurance premium surges (from approximately 0.05% to 0.3–0.4% of cargo value post-conflict), would render many voyages economically impractical at prevailing prices even when physical transit appears technically feasible.

8.2 Price Shock Transmission: Documented Market Effects

The price transmission from a Strait of Hormuz disruption through global fertilizer markets to farm-level costs would be rapid and substantial. Under a hypothetical conflict scenario, key price benchmarks would evolve as follows. Middle Eastern granular urea – the primary export product of Saudi, Qatari, and UAE producers – would rise from approximately USD 310/tonne (pre-crisis baseline) to approximately USD 369/tonne within six weeks, a 19% increase. Egyptian urea (a major alternative source) would surge even more sharply to USD 368–396/tonne given speculative purchasing and contract cancellations from regular Middle East sources. Baltic urea (traded in Northwest Europe) would rise from USD 380/tonne to USD 440/tonne, reflecting European concern about Russian supply reliability amid the broader geopolitical environment.

Indian import prices would rise from approximately USD 290/tonne CNF (cost and freight) pre-crisis to approximately USD 375–395/tonne within two months – a 29–36% increase.

DAP prices would follow a parallel trajectory, rising from approximately USD 560/tonne (pre-crisis) to USD 640–660/tonne. MOP prices would rise more modestly (approximately 8–12%) given that Canadian and Russian supply would not be directly affected by the conflict zone, with price tension driven primarily by speculative demand increases and logistics complications rather than physical supply losses. Ammonia prices – most sensitive to gas supply disruptions – would rise approximately 18–22% in the same period, transmitting upstream through the nitrogen fertilizer supply chain.

Table 5 presents estimated global fertilizer price movements under a hypothetical conflict scenario.

TABLE 5
ESTIMATED GLOBAL FERTILIZER PRICE MOVEMENTS UNDER HYPOTHETICAL CONFLICT SCENARIO (PRE-CRISIS TO +2 MONTHS)

Product	Pre-Crisis (USD/t)	Crisis (USD/t)	Change	% Change	Primary Cause
Middle East Granular Urea	$310	$369	+$59	19%	Export disruption
Egyptian Urea	$295	$378	+$83	28%	Demand substitution
Baltic Urea	$380	$440	+$60	16%	European stockpiling
India CFR Urea	$290	$385	+$95	33%	Gulf supply loss
DAP (India CFR)	$560	$645	+$85	15%	Ma'aden disruption
MOP (Standard)	$270	$302	+$32	12%	Logistics premium
Ammonia (Baltic)	$280	$332	+$52	19%	Gas market linkage

Source: S&P Global Platts Fertilizer; Argus Media; ICIS (estimated scenario impacts)

8.3 Shipping, Insurance, and Freight Rate Dynamics

Beyond direct commodity price movements, a Gulf conflict would generate unprecedented disruptions in the freight and insurance markets that service fertilizer trade. Marine insurance premiums for vessels transiting or planning to transit the Persian Gulf and Strait of Hormuz would increase from approximately 0.05% of hull value (standard industry baseline) to 0.35–0.45% within weeks – representing a seven- to nine-fold increase. For a Panamax bulk carrier with hull value of USD 25 million carrying 65,000 tonnes of urea, the single-voyage insurance premium would increase from approximately USD 12,500 to USD 87,500–112,500, equivalent to adding USD 1.15–1.73/tonne to cargo costs – modest in absolute terms but significant given the industry's thin margins.

More consequential than direct insurance costs would be the decisions by several major P&I (Protection and Indemnity) clubs and commercial marine insurers to apply war-risk exclusion clauses or require separate war-risk coverage endorsements for Gulf voyages. This would effectively make many charterers unable or unwilling to commit to Gulf loading ports, as potential liability for cargo loss would exceed available coverage limits at commercially viable premium levels. The resulting reduction in vessel availability would drive freight rates for Gulf-loading bulk carriers to unprecedented levels, with Panamax time-charter rates rising approximately 45% within the first months of such a crisis.

8.4 Historical Comparison: The 2022 Russia-Ukraine Fertilizer Disruption

The 2022 Russia-Ukraine conflict provides the most instructive historical precedent for understanding the potential mechanisms and trajectory of a Gulf disruption, though important structural differences exist. The 2022 shock removed Russia from approximately 20–22% of global fertilizer trade through a combination of Western sanctions, export restrictions implemented by Russia itself, and logistical complications. Russian urea, ammonium nitrate, and complex fertilizer exports fell approximately 30–40% from pre-war levels through the first six months of 2022, before alternative purchasing patterns

centered on India, Brazil, and African nations declining to comply with Western sanctions restored most Russian export volumes by late 2022 and 2023. Simultaneously, Russian natural gas supply disruption to Europe elevated European fertilizer production costs sharply, with many European ammonia producers reducing output by 50–80% at peak gas price levels in August–September 2022.

A Gulf conflict would differ structurally in several important respects. First, the volume of fertilizer supply disrupted would be potentially larger: GCC nations collectively produce approximately 14.5–16 Mt of urea (approximately 8–10% of global production), concentrated in the most trade-dependent export-oriented producers. Second, the disruption would be primarily logistical rather than sanctions-based, meaning there would be no sanction-evasion route available – physically blocking the strait would prevent exports regardless of buyer and seller willingness. Third, the disruption would simultaneously affect energy (LNG) and fertilizer supply, creating compound stress rather than isolated fertilizer market tightening.

The 2022 experience demonstrated that global markets, while experiencing severe price spikes (urea peaked at approximately USD 900/tonne in 2022), eventually adapted through expanded production by non-disrupted suppliers (primarily China initially, before China implemented export restrictions, and subsequently through North American and Middle Eastern non-Russian producers) and demand destruction in price-sensitive markets. Whether similar adaptation could occur within the timeline relevant to planting seasons remains uncertain, particularly for India whose Kharif planting window leaves minimal time for supply chain restructuring.

IX. BIOLOGICAL INPUTS AS CRISIS MITIGATION: EXPANDED ANALYSIS

9.1 Biofertilizers: Scientific Basis and Field Performance

Crisis-driven interest in biofertilizers as partial substitutes for synthetic nitrogen and phosphate fertilizers demands rigorous evaluation grounded in field performance data rather than promotional claims. Biofertilizers – preparations containing viable microorganisms including nitrogen-fixing bacteria (Rhizobium, Azotobacter, Azospirillum), phosphate-solubilizing bacteria (PSB), mycorrhizal fungi, and plant growth-promoting rhizobacteria (PGPR) – represent scientifically validated technologies with substantial agronomic evidence.

For leguminous crops, the case for biological nitrogen fixation is overwhelming. Effective Rhizobium inoculation of soybeans can supply 100–150 kg N/ha biologically, completely eliminating nitrogen fertilizer requirements for this crop. For non-legume crops (cereals, vegetables), the benefits are substantial but partial: meta-analyses of 130+ field studies across wheat, maize, and rice indicate that optimally formulated PGPR inoculants combined with mycorrhizal fungi could reduce nitrogen fertilizer requirements by 20–30% while maintaining yields within 5% of fully fertilised controls. Phosphate-solubilizing bacteria applications demonstrate reductions in phosphate fertilizer requirements of 15–25% in well-designed studies. The key qualification is consistency: results vary substantially with soil type, climate, crop variety, and application quality – meaning that blanket claims of 40–50% fertilizer substitution across all systems are agronomically unrealistic, though achievable in optimised systems.

9.2 Economic Feasibility and Scaling Constraints

The economic case for biofertilizer adoption as a crisis mitigation strategy is compelling in principle but faces practical scaling constraints. At current market prices (pre-crisis) in India, for example, biofertiliser inoculants are commercially available at approximately INR 50–120/ha (USD 0.60–1.45/ha) – representing a fraction of the INR 800–2,500/ha nitrogen fertilizer cost they would partially substitute. The cost-benefit ratio is clearly favourable for farmers. However, actual adoption rates for biofertilisers in India, despite subsidised availability and government promotion since the 1970s, remain below 15% of sown area – reflecting skepticism about consistency, inadequate extension services, poor quality control in commercial products, and habitual reliance on chemical inputs.

Scaling biofertiliser production rapidly in response to a crisis would face additional constraints. High-quality biofertiliser preparations require controlled fermentation conditions maintaining microbial viability above 10^8 colony-forming units per gram, refrigerated or cool storage logistics, and short shelf lives (typically 6–12 months). India's national biofertiliser production capacity of approximately 64,000 Mt annually could theoretically serve approximately 30–35% of sown area at

recommended application rates, but actual effective production quality reaching farmers falls significantly below this nominal capacity due to quality control failures along the supply chain.

X. POLICY RECOMMENDATIONS FOR ENHANCED FERTILIZER SECURITY

10.1 Strategic Fertilizer Reserve Systems

The most immediate and high-impact policy intervention available to import-dependent nations would be establishment of adequate strategic fertilizer reserves analogous in design to petroleum strategic reserves. India's current working stock of approximately 30–35 days for urea and 25–30 days for DAP is manifestly insufficient given the 45–60 day shipping transit time for alternative supply from non-Gulf sources to reach Indian ports. A strategic reserve of 90–120 days consumption would require capital investment of approximately USD 4–6 billion for India alone, plus ongoing carrying costs – a significant but justifiable expenditure given the USD 21+ billion annual subsidy cost and the economic consequences of inadequate supply.

The United States, despite being less import-dependent, should similarly consider establishing a strategic potash reserve given its 85–90% import dependence for this essential nutrient. The 2022 Belarus potash crisis (when Western sanctions removed approximately 20% of global potash export capacity within months) demonstrated that even Canada's large reserve capacity cannot instantaneously substitute for lost supply. A U.S. strategic potash reserve of 60–90 days consumption (approximately 3.0–4.5 Mt) would require approximately USD 0.8–1.2 billion at current prices – a manageable investment against the scale of U.S. agricultural output.

10.2 Supply Chain Diversification and New Source Development

All reviewed countries and regions require deliberate investment in fertilizer source diversification to reduce concentration risk. For nitrogen, this includes accelerating domestic ammonia-urea production from renewable hydrogen (green ammonia), which remains costly but represents a long-term path toward supply independence. Several jurisdictions – Germany, Australia, Morocco – have announced major green ammonia projects targeting 2027–2030 startup. For phosphate, Morocco's OCP Group dominates global trade to an extent that creates systemic risk: major phosphate-importing nations including India, Brazil, and various African states should consider joint ventures with OCP to secure dedicated offtake agreements and shared equity in production expansion, reducing exposure to any future supply restriction.

Regional cooperation frameworks can significantly enhance individual country resilience. Within South Asia, India and Bangladesh could negotiate pooled fertilizer procurement and shared strategic reserve arrangements, reducing per-country holding costs while maintaining collective security. The Gulf Cooperation Council's existing coordination mechanisms could be extended to cover fertilizer trade security, including provisions for maintaining production and export continuity during regional conflicts – potentially a confidence-building measure with broader diplomatic benefits.

10.3 Accelerating Nutrient Use Efficiency and Precision Application

The most sustainable path to reduced fertilizer import dependence is improving the efficiency with which applied nutrients translate into crop yields. India's nitrogen use efficiency (NUE) – the fraction of applied nitrogen that is actually taken up by the crop – averages approximately 30–35%, versus 50–60% achievable through split application timing, deep placement, enhanced-efficiency fertilizer formulations, and soil testing-guided rate calibration. If India's NUE could be improved from 33% to 45% (a realistic target within 5–7 years through technology diffusion), total nitrogen consumption would fall by approximately 8–10 Mt annually, reducing import dependence proportionally.

Israel's fertigation model – applying fertilizer in precisely calibrated doses through drip irrigation systems – represents the global standard for NUE, achieving 85–95% efficiency versus the global average of approximately 50%. Adapting fertigation principles for semi-arid crop systems in India, Pakistan, Egypt, and Sub-Saharan Africa presents significant practical challenges given investment costs, but targeted adoption in high-value crops (vegetables, fruits, cotton) could generate significant aggregate savings while demonstrating the technology's agronomic benefits to adjacent grain farmers.

10.4 Biological Transition Roadmaps

Governments of import-dependent nations should develop formal biological input transition roadmaps establishing clear adoption targets, quality standards, technology development milestones, and subsidy frameworks that progressively shift support from synthetic to biological inputs while maintaining farm profitability through the transition. India's PM PRANAM (Programme for Restoration, Awareness, Nourishment and Amelioration of Mother Earth) scheme – which incentivises state

governments to reduce chemical fertilizer consumption – provides a useful template that should be strengthened with binding reduction targets and expanded biofertiliser quality assurance infrastructure.

The United States, Israel, and GCC nations – despite being less import-dependent – have strong incentives to develop and export biological input technologies as a new component of agricultural technology trade. U.S. agricultural biotechnology companies (Corteva, BASF, Syngenta, and emerging startups) have invested substantially in biological nitrogen fixation and PGPR technologies that are approaching commercial-scale reliability. Development of these technologies for export to import-dependent nations represents both a commercial opportunity and a tool of agricultural development diplomacy that could contribute to long-term geopolitical stability.

XI. DISCUSSION

The convergence of geopolitical conflict, supply chain disruption, and the intensifying search for agricultural resilience revealed by the scenario analysed in this review would represent more than an episodic market disturbance – it would constitute a structural stress test for the global fertilizer system. The evidence examined in this review supports several overarching conclusions that merit sustained attention from policymakers, agronomists, economists, and strategic planners.

First, the geographic concentration of fertilizer production and export capacity in geopolitically volatile regions has created a systemic vulnerability that markets alone cannot efficiently manage. The fertilizer industry's response to the 2022 Russia-Ukraine crisis – price spikes followed by demand substitution, trade route adaptation, and modest production diversification – provided partial and temporary relief but did not address the underlying structural concentration risk. A Gulf crisis would affect a different but equally concentrated production region, suggesting that sequential shocks targeting different concentrations are not merely possible but arguably probable over a decade of sustained geopolitical tension.

Second, the differential vulnerability profiles of the reviewed countries illuminate the distributional justice dimensions of global fertilizer system fragility. India – with over 600 million people dependent on agriculture and a government committed to providing affordable fertilizer through substantial subsidy expenditure – would bear far greater proportional cost from supply disruptions than the United States, which has domestic production buffers, financial capacity to absorb price increases, and fewer people living near the margin of food insecurity. The political economy of global fertilizer governance is fundamentally asymmetric in ways that deserve recognition in international policy forums.

Third, the technological alternatives to synthetic fertilizer dependency – biofertilisers, precision application, enhanced-efficiency formulations, and ultimately green ammonia – are sufficiently developed to form the basis of a credible long-term transition strategy, though they require sustained investment, quality infrastructure, and behavioural change among millions of smallholder farmers. This transition cannot occur within a single growing season or even a single year, making the potential crisis primarily a wake-up call for investment that must begin immediately to yield security benefits within 5–10 years.

Fourth, international governance frameworks for fertilizer security are dramatically underdeveloped relative to frameworks for energy security (IEA's strategic petroleum reserve coordination), food security (FAO's emergency response mechanisms), and financial security (G20 stabilisation mechanisms). No equivalent institution monitors, coordinates, or provides emergency response for global fertilizer supply disruptions despite fertilizer's fundamental role in food production. The creation of an International Fertilizer Security Agency with mandate to monitor supply disruption risks, coordinate strategic reserve adequacy, facilitate emergency trade, and invest in supply diversification represents a governance gap whose costs would be borne by the world's most vulnerable agricultural populations during any future crisis.

XII. CONCLUSION

This comprehensive review has examined global fertilizer production, consumption, trade, and import dependence across the United States, Israel, Gulf Cooperation Council nations, and India, before systematically analysing the potential impacts of a hypothetical Iran-U.S.-Israel conflict on the global fertilizer system. The evidence establishes that global fertilizer supply chains are structurally fragile, geographically concentrated, and poorly protected against the recurring disruptions that characterise an era of elevated geopolitical tension.

Under such a scenario, the United States, as both a significant fertilizer producer and a potential military participant, would face paradoxical domestic agricultural costs including urea price increases of approximately 33% and elevated production costs that would threaten farm profitability in the approaching planting season. Israel, through ICL's Dead Sea potash operations, occupies a globally significant production position whose operational continuity during conflict would provide

some price stability in potash markets even as logistics costs rise. GCC nations – whose combined urea production capacity of approximately 14.5 Mt represents approximately 8–10% of global supply and 30% of globally traded volumes – would experience production continuity disruption through a Strait of Hormuz shipping crisis, with Qatar alone potentially losing approximately 60–70% of export capacity within the first month. India, with import dependence exceeding 90% for potash, 55–60% for DAP, and 23% for urea, facing strategic reserves measured in weeks rather than months, and with over 600 million agricultural livelihoods at stake, would confront the most severe and immediate crisis of all reviewed entities.

The policy framework needed to address this vulnerability is multi-dimensional: strategic reserve systems providing 90–120 days of consumption security; supply chain diversification reducing dependence on any single geographic chokepoint; NUE improvement programmes reducing absolute consumption requirements; biological input transition roadmaps progressively reducing synthetic fertilizer dependency; and international governance architecture capable of coordinating emergency response across the fragmented global fertilizer trading system. None of these measures is individually sufficient; collectively implemented, they offer a credible path toward a more resilient global fertilizer system capable of sustaining food security through the geopolitical uncertainties of the coming decades.

A hypothetical Gulf crisis would ultimately pass through conflict resolution, route adaptation, or demand response – as the 2022 crisis did. But the underlying structural vulnerabilities it would expose would persist until deliberately and systematically addressed. The most important legacy of such a scenario would be the political will to invest in that structural transformation before the next disruption occurs. Along with supply-side measures, strengthening agricultural extension services is equally important. Farmers need proper guidance on efficient fertilizer use and pest management practices. Combining nutrient management with pest control can help in reducing risk and improving sustainability.

ACKNOWLEDGEMENTS

The authors are grateful to the International Fertilizer Association (IFA), Food and Agriculture Organization of the United Nations (FAO), and the Fertiliser Association of India (FAI) for publicly accessible data repositories that informed this review. The views expressed are those of the authors and do not represent the positions of any government, institution, or company referenced in the text. The authors declare no financial conflict of interest

CONFLICT OF INTEREST

The authors declare that there is no conflict of interest regarding the publication of this research paper.

REFERENCES

[1] Al Jazeera. (2026, April 14). *Iran war: What is happening on day 46 of the US-Iran conflict?* https://www.aljazeera.com/news/2026/4/14/iran-war
[2] Argus Media. (2026, April 5). *Argus Fertilizer Daily: Gulf disruption drives global urea surge*. Argus Media Group.
[3] Britannica. (2026, April 14). *2026 Iran war*. https://www.britannica.com/event/2026-Iran-war
[4] CNN. (2026, April 13). *Trump warns Iran as US military blockade on Iranian ports takes effect*. https://www.cnn.com/2026/04/13/world/live-news/iran-us-war-trump-hormuz
[5] Cordesman, A. H. (2024). *The Gulf and the geopolitics of critical minerals and agricultural inputs*. Center for Strategic and International Studies.
[6] Department of Fertilizers, Government of India. (2025). *Annual report 2024–25*. Ministry of Chemicals and Fertilizers.
[7] Food and Agriculture Organization of the United Nations. (2026, April 3). *FAO Chief Economist warns of severe global food security risks from disruption to Strait of Hormuz trade corridor*. FAO.
[8] Food and Agriculture Organization of the United Nations. (2025). *World food and agriculture statistical yearbook 2025*. FAO.
[9] Fertiliser Association of India. (2025). *Fertiliser statistics 2024–25*. FAI.
[10] Gulf Petrochemicals and Chemicals Association. (2025). *Annual fertilizer report 2025*. GPCA.
[11] ICIS. (2026). *ICIS fertilizer price reports — Urea, DAP, potash, ammonia* (March–April). ICIS.
[12] International Fertilizer Association. (2025). *Assessment of fertilizer use by crop at the global level*. IFA.
[13] International Fertilizer Association. (2025). *World fertilizer trends and outlook to 2028*. IFA.
[14] Ma'aden (Saudi Arabian Mining Company). (2025). *Annual report 2024*. Ma'aden.
[15] McKinsey Agriculture Practice. (2022). *A reflection on global food security challenges amid the war in Ukraine*. McKinsey & Company.
[16] Mordor Intelligence. (2026). *Biopesticides market — 11% CAGR forecast 2026–2031*. Mordor Intelligence.
[17] Mosaic Company. (2025). *2024 annual report to shareholders*. The Mosaic Company.
[18] Nayak, K. K. (2021). *Bacillus subtilis* in sustainable agriculture: Versatility in pest management and plant growth promotion. *Environmental and Experimental Botany, 178*, Article 104210.
[19] Nutrien Ltd. (2025). *2024 annual report*. Nutrien.
[20] OCP Group. (2025). *Annual report and sustainability report 2024*. OCP S.A.

[21] Orozco-Mosqueda, M. C., Rocha-Padilla, A., Glick, B. R., & Santoyo, G. (2023). Plant growth-promoting bacteria as biofortification agents. *Trends in Plant Science, 28*(6), 645–659.
[22] Precedence Research. (2025). *Agricultural biologicals market size, USD 68.36 Bn by 2035*. Precedence Research.
[23] Qatar Fertiliser Company. (2025). *Operations and production report 2024–25*. QAFCO.
[24] Riaz, S., Ahmad, M., Hassan, M. U., & [Additional authors if available]. (2021). *Bacillus subtilis* as multifunctional bioinoculant for sustainable agriculture. *Microbiological Research, 254*, Article 126903.
[25] S&P Global. (2026, March 13). *Middle East war impacts global food security over fertilizer, fuel and freight*. S&P Global Commodity Insights.
[26] SABIC (Saudi Basic Industries Corporation). (2025). *Annual report 2024*. SABIC.
[27] Smil, V. (2004). *Enriching the Earth: Fritz Haber, Carl Bosch, and the transformation of world food production*. MIT Press.
[28] Springer Nature. (2025). Biofertilizers in sustainable agriculture: Mechanisms, applications, and future prospects. *Journal of Plant Growth Regulation*. https://doi.org/10.1007/s44279-025-00318-0
[29] United States Geological Survey. (2025). *Mineral commodity summaries 2025: Potash, phosphate rock, nitrogen*. USGS.
[30] Wikipedia. (2026, April 14). *2026 Iran war*. https://en.wikipedia.org/wiki/2026_Iran_war
[31] World Bank. (2025). *Commodity markets outlook: Fertilizer price projections 2025–2027*. World Bank Group.
[32] World Bank. (2026, April). *Food security update: Geopolitical impacts on fertilizer markets*. World Bank Group.

International Journal of Environmental & Agriculture Research (IJOEAR)
ISSN: [2454-1850]
[Vol-12, Issue-4, April- 2026]
Website: www.ijoear.com
Journal DOI: 10.25125/agriculture-journal

Horizontal Spread of Vanaraja Poultry Bird in Chandel District of Manipur after Intervention of FLD

Asem Ameeta Devi[1*]; Khumlo Levish[2]; K. Sonamani Singh[3]; Ts. Leenda[4]; P.S. Lavid[5]; Deepak Singh[6]

ICAR-Krishi Vigyan Kendra, Chandel
ICAR Research Complex for NEH Region, Manipur Centre, Lamphelpat-795004 (Imphal), Manipur
*Corresponding Author

Received:- 07 April 2026/ Revised:- 13 April 2026/ Accepted:- 19 April 2026/ Published: 30-04-2026

Abstract— *In Chandel district of Manipur, almost every rural household rears one or two livestock along with 5-10 desi birds under backyard poultry farming (BPF). Rearing of desi chickens is interwoven with the culture and tradition of tribal people and is kept for ritual purposes. According to traditional knowledge, black-coloured birds are used for medicinal purposes. However, the poultry sector in the district has remained rather stagnant due to the low productivity of native poultry varieties reared under the backyard system. Vanaraja is a breed of choice under the backyard system to augment poultry production in Chandel district of Manipur due to its coloured plumage, disease resistance, coupled with higher egg production and faster growth rate. This paper documents the horizontal spread of Vanaraja poultry birds following Front Line Demonstrations (FLD) conducted by Krishi Vigyan Kendra (KVK), Chandel, and assesses the impact on livelihood security of tribal farm women.*

Keywords— Vanaraja, Horizontal spread, Front Line Demonstration, Backyard poultry, Chandel district, Manipur.

I. INTRODUCTION

Poultry farming plays a vital role in improving the livelihood and nutritional security of rural households. Among the improved poultry varieties developed for backyard farming, Vanaraja birds have gained significant popularity due to their adaptability, higher productivity, and low input requirements. Developed by the ICAR-Directorate of Poultry Research, Hyderabad, Vanaraja birds are specifically suited for free-range and semi-intensive systems commonly practiced in villages.

Vanaraja birds are dual-purpose, providing both eggs and meat, which makes them an excellent source of regular income for farmers. They are hardy in nature, resistant to common diseases, and can thrive under scavenging conditions with minimal supplementary feeding. Compared to local indigenous birds, Vanaraja birds grow faster, attain higher body weight, and produce more eggs, thereby enhancing overall productivity.

Rearing Vanaraja birds requires relatively low investment, making it accessible to small and marginal farmers, landless labourers, and women entrepreneurs. Their ability to utilize locally available feed resources further reduces the cost of production. Additionally, the demand for desi-type eggs and meat in local markets ensures better pricing, contributing to increased profitability. Thus, Vanaraja bird rearing has emerged as a sustainable and profitable enterprise that supports rural livelihoods.

In Chandel district of Manipur, almost every rural household rears one or two livestock along with 5-10 desi birds under backyard poultry farming. Rearing of desi chickens is interwoven with the culture and tradition of tribal people and is kept for ritual purposes. According to traditional knowledge, black-coloured birds are used for medicinal purposes. However, the poultry sector in the district has remained rather stagnant due to the low productivity of native poultry varieties reared under the backyard system. The present study aims to document the horizontal spread of Vanaraja poultry birds in Chandel district following FLD intervention and assess its impact on livelihood security.

II. MATERIALS AND METHODS

The present investigation is based on Front Line Demonstrations (FLD) conducted on promoting backyard poultry in Chandel district by KVK Chandel. Under mandatory activities after standardization by ICAR Manipur Centre during 2000, the dual-purpose bird Vanaraja, a strain cross of PDP, Hyderabad, was reintroduced during 2009-10 (in September to November months) under the FLD programme.

Initially, KVK selected three villages in Chandel district: Tuishemi, Teraphai, and Khangshim. A total of 30 farmers (10 tribal farm women from each village) were selected. Each farm woman was provided with 25 started chicks (3-4 weeks old) in a ratio of 5:20 (male:female). Most of the farm women maintained Vanaraja birds under a semi-range system.

Initially, Vanaraja birds were introduced in selected villages through Krishi Vigyan Kendra, Chandel. Farmers were provided with chicks, training, and technical guidance on scientific rearing practices. These initial beneficiary farmers acted as demonstrators of the technology.

As the birds started showing better performance—such as faster growth, higher egg production, and better income—neighbouring farmers observed the benefits and became interested in adopting the practice. This led to horizontal spread through informal channels such as sharing of chicks, exchange of fertile eggs, and farmer-to-farmer learning.

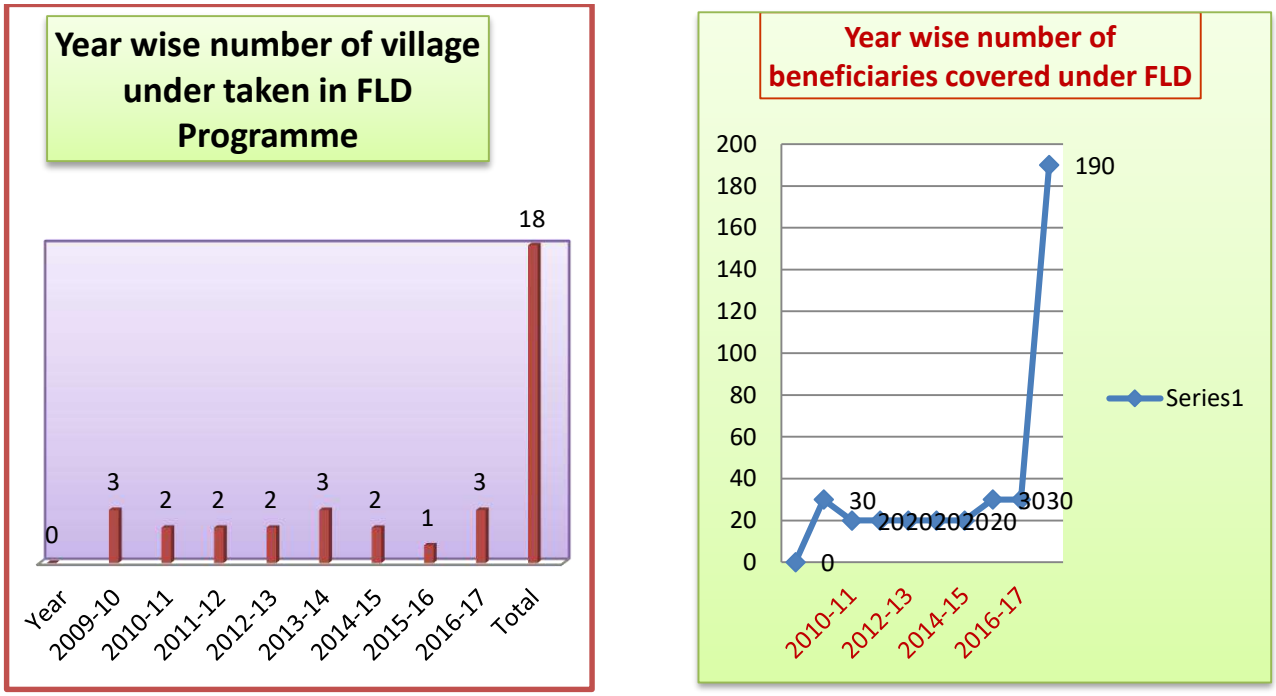

FIGURE 1: Details of villages adopted, number of birds distributed, and beneficiaries

III. RESULTS AND DISCUSSION

Vanaraja birds are more remunerative than the local desi bird (Kakyen). For this reason, Vanaraja has been widely accepted by many villagers. The acceptability among the people was found to be high, as these birds have a triple advantage in terms of colour and hardiness similar to local birds, early laying age, high egg-laying capacity, and higher weight gain over local

birds with minimal supplementation of locally available feed ingredients. Under these conditions, there is a wide demand for new improved birds among farmers, which started the popularization of Vanaraja from farmer to farmer and horizontal spread from village to village.

Villagers used to sell eggs for hatching purposes, which were brooded by local desi hens. Likewise, propagation expanded, and many villagers approached KVK for more training and more demand for Vanaraja chicks. The details of FLD results are described in graphical form.

FIGURE 2: Results of Front Line Demonstrations on Vanaraja birds

The rearing of Vanaraja birds under backyard or semi-intensive systems has shown significant improvement in growth performance, egg production, and income generation compared to local indigenous birds. The results from various field observations indicate that Vanaraja birds attain an average body weight of about 2.5–3.0 kg at 15–16 weeks of age, which is considerably higher than local birds of the same age. This faster growth rate contributes to early marketing and quicker returns.

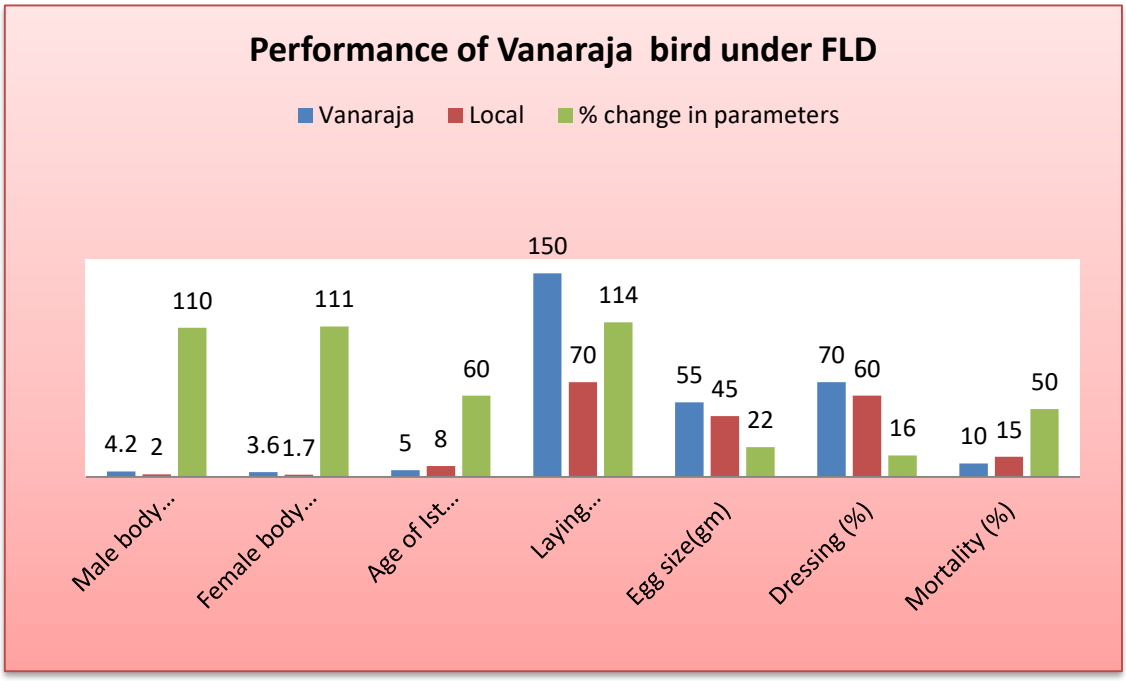

In terms of egg production, Vanaraja birds lay around 140–160 eggs per year under improved management practices, whereas local birds usually produce only 70–80 eggs annually. The eggs are larger in size and have good consumer preference due to their brown shell and desi-type characteristics, which fetch a higher market price.

Mortality rate in Vanaraja birds is relatively low when basic healthcare, vaccination, and proper housing are provided. Their hardy nature and adaptability to scavenging conditions reduce the risk and cost associated with intensive management. Farmers reported better survivability and disease resistance compared to exotic breeds.

Economically, Vanaraja bird rearing has proven to be profitable. The combination of higher egg production, better growth rate, and premium market value of eggs and meat results in increased net income. The use of locally available feed resources and minimal input costs further enhances the benefit-cost ratio. Additionally, this enterprise provides supplementary income, especially for rural women and smallholder farmers, contributing to household livelihood security.

Rearing of Vanaraja birds can offer immense potential in rural areas by providing regular income throughout the year, along with suitable employment, food security, and other livelihood benefits in Chandel district. The horizontal spread of Vanaraja bird rearing from one village to another in Chandel district demonstrates the effectiveness of farmer-led technology dissemination supported by extension services. The visible success in terms of higher egg production, better growth performance, and increased income has encouraged neighbouring farmers to adopt this improved poultry variety.

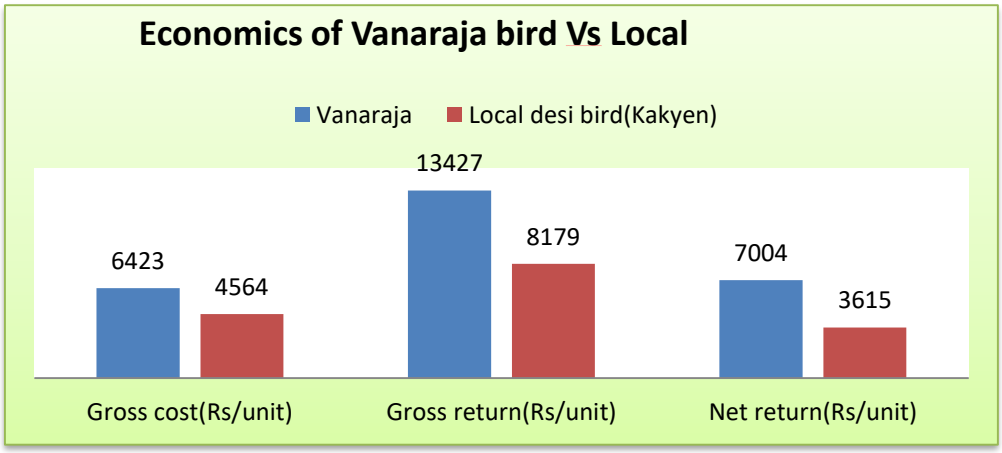

TABLE 1

COMPARATIVE PERFORMANCE OF VANARAJA AND LOCAL DESI BIRDS UNDER BACKYARD SYSTEM

Parameter	Vanaraja Birds	Local Desi Birds (Kakyen)
Average body weight at 15-16 weeks	2.5-3.0 kg	1.0-1.5 kg
Annual egg production	140-160 eggs	70-80 eggs
Egg colour	Brown	White/tinted
Disease resistance	High	Moderate
Age at first laying	5-6 months	6-8 months
Market preference	High (desi-type)	Moderate

IV. CONCLUSION

The widespread adoption of Vanaraja bird rearing has contributed significantly to livelihood improvement, nutritional security, and employment generation in Chandel district. It serves as a sustainable and scalable model for rural development, particularly benefiting small and marginal farmers and women in the district. The widespread performance of Vanaraja birds across villages indicates their acceptability among farmers due to low input requirements, scavenging ability, and comparatively higher productivity than local indigenous birds. Overall, the rearing of Vanaraja birds can be considered a sustainable and profitable enterprise, especially for small and marginal farmers, playing a significant role in improving the rural economy and supporting poverty alleviation.

ACKNOWLEDGEMENT

The authors are highly thankful to the Director of ICAR Barapani, Director of ATARI, and HORC, ICAR Manipur Centre for financial support for carrying out the FLD on Vanaraja birds.

REFERENCES

[1] ICAR-Directorate of Poultry Research. (2015). *Vanaraja poultry: A dual purpose bird for rural backyard farming*. Hyderabad, India.

[2] Singh, R. K., Sharma, P., & Kumar, A. (2017). Performance of Vanaraja birds under backyard system in rural areas. *Indian Journal of Poultry Science, 52*(2), 215–218.

[3] Roy, A., Datta, S., Roy, P. S., Biswas, S., & Mishra, S. P. (2018). Comparative assessment of production and hatchability performance of Vanaraja, Rhode Island Red and indigenous poultry birds under backyard rearing system at West Bengal. *International Journal of Livestock Research, 8*(7), 296–303.

[4] Devi, A. A., Levish, K., Singh, K. S., Monsang, T. L., Anal, P. L., & Kumar, H. (2025). Comparative performance of CARI Nirbheek, Vanaraja and local desi bird under backyard system of rearing in Chandel District of Manipur, India. *Journal of Advances in Biology & Biotechnology, 28*(9), 888–893.

[5] Kumar, V., Rajkumar, U., Prince, L. L. L., Rama Rao, S. V., & Chatterjee, R. N. (2021). *Geographical distribution of Vanaraja chicken variety and its impact on poultry sector in India*. Indian Poultry Science Association.

[6] Banja, B. K., Ananth, P. N., Singh, S., Behera, S., & Jayasankar, P. (2017). A study on the frontline demonstration of backyard poultry in rural Odisha. *Livestock Research for Rural Development, 29*(5).

International Journal of Environmental & Agriculture Research (IJOEAR)
ISSN: [2454-1850]
[Vol-12, Issue-4, April- 2026]
Website: www.ijoear.com
Journal DOI: 10.25125/agriculture-journal

The Effect of Papaya Fruit Peel Extract (*Carica papaya* L.) on The Percentage of External Offal in Broiler Chickens

Sebayang, N. D.[1]; G. A. M. K. Dewi[2]; M. Wirapartha[3]; dan N. P. M. Suartiningsih[4*]

Faculty of Animal Husbandry, Udayana University, Indonesia
*Corresponding Author

Received:- 07 April 2026/ Revised:- 16 April 2026/ Accepted:- 21 April 2026/ Published: 30-04-2026

Abstract— *This study aims to determine the effect of papaya peel extract (Carica papaya L.) administered through drinking water on the percentage of external offal in 35-day-old broiler chickens. The study was conducted at the Sesetan Farm, Faculty of Animal Science, Udayana University in February 2025. The study involved 80 broilers that were given papaya peel extract in drinking water at different concentrations, namely 4%, 6% and 8%. The study was designed using a completely randomized design (CRD) with 4 treatments and 5 replications: P0 as the control (drinking water without papaya peel extract), P1 (drinking water with 4% papaya peel extract), P2 (drinking water with 6% papaya peel extract), and P3 (drinking water with 8% papaya peel extract). The variables observed were the percentage of external offal (head, neck, feet, blood, and feathers). The results showed that the administration of papaya peel extract at concentrations of 4%, 6% and 8% had no significant difference (P>0.05) on external offal. Therefore, this study concluded that the administration of papaya peel extract at concentrations of 4%, 6% and 8% in drinking water produced similar results on the percentage of external offal (head, neck, feet, blood and feathers) in 35-day-old broiler chickens.*

Keywords— Broiler chickens, External offal, Papaya peel extract.

I. INTRODUCTION

The growth in the population and the improvement in the standard of living of the Indonesian people have led to an increase in food demand, especially animal protein. Based on data from the Central Statistics Agency (BPS), the population of Indonesia continues to increase year by year. In 2020, the Population Census recorded a population of 270.20 million people. Population projections indicate an increase to 275.77 million people in 2022, 278.70 million people in 2023, and 281.60 million people in 2024. The need for animal protein can be met by one type of animal meat, namely broiler chicken. In 2013, per capita consumption was recorded at 3.65 kg per year and increased to 5.68 kg per year in 2017. In total, national consumption of broiler chicken during the 2017–2021 period reached an average of 1.62 million tons per year, placing Indonesia as the sixteenth largest consumer of broiler chicken in the world. This increase in consumption reflects the important role of broiler chicken as an affordable and popular source of animal protein among the Indonesian population.

Broiler chickens are the result of crossbreeding various chicken breeds with high meat production capabilities, making them one of the main commodities. Along with the growth in population, the production of broiler chicken meat in Indonesia has also shown an increase. Data on broiler chicken meat production per province from the Central Bureau of Statistics (BPS) in 2024 shows variations in production across different regions, with broiler chicken meat production in Bali reaching 93,596.37 tons. Denpasar City produced 8,268 tons of poultry meat in 2022. This increase in broiler chicken meat production reflects efforts to meet the rising demand in line with the growing population and the need for animal protein consumption in Bali. According to the Central Bureau of Statistics (BPS) data in 2024, the population of broiler chickens in Indonesia reached 3.11 billion, an increase of 6.43% compared to the previous year, which recorded 2.93 billion.

Since 1946, antibiotics have been used as additives in livestock feed in Indonesia with the aim of improving digestibility, growth, and the health of livestock. However, the use of Antibiotic Growth Promoters (AGP) has been banned in Indonesia since January 1, 2018, in accordance with the Minister of Agriculture Regulation Number 14 of 2017 concerning the Classification of Veterinary Drugs (Dwi Cahyono and Nurul, 2022). One of the natural feed additive ingredients is papaya fruit peel extract. Papaya fruit peel is a byproduct of the papaya fruit that has almost the same nutritional content as the fruit itself. Papaya fruit peel contains antibacterial compounds such as alkaloids, tannins, steroids, saponins, and flavonoids. Papaya fruit peel also has active compounds such as papain, vitamin C, vitamin A, magnesium, copper, pantothenic acid, B complex vitamins, beta-carotene, lutein, zeaxanthin, vitamin E, calcium, potassium, vitamin K, and lycopene (Armando, 2020).

Prabayanti et al. (2022) stated that the administration of garlic skin extract at 1%, 2%, and 3% in drinking water did not affect the percentage of external offal (head, neck, feet, blood, and feathers) of 4-week-old broilers. Additionally, according to Triwibowo et al. (2021), the addition of papaya leaf juice in drinking water up to a level of 1.5% did not have a significant effect ($P>0.05$) on feed consumption, drinking water consumption, body weight gain, and feed conversion. Research by Wiriani (2023) reported that the administration of papaya seed extract (Carica papaya L.) through drinking water at levels of 1%, 2%, and 3% yielded similar results regarding the percentage of external offal in 4-week-old broilers. Based on this background, this study was conducted to determine the effect of administering drinking water with added papaya peel extract (Carica papaya L.) on the percentage of external offal in 5-week-old broilers.

II. MATERIALS AND METHODS

2.1 Place and Time of the Research

This research was conducted at the Faculty of Animal Husbandry, located on Jalan Raya Sesetan Gang Markisa, Denpasar, Bali. The research lasted for 2 months, from preparation to data processing.

2.2 Broiler Chickens

The broiler chickens used in this study did not differentiate between specific sexes (unsexed) and the broilers used were 2 days old. A total of 100 Day Old Chickens (DOC) were obtained, from which 80 were selected based on weight uniformity with a standard deviation of ±5% of the mean weight.

2.3 Cages and Equipment

This study uses colony-type cages made of iron, measuring 75 cm in length, 75 cm in width, and 50 cm in height. The colony cages are placed inside a building measuring 16 meters x 6 meters, with an asbestos roof and a concrete floor. A total of 20 units of cages were used in this study, with each cage housing 4 livestock. Each cage is equipped with a plastic feeder and a special drinking place for poultry. This research also uses various additional equipment, such as buckets to mix papaya peel extract with water, measuring cups to measure the amount of drinking water, blenders to make papaya peel extract, strainers to separate the pulp from the extract, and stationery to record data during the research.

2.4 Ration and Drinking Water

This study used the commercial ration CP 511B from PT Charoen Pokhpand and papaya fruit peels. The provision of feed and drinking water was given ad libitum and the leftovers were measured the next day. The drinking water used is sourced from a well. The nutritional content of the commercial feed used can be seen in Table 1.

TABLE 1
NUTRITIONAL CONTENT OF CP 511

Nutrient	Composition (%)	Standard Requirements for Broiler Starters (%)	Standard Requirements for Broiler Finisher (%)
Water	13	Max. 14.0	Max. 14.0
Proteins	21	Max. 19.0	Min. 18.0
Fat	4	Max. 7.4	Max. 8.0
Fiber	4	Max. 6.0	Max. 6.0
Ash	6.5	Max. 8.0	Max. 8.0
Calcium	0.9	0.9 – 1.20	0.9 – 1.20
Phosphorus	0.7	0.6 – 1.00	0.6 – 1.00

Information:

- PT. Charoen Phokphand Indonesia
- Standard Requirements for Broiler Starters according to SNI 01-3930-2006
- Standard Requirements for Broiler Finisher according to SNI 01-3930-2006

2.5 Research Design

In this study, the design that was used is a Completely Randomized Design (CRD) with 4 treatments and 5 replications, each replication consisting of 4 broiler chickens. The treatment involves administering papaya peel extract through drinking water with the following groups:

- P0: Drinking water without papaya peel extract (control)
- P1: Drinking water with 4% papaya peel extract
- P2: Drinking water with 6% papaya peel extract
- P3: Drinking water with 8% papaya peel extract

2.6 Randomization of Broiler Chickens

In this study, 100 chickens were used, with a weight range of approximately 5% standard deviation. The randomization of the chickens was carried out to select 80 DOC from 100 DOC according to the weight with a standard deviation of ±5%. They were then divided into 4 treatments with 5 replications and 20 randomly assigned cages. Each cage was filled with 4 chickens.

2.7 Making Papaya Peel Extract

The making of papaya peel extract was done by collecting the papaya peels that had been separated from the flesh. After separation, the papaya peels were cut into small pieces to make it easier to put them into the blender. Once cut, they were put into the blender and mixed with water using a 1:1 ratio, meaning 1 kg of papaya peel equals 1 liter of water. After blending, the mixture was strained and given to the livestock according to the treatment.

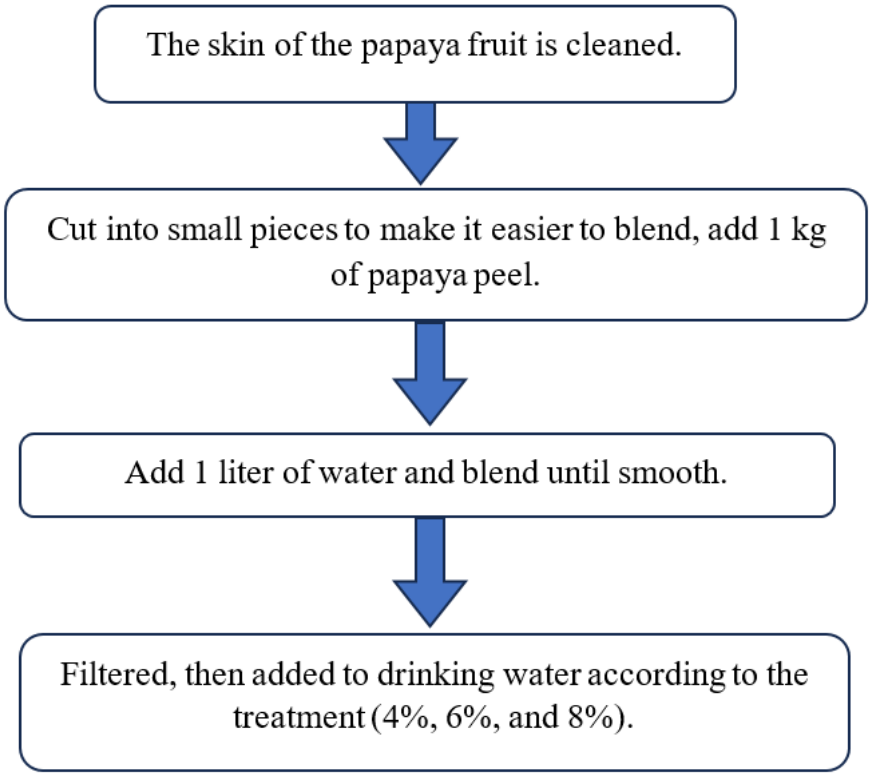

FIGURE 1: Method of making papaya peel extract

2.8 Administration of Papaya Peel Extract

Administration of drinking water:

- P0: Drinking water without papaya peel extract
- P1: Drinking water with 4% papaya peel extract (960 ml water + 40 ml extract)
- P2: Drinking water with 6% papaya peel extract (940 ml water + 60 ml extract)
- P3: Drinking water with 8% papaya peel extract (920 ml water + 80 ml extract)

In this study, the provision of drinking water was done ad libitum, meaning the water was available throughout the day and the remainder was measured the next day.

2.9 Research Preparation

One week before the research began, the cages and equipment were prepared, and the cage area was sanitized using an antiseptic diluted at a ratio of 1:5 (1 ml of antiseptic added to 5 liters of water) as a disinfectant. On the first day, the DOC was weighed to determine the initial body weight and marked with paint on the broiler's wing to facilitate the recording process.

2.10 Broiler Chicken Slaughtering

Chickens were slaughtered to obtain by-products such as heads, necks, feet, blood, and feathers. The number of chickens slaughtered was 4 chickens from each poultry unit that had been given drinking water with papaya peel extract. However, before slaughter, the chickens were fasted for 12 hours but were still given drinking water. The slaughtering process was carried out according to the USDA (United States Department of Agriculture, 1997) and Soeparno (2009) method, which states that the jugular vein and carotid artery located between the first neck vertebra should be cut. The blood that flows out was collected and weighed to determine its weight. After the chicken was confirmed dead, its body was submerged in warm water at a temperature of 50°-65°C for 30-60 seconds, followed by feather plucking. The next step involved cutting off the external offal of the chicken that had been separated from the carcass, followed by weighing to determine its weight.

2.11 Observed Variables

The observed variables in the research were as follows:

- **Head:** The head weight was calculated by weighing the chicken's head that had been separated from the neck after slaughter. The separation of the head was done by cutting at the joint (atlanto-occipitalis), which is the meeting point between the atlas bone (Os vertebrae cervicalis I) and the back of the skull.

$$\text{Percentage of head} = \frac{Head\ weight}{Cut-off\ weight} \times 100\% \quad (1)$$

- **Neck:** The weight of the neck was obtained by weighing the chicken's neck that had been separated from the head. The cutting was done at the joint between the last neck bone (Os vertebrae cervicalis) and the first back bone (Os vertebrae thoracalis).

$$\text{Percentage of neck} = \frac{neck\ weight}{Cut-off\ weight} \times 100\% \quad (2)$$

- **Feet:** The weight of the feet was calculated by weighing the chicken feet that had been separated from the carcass. The cutting was done at the junction between the tarsal bone (Os tarsal) and the tibia bone (Os tibia).

$$\text{Percentage of feet} = \frac{Feet\ weight}{Cut-off\ weight} \times 100\% \quad (3)$$

- **Blood:** The weight of the blood was obtained by weighing the collected blood of the chicken after slaughter.

$$\text{Percentage of blood} = \frac{Blood\ weight}{Cut-off\ weight} \times 100\% \quad (3)$$

- **Feathers:** The weight of the feathers was calculated by weighing the total body weight of the chicken without feathers, then subtracting the weight of the blood.

$$\text{Percentage of feather} = \frac{Feather\ weight}{Cut-off\ weight} \times 100\% \quad (3)$$

2.12 Data Analysis

The data were analyzed using analysis of variance; if there was a significant difference (P<0.05), it would be followed by Duncan's Multiple Range Test (Steel and Torrie, 1993).

III. RESULTS AND DISCUSSION

The results of the study on the effect of administering papaya fruit peel extract (Carica papaya L.) on the percentage of external offal in broiler chickens can be seen in Table 2.

TABLE 2
RESULTS OF THE ANALYSIS OF THE EFFECT OF ADMINISTERING PAPAYA FRUIT PEEL EXTRACT (CARICA PAPAYA L.) ON THE PERCENTAGE OF EXTERNAL OFFAL IN BROILER CHICKENS AT DIFFERENT LEVELS

Variable	P0	P1	P2	P3	SEM[1])
Head (%)	2.39a	2.46a	2.13a	2.24a	0.09
Neck (%)	4.18a	3.68a	3.91a	3.47a	0.45
Feet (%)	3.85a	4.31a	4.01a	4.26a	0.19
Blood (%)	5.65a	3.37a	4.58a	4.36a	1.34
Feathers (%)	8.76a	5.34a	5.44a	6.11a	0.99

Explanation:

P0: Drinking water without papaya peel extract (control)

P1: Drinking water with 4% papaya peel extract

P2: Drinking water with 6% papaya peel extract

P3: Drinking water with 8% papaya peel extract

[1]) SEM = Standard Error of the Treatment Means

Values with the same letter in the same row indicate no significant difference (P>0.05)

3.1 Percentage of Head

The average head percentage based on the research results on broiler chickens that were not given papaya fruit peel extract (P0) as a control was 2.39% (Table 2). Broiler chickens that received treatment P1 had a head percentage of 2.46%, which was higher compared to treatment P0 but statistically not significantly different (P>0.05). In treatments P2 and P3, the head percentages were 10.88% and 6.28% lower compared to treatment P0, respectively, but statistically not significantly different (P>0.05).

3.2 Percentage of Neck

The average neck percentage based on the research results on broiler chickens that were not given papaya fruit peel extract (P0) as a control was 4.18% (Table 2). Broiler chickens that received treatments P1, P2, and P3 had neck percentages of 11.96%, 6.46%, and 16.99% lower compared to treatment P0, respectively, and were statistically not significantly different (P>0.05).

3.3 Percentage of Feet

The average percentage of feet based on the research results on broiler chickens that were not given papaya fruit peel extract (P0) as a control was 3.85% (Table 2). Broiler chickens that received treatments P1, P2, and P3 had percentages of 11.95%, 4.16%, and 10.65% higher compared to treatment P0, respectively, and were statistically not significantly different (P>0.05).

3.4 Percentage of Blood

The average blood percentage based on the research results on broiler chickens that were not given papaya fruit peel extract (P0) as a control was 5.65% (Table 2). The blood percentage of broiler chickens receiving treatments P1, P2, and P3 were

40.35%, 18.94%, and 22.83% lower, respectively, compared to treatment P0 and were statistically not significantly different (P>0.05).

3.5 Percentage of Feathers

The average feather percentage based on the research results on broiler chickens that were not given papaya fruit peel extract (P0) as a control was 8.76% (Table 2). The feather percentage of broiler chickens receiving treatments P1, P2, and P3 were 39.04%, 37.90%, and 30.25% lower, respectively, compared to treatment P0 and were statistically not significantly different (P>0.05).

IV. DISCUSSION

Statistically, Table 2 shows that the percentage of head, neck, feet, blood, and feathers with the administration of drinking water containing papaya peel extract at levels of 4%, 6%, and 8% showed no significant difference (P>0.05). This is because the head, neck, and feet of broiler chickens are mostly composed of bone tissue, whose growth is more influenced by age and genetic factors rather than the effect of feed additives. Irham (2012) in Suryanti et al. (2019) states that the rate of bone growth does not depend on the influence of feed but rather on the age of the livestock. Furthermore, Wulandari (2014) reported that the process of bone calcification and skeletal formation (skeletogenesis) begins during the embryonic phase, long before the chicks hatch, so the subsequent growth phase has a relatively limited influence of feed additive supplementation on the percentage of the head, neck, and feet.

The head has an important role as the center of the nervous and sensory systems. The head of broiler chickens grows from the embryonic stage inside the egg through intramembranous ossification, accompanied by the development of the brain, eyes, and beak. Wahju (2004) also stated that bones form early in growth, so the influence of additional nutrition during the starter phase is relatively limited on the growth of head size structures. The administration of 4%, 6%, and 8% has not yet been able to influence the growth or percentage of the head in broiler chickens. This is in line with the research by Raillah et al. (2021), which states that the insignificant increase in head weight is related to the final weight of broiler chickens, which also does not show a significant difference, resulting in larger body organs and greater body weight.

Suryantiyanti et al. (2019) added that the weight of livestock organs generally corresponds with the final body weight produced. Additionally, the insignificance of this study can also be attributed to the homogeneity in the research, such as genetics, livestock age, management practices, and the feed used, which are the same, resulting in no significant differences between treatments. Jihad's research (2025) reported that herbal supplements generally have a greater impact on internal parameters such as the digestive system or immune system than on external parameters like head size.

The neck of broiler chickens begins to develop from the embryo through the process of ossification of the cervical vertebrae, which are composed of calcium, phosphorus, and collagen. The main nutrients that play a role in supporting neck growth include protein (especially essential amino acids like arginine), calcium, phosphorus, vitamin D3, and iron, which function in the formation and strengthening of bone and muscle tissue (Pratiwi and Firmawati, 2019). Based on the average results in Table 2, the addition of papaya peel extract through drinking water at levels of 4%, 6%, and 8% did not have a significant effect on the percentage of broiler chicken necks (P>0.05). This indicates that the neck is an external part of the body whose muscle tissue growth is relatively stable and unresponsive to variations in feed or phytochemical supplementation. The absence of significant differences observed can be attributed to the homogeneity in the study, such as the age of broiler chickens, genetic factors, management practices, and the uniform provision of feed and drinking water.

Chicken feet function as the main support of the body and play an important role in supporting body weight during the growth phase of broiler chickens. Based on the average results in Table 2, the administration of papaya fruit peel extract through drinking water at levels of 4%, 6%, and 8% showed no statistically significant difference in the percentage of broiler chicken feet (P>0.05). This indicates that the treatment has not yet been able to provide a significant effect on the growth of the feet parts. Bones are formed from the early stages of growth, so after passing the starter phase, the influence of additional nutrition on bone growth is relatively small (Wahju, 2004). The growth of the feet begins with the process of transforming cartilage tissue into hard bone through endochondral ossification, a process that highly depends on the adequacy of calcium, phosphorus, and vitamins that play a role in maintaining the density and strength of the feet bones (David et al., 2023).

Blood is the main component of the circulatory system that serves as a transport medium for various substances important to the body, such as oxygen, nutrients, hormones, and metabolic waste (Soeparno et al., 2011). The volume and composition of broiler chicken blood are influenced by several factors, including age, physiological condition, nutritional status, and

hormonal balance. Based on the research results, the administration of papaya peel extract through drinking water at levels of 4%, 6%, and 8% has not met the nutritional needs of broilers required to stimulate blood formation, thus showing no significant changes. Statistically, although the blood percentage in treatments P1, P2, and P3 tended to be lower compared to P0, the differences were not significant (P>0.05). This indicates that the administration of papaya fruit peel extract does not have a significant effect on the blood volume of broiler chickens. Physiologically, blood formation is closely related to the process of hematopoiesis, where red blood cells (erythrocytes) begin to form during the embryonic phase in the liver, then shift to the bone marrow as the main production center after hatching (Guedes et al., 2014).

Feathers are the outer part of broiler chickens that continue to grow, but as the livestock ages, the growth rate of the feathers tends to reach a fixed or constant point (Utari et al., 2025). The formation and growth of feathers in broiler chickens are greatly influenced by the adequacy of energy, protein, and minerals obtained from feed and drinking water (Chen et al., 2020). Based on the average results in Table 2, the administration of papaya peel extract through drinking water showed no significant difference in the percentage of broiler chicken feathers (P>0.05). The absence of significant differences between treatments can be attributed to the homogeneity of research conditions such as the age of the livestock, environment, management practices, and relatively similar feed, resulting in uniform feather growth across all treatments. In addition to nutritional factors, the growth and molting of broiler feathers are also influenced by environmental factors, especially temperature, which plays a role in regulating metabolism and feather molting (Achmad et al., 2018). Radhitya (2014) reported that the difference in the weight of broiler feathers in diets with different protein levels did not show significant results when the protein requirements were adequately met. This is in line with the research findings of Widelitz (2019), which reported that all treatments received the same feed additive, so there was no difference in feather growth response between treatments. The main functions of feathers include maintaining body temperature, protecting the body from injury, and forming a protective layer through the growth of feathers from the epidermal follicles outward to the surface of the body.

V. CONCLUSION

Based on the research results, it can be concluded that the administration of 4%, 6%, and 8% papaya fruit peel extract in drinking water does not affect the percentage of external offal (head, feet, neck, blood, and feathers) in broiler chickens aged 35 days. Future studies should investigate higher concentrations of papaya peel extract or explore its effects on internal organ development, growth performance, or meat quality.

ACKNOWLEDGEMENT

The authors gratefully acknowledge the support of the Dean, Head of Research and Community Service, supervising lecturers and staff of the Animal Feed Nutrition Chemistry and Poultry Science Laboratories, Faculty of Animal Husbandry, Udayana University, Bali, Indonesia, for funding and laboratory facilities.

CONFLICT OF INTEREST

The authors declare that there is no conflict of interest regarding the publication of this research. The materials used in this study, including papaya fruit peel extract, were prepared independently by the researchers and were not influenced by any commercial or financial interests.

REFERENCES

[1] Achmad, G. A., Darwati, S., & Sumantri, C. (2018). [Title missing]. *Jurnal Ilmu dan Teknologi Peternakan Tropis, 6*(1), 38–47.

[2] Armando Paat, C. S. (2020). Pemanfaatan tepung kulit buah pepaya (*Carica papaya* L.) dalam ransum. *[Journal Name], 40*(2), 418–427.

[3] Badan Pusat Statistik. (2022). *Produksi tanaman buah-buahan di Indonesia tahun 2021–2022*.

[4] Badan Pusat Statistik. (2023). *Rata-rata harian konsumsi protein per kapita dan konsumsi kalori per kapita tahun 1990–2024*.

[5] Badan Pusat Statistik. (2023). *Rata-rata konsumsi per kapita seminggu beberapa macam bahan makanan penting, 2007–2023*.

[6] Badan Pusat Statistik. (2024). *Jumlah penduduk pertengahan tahun (Ribu Jiwa), 2022–2024*.

[7] Badan Pusat Statistik. (2024). *Produksi daging ayam ras pedaging menurut provinsi (Ton), 2024*.

[8] Badan Pusat Statistik. (2021). *Jumlah ayam pedaging di Indonesia*. https://dataindonesia.id/sektor-riil/detail/jumlah-ayam-pedaging-di-indonesia-capai-311-miliar-pada-2021

[9] Chen, M., Xie, W., Jiang, S., Wang, X., Yan, H., & Gao, C. (2020). Molecular signaling and nutritional regulation in the context of poultry feather growth and regeneration. *Frontiers in Physiology, 11*, Article 1609, 1–14.

[10] David, L. S., Anwar, M. N., Abdollahi, M. R., Bedford, M. R., & Ravindran, V. (2023). Calcium nutrition of broilers: Current perspectives and challenges. *Animals*.

[11] Dwi Cahyono, P., & Nurul, H. (2022). Efektifitas probiotik sebagai pengganti antiprobotik growth promotor (AGP) pada unggas. *Jurnal Penelitian, Fakultas Peternakan, Universitas Islam Malang*.

[12] Guedes, P. T., Oliveira, B. C. E. P. D., Manso, P. P. A., Caputo, L. F. G., Cotta-Pereira, G., & Pelajo-Machado, M. (2014). Histological analyses demonstrate the temporary contribution of yolk sac, liver, and bone marrow to hematopoiesis during chicken development. *PLoS ONE, 9*(3), 1–15.

[13] Irham, M. (2012). *Pengaruh penggunaan enceng gondok (Eichornia crassipes) fermentasi dalam ransum terhadap persentase karkas, nonkarkas dan lemak abdominal itik lokal jantan umur delapan minggu* [Skripsi, Universitas Sebelas Maret Surakarta].

[14] Jihad, A. (2025). *Pengaruh ekstrak daun kelor terfermentasi melalui air minum terhadap persentase offal eksternal broiler* [Skripsi, Universitas Udayana].

[15] Prabayanti, I. A. S. T., Dewi, G. A. M. K., & Wijana, I. W. (2022). Pengaruh ekstrak kulit bawang putih (*Allium sativum*) pada air minum terhadap persentase eksternal offal broiler umur 4 minggu. *Peternakan Tropika, 2*(1).

[16] Pratiwi, H., & Firmawati, A. (2019). *Embriologi hewan*. Universitas Brawijaya Press.

[17] Radhitya, A. (2014). Pengaruh pemberian tingkat protein ransum pada fase grower terhadap pertumbuhan puyuh (*Coturnix coturnix japonica*). *Students e Journal, Universitas Padjadjaran*.

[18] Raillah, H. S., Dewi, G. A. M. K., & Wirapartha, M. (2021). Pemberian tepung kulit kerang dalam ransum terhadap persentase offal eksternal ayam Isa Brown umur 100 minggu. *Jurnal Peternakan Tropika, 9*.

[19] Soeparno. (2009). *Ilmu teknologi daging*. Gadjah Mada University Press.

[20] Suryanti, N. L. A., Dewi, G. A. M. K., & Dewantari, M. (2019). The effect of use of red dragon skin (*Hylocereus polyrhizus*) fermented in the break of external offal broiler. *Jurnal Peternakan Tropika, 7*.

[21] Tribowo, A., Wati, N. E., & Suhadi, M. (2021). Pengaruh penambahan air perasan daun buah pepaya (*Carica papaya* L.) dalam air minum terhadap performa ayam broiler. *Jurnal Wahana Peternakan, 5*(1), 32–40.

[22] Utari, G. A. D. D., Ariana, I. N. T., & Mahardika, I. G. (2025). Kualitas fisik daging itik Bali jantan yang diberi pakan konsentrat protein limbah peternakan ayam (KPLA). *Peternakan Tropika, 13*(2), 249–261.

[23] Wahju, J. (2004). *Ilmu nutrisi ternak unggas* (5th ed.). Gadjah Mada University Press.

[24] Wahju, J. (2004). *Ilmu nutrisi ternak unggas* (5th ed.). Gadjah Mada University Press.

[25] Widelitz, R. B. (2019). Morpho regulation in diverse chicken feather formation. *Developmental Dynamics, 248*(8), 666–676. https://onlinelibrary.wiley.com/doi/10.1111/dgd.12584

[26] Wiriani. (2023). *Pengaruh pemberian ekstrak biji pepaya (Carica papaya L.) melalui air minum terhadap persentase eksternal offal broiler umur 4 minggu* [Skripsi, Universitas Udayana].

[27] Wulandari, R. (2014). *Struktur dan perkembangan rangka embrio ayam (Gallus gallus domesticus)* [Skripsi, Universitas Gadjah Mada]. https://etd.repository.ugm.ac.id/home/detail_pencarian/73657?utm_source.

International Journal of Environmental & Agriculture Research

Published by
AD Publications

Contact us +91-7665235235 www.ijoear.com info@ijoear.com